7.8 The object of this problem is to verify that Equation (7.59) is the solution to Equations (7.56) – (7.58).

(a) Integrate Equations (7.56) once and impose the freestream boundary condition [Equation (7.58)].

(b) Observing that $\sigma = \sigma^* = 1/2$ for Saffman's model, combine the k and ω^2 equations to show that

$$\frac{dk}{d\omega^2} = \frac{k}{\omega^2}$$

Solve this equation subject to the boundary conditions.

(c) Introduce the dimensionless variables

$$\bar{y} = \frac{|V|(\delta - y)}{\nu} \qquad \text{and} \qquad \bar{\omega} = \frac{V^2\omega}{\mathcal{K}\nu}$$

and substitute the solution for k into the equation for ω. Set any arbitrary constant of integration equal to zero, and verify the solution for $\delta - y$.

(d) Letting $\bar{U} = U/|V|$, rewrite the momentum equation. Using the dimensionless equation for $\bar{\omega}$ derived in Part (c), verify that

$$\left(\frac{1+\bar{\omega}}{2+\bar{\omega}}\right)\frac{d\bar{U}}{d\bar{\omega}} = \frac{\bar{U} - \bar{U}_e}{\bar{\omega}}$$

and verify the solution for $U_e - U$.

7.9 This problem illustrates how nonlinear terms affect numerical stability for parabolic marching methods. Consider the following limiting form of the k-ω model.

$$U\frac{\partial\omega}{\partial x} = \alpha\left(\frac{\partial U}{\partial y}\right)^2 - \beta_o\omega^2$$

We wish to analyze the stability of the solution to this equation under the following discretization approximations.

$$U\frac{\partial\omega}{\partial x} \doteq \frac{U}{\Delta x}\left[3\omega^i_{m+1} - 4\omega_m + \omega_{m-1}\right]$$

$$\alpha\left(\frac{\partial U}{\partial y}\right)^2 \doteq \frac{\alpha(\partial U/\partial y)^2}{\omega^{i-1}_{m+1}}\omega^i_{m+1}$$

$$\beta_o\omega^2 \doteq (1+\psi_\omega)\beta_o\omega^{i-1}_{m+1}\omega^i_{m+1} - \psi_\omega\beta_o(\omega^{i-1}_{m+1})^2$$

(a) Assuming that ω^i_{m+1} is the sum of the exact solution to the discretized equation, ω_{m+1}, and an error term, $\delta\omega^i$, viz.,

$$\omega^i_{m+1} = \omega_{m+1} + \delta\omega^i$$

linearize the discretized equation for ω and verify that

$$\frac{\delta\omega^i}{\delta\omega^{i-1}} = \frac{(\psi_\omega - 1)\beta_o\omega^2_{m+1} - \alpha(\partial U/\partial y)^2}{3U\omega_{m+1}/\Delta x - \alpha(\partial U/\partial y)^2 + (\psi_\omega + 1)\beta_o\omega^2_{m+1}}$$

(b) Using the fact that ω_{m+1} satisfies the exact discretized equation, simplify the denominator and show that

$$\frac{\delta\omega^i}{\delta\omega^{i-1}} = \frac{(\psi_\omega - 1) - \alpha(\partial U/\partial y)^2/(\beta_o\omega_{m+1}^2)}{\psi_\omega + U(4\omega_m - \omega_{m-1})/(\beta_o\omega_{m+1}^2\Delta x)}$$

(c) Assuming the term proportional to U is negligible, determine the condition that ψ_ω must satisfy in order to insure that $|\delta\omega^i/\delta\omega^{i-1}| < 1$.

7.10 Using von Neumann stability analysis, determine G and any condition required for stability of the following finite-difference schemes. Assume $U > 0$, $\nu > 0$ and $S < 0$.

(a) Euler's method:

$$k_j^{n+1} = k_j^n - \frac{U\Delta t}{2\Delta x}\left(k_{j+1}^{n+1} - k_{j-1}^{n+1}\right)$$

(b) Richardson's method:

$$k_j^{n+1} = k_j^{n-1} + \frac{2\nu\Delta t}{(\Delta x)^2}\left(k_{j+1}^n - 2k_j^n + k_{j-1}^n\right)$$

(c) Crank and Nicolson's method:

$$k_j^{n+1} = k_j^n - \frac{U\Delta t}{4\Delta x}\left(k_{j+1}^{n+1} + k_{j+1}^n - k_{j-1}^{n+1} - k_{j-1}^n\right) + \frac{1}{2}S\Delta t\left(k_j^{n+1} + k_j^n\right)$$

7.11 Using von Neumann stability analysis, determine G and any condition required for stability of the following first-order accurate scheme applied to the inviscid Burgers' equation, $u_t + Uu_x = 0$:

$$u_j^{n+1} = u_j^n - \frac{U\Delta t}{2\Delta x}\left(u_{j+1}^{n+1} - u_{j-1}^n\right), \qquad U > 0$$

7.12 Consider the following one-dimensional wave equation with source and diffusion terms.

$$\frac{\partial k}{\partial t} + U\frac{\partial k}{\partial x} = Sk + \nu\frac{\partial^2 k}{\partial x^2}$$

where $U > 0$, $\nu > 0$ and S can be either positive or negative.

(a) Cast this equation in finite-difference form using Crank-Nicolson differencing and the following approximation for the source term.

$$Sk \doteq S\left[\psi k_j^n + (1-\psi)k_j^{n+1})\right], \qquad 0 \le \psi \le 1$$

(b) Using von Neumann stability analysis, determine G and any condition required for stability of this finite-difference scheme. How do your results compare to the analysis of Equation (7.93) in Section 7.4?

7.13 Using von Neumann stability analysis, determine G and any condition required for stability of *Lax's method* applied to the inviscid Burgers' equation, $u_t + Uu_x = 0$:

$$\frac{u_j^{n+1} - \frac{1}{2}\left(u_{j+1}^n + u_{j-1}^n\right)}{\Delta t} + U\frac{u_{j+1}^n - u_{j-1}^n}{2\Delta x} = 0, \qquad U > 0$$

7.14 Verify that the dependent-variable and inviscid-flux vectors in Equation (7.117) can be written as

$$\mathbf{Q} = \begin{Bmatrix} Q_1 \\ Q_2 \\ Q_3 \\ Q_4 \\ Q_5 \end{Bmatrix}, \quad \mathbf{F} = \begin{Bmatrix} Q_2 \\ (\frac{3-\gamma}{2})Q_2^2/Q_1 + (\gamma-1)Q_3 - (\gamma-1)Q_4 \\ \gamma Q_2 Q_3/Q_1 - (\frac{\gamma-1}{2})Q_2^3/Q_1^2 - (\gamma-1)Q_2 Q_4/Q_1 \\ Q_2 Q_4/Q_1 \\ Q_2 Q_5/Q_1 \end{Bmatrix}$$

and show that the flux-Jacobian matrix is given by Equation (7.121).

7.15 Suppose a finite-difference method is only first-order accurate. When this is true, Richardson's estimate of the error must be revised. Assuming

$$E_h = e_1 h + e_2 h^2 + \cdots$$

propose an alternative to Equation (7.138).

7.16 The following table represents partial results for one-dimensional finite-difference computations using a second-order accurate, time-marching method. The computations have been done on grids with 50, 100 and 200 points. Use Richardson extrapolation to estimate the discretization error at each point for the two finest grids. Based on your results, make a table of the results below and add a column with your best estimate of the continuum solution (grid-point spacing $\rightarrow$ 0) to the differential equation.

j	ϕ_{50}	j	ϕ_{100}	j	ϕ_{200}
1	0.5592	1	0.5628	1	0.5607
2	0.5700	3	0.5740	5	0.5726
3	0.5737	5	0.5748	9	0.5745
4	0.5615	7	0.5557	13	0.5573

7.17 The following table represents partial results for one-dimensional finite-difference computations using a second-order accurate, time-marching method. The computations have been done on grids with 50, 100 and 200 points. Use Richardson extrapolation to estimate the discretization error at each point for the two finest grids. Based on your results, make a table of the results below and add a column with your best estimate of the continuum solution (grid-point spacing $\rightarrow$ 0) to the differential equation.

j	ϕ_{50}	j	ϕ_{100}	j	ϕ_{200}
1	3.00361	1	2.96624	1	2.95443
2	3.07446	3	3.06157	5	3.05965
3	3.09224	5	3.06523	9	3.07557
4	3.54523	7	3.53756	13	3.52365

7.18 The object of this problem is to verify that Program **WAKE** (see Appendix C) is second-order accurate and to compute the grid-convergence index (GCI).

(a) Select default conditions in Program **WAKE_DATA** to clear any previous applications. Then, run computations with $N = 101$, 151 and 201 grid points. Record the 5-significant-digit spreading rate, δ', from the printed output for each computation.

(b) Use Richardson extrapolation for the 101- and 201-point computations to infer δ'_∞, the "exact" value of δ'.

(c) Define the error, $E_h = \delta' - \delta'_\infty$ for the three computations. Make a log-log plot of E_h versus $h = 1/(N-1)$ and confirm that the order of accuracy of the numerical method implemented in **WAKE** is $p = 2$.

(d) Compute the GCI (expressed as a percent) for the 151- and 201-point grids with the 101-point grid results as the basis in both cases.

7.19 The object of this problem is to verify that Program **SUBLAY** (see Appendix C) is second-order accurate and to compute the grid-convergence index (GCI).

(a) Select default conditions in Program **SUBLAY_DATA** to clear any previous applications. Then, run computations with $N = 101$, 151, 201, 301 and 401 grid points. Each time you change N, set the value of y^+ at the point nearest the surface to $y_2^+ = 10/(N-1)$. Record the 6-significant-digit constant in the law of the wall, C, from the printed output for each computation.

(b) Use Richardson extrapolation for the 201- and 401-point computations to infer C_∞, the "exact" value of C.

(c) Define the error, $E_h = C - C_\infty$ for the five computations. Make a log-log plot of E_h versus y_2^+ and confirm that the order of accuracy of the numerical method implemented in **SUBLAY** is $p = 2$.

(d) Compute the GCI (expressed as a percent) for the 151- through 401-point grids with the next smallest grid results as the basis in all cases.

7.20 The object of this problem is to verify that Program **EDDYBL** (see Appendix C) is second-order accurate and to compute the grid-convergence index (GCI).

(a) Use Program **EDDYBL_DATA** and the input data supplied on the companion CD for Flow 1400. Run computations with $N = 101$, 151 and 201 grid points. Each time you change N, you must select the proper "Geometric Progression Ratio," k_g, to adjust grid-cell spacing. Use $k_g = 1.07$, 1.046 and 1.0345 for $N = 101$, 151 and 201, respectively. Record the 6-significant-digit skin friction, c_{fe}, from the "long" printed output for each computation.

(b) Use Richardson extrapolation for the 101- and 201-point computations to infer $c_{f\infty}$, the "exact" value of c_{fe}.

(c) Define the error, $E_h = c_{fe} - c_{f\infty}$ for the three computations. Make a log-log plot of E_h versus $y_2^+ = 27/(N-1)$ and confirm that the order of accuracy of the numerical method implemented in **EDDYBL** is $p = 2$.

(d) Compute the GCI (expressed as a percent) for the 151- and 201-point grids with the 101-point grid results as the basis in both cases.

Chapter 8

New Horizons

The focus of the previous chapters has been on approximate, Reynolds-averaged, models for use in general engineering applications. Throughout this text, we have stressed the virtue of using the minimum amount of complexity while capturing the essence of the relevant physics. This is the same notion that G. I. Taylor described as the "simple model/simple experiment" approach.

Nevertheless, no pretense has been made that any of the models devised in this spirit applies to all turbulent flows: such a "universal" model probably doesn't exist. We must always proceed with some degree of caution since there is no guarantee that Reynolds-averaged models are accurate beyond their established data base. Thus, while simplicity has its virtues for many practical engineering applications, there is a danger that must not be overlooked. Specifically, as quipped by H. L. Mencken...

> *"There is always an easy solution to every human problem – neat, plausible and wrong."*

This chapter discusses modern efforts that more directly address the physics of turbulence without introducing Reynolds-averaged closure approximations. We begin by discussing Direct Numerical Simulation (DNS) in which the exact Navier-Stokes and continuity equations are solved, though currently at relatively low Reynolds numbers because of the limitations of present-day computers. We then turn to Large Eddy Simulation (LES) in which the largest eddies are computed exactly and the smallest, "subgrid-scale" (SGS) eddies are modeled, hopefully with a less critical impact on the simulation than in Reynolds-stress modeling. Next, we address the recently developed Detached Eddy Simulation (DES) method that computes the very largest eddies from first principles and uses a conventional Reynolds-averaged model for the "smaller eddies." In comparison to the LES method, the smaller eddies are much larger than the SGS cell size.

Finally, we discuss current efforts in chaos studies, and their possible relevance to turbulence.

8.1 Background Information

Before plunging into these topics, it is worthwhile to pause and review the key aspects of turbulence that we discussed in Chapters 1 and 2. It may even be helpful for the unhurried reader to revisit Sections 1.3 and 2.5 before proceeding. Note that in pursuing a more fundamental approach to turbulence in DNS, LES and DES studies, we still have a need to understand important aspects of turbulence such as the roles played by the largest and smallest eddies and the cascade process. The reason for this need changes however. In developing a turbulence model, we are trying to mimic the physics in our mathematical formulation. As our understanding of turbulent-flow physics improves, so the quality of our approximations improves (assuming we make intelligent use of the improved understanding). Even in DNS we need some knowledge of turbulence physics to check for the physical soundness of the numerical results, for example, to be certain that inadequate resolution or even programming errors are not causing spurious results. The same applies to LES and DES. Note, for example, that formulating SGS models requires at least as detailed an understanding of turbulence physics as Reynolds-averaged models.

The first important point we must consider in DNS, LES and DES is that of the smallest scales of turbulence. Our primary focus in devising Reynolds-averaged closure approximations has been on the dynamics of the largest eddies, which account for most of the transport of properties in a turbulent flow. Our use of dimensional analysis, in which molecular viscosity has been ignored, guarantees that the closure approximations involve length scales typical of the energy-bearing eddies whose Reynolds number — however defined — is much larger than unity except close to a solid surface, i.e. in the viscous sublayer, $y^+ < 3$, say. This is the reason that viscous-damping functions are often needed close to a solid boundary where the dissipating eddies dominate, and even the energy-bearing eddies have Reynolds numbers of order unity. DNS is supposed to resolve the whole range of eddy sizes, while in LES and DES we try to resolve all the important (larger) eddies so that the SGS model for the small eddies does not have a critical influence on the overall results. In all three cases we need to know the typical scales of the smallest eddies.

As shown in Subsection 1.3.3, the smallest scales of turbulence are the **Kolmogorov scales** of length, time and velocity, viz.,

$$\eta \equiv \left(\nu^3/\epsilon\right)^{1/4}, \quad \tau \equiv \left(\nu/\epsilon\right)^{1/2}, \quad \upsilon \equiv \left(\nu\epsilon\right)^{1/4} \tag{8.1}$$

where ν is kinematic viscosity and ϵ is dissipation rate. Note that the Reynolds

number $v\eta/\nu$ is equal to unity, which is plausible in view of the basic definition of Reynolds number as a ratio of inertial forces to viscous forces. Necessarily, inertial and viscous effects just balance in the smallest eddies (this is merely an order-of-magnitude argument, and $v\eta/\nu$ comes out as exactly unity simply because the above definitions contain no numerical factors). To relate the Kolmogorov length scale to the length scale we have been dealing with in standard turbulence models, consider the following. By hypothesis, we have been using the length scale appropriate to the energy-bearing eddies, ℓ. This length scale is often chosen as the **integral length scale** in statistical turbulence theory, and is related to ϵ by Equation (4.10), so that [see Equation (1.6)]

$$\frac{\eta}{\ell} \sim Re_T^{-3/4} \tag{8.2}$$

where $Re_T = k^{1/2}\ell/\nu$ is the usual turbulence Reynolds number. Since values of Re_T in excess of 10^4 are typical of fully-developed turbulent boundary layers and $\ell \sim 0.1\delta$ where δ is boundary-layer thickness, the Kolmogorov length scale, η, outside the viscous wall region is less than one ten-thousandth times the thickness of the boundary layer.

DNS, LES and DES studies also make use of another length scale from the statistical theory of turbulence, the **Taylor microscale**, λ [c.f., Tennekes and Lumley (1983) or Hinze (1975)]. The basic definition is

$$\lambda^2 = \frac{\overline{u'^2}}{\overline{(\partial u'/\partial x)^2}} \tag{8.3}$$

For locally isotropic turbulence (i.e. turbulence in which the small scales are statistically isotropic even if the large ones are not, which is usually the case at high Reynolds numbers), the exact expression for dissipation rate, ϵ, leads to

$$\epsilon = 15\nu\overline{\left(\frac{\partial u'}{\partial x}\right)^2} \equiv 15\nu\frac{\overline{u'^2}}{\lambda^2} \tag{8.4}$$

Other definitions of λ can be constructed by using different velocity components and gradients in the basic definition, but in locally-isotropic turbulence they are simply related. Using Equation (4.10), and assuming $k \sim \overline{u'^2}$, we conclude that

$$\frac{\lambda}{\ell} \sim Re_T^{-1/2} \qquad \text{or} \qquad \lambda \sim (\ell\eta^2)^{1/3} \tag{8.5}$$

Thus, in general we can say that for high-Reynolds-number turbulence there is a distinct separation of these scales, i.e.,

$$\eta \ll \lambda \ll \ell \tag{8.6}$$

Now the basic definition shows that λ is a composite quantity, depending on properties of the large-scale eddies as well as the small ones. Unlike ℓ and η, it cannot be identified with any meaningful range of eddy sizes. However, results of numerical simulations are often characterized in terms of the **microscale Reynolds number**, Re_λ, defined by

$$Re_\lambda = k^{1/2}\lambda/\nu \tag{8.7}$$

Substitution for λ from Equation (8.4) leads to

$$Re_\lambda \sim (k^{1/2}L_\epsilon/\nu)^{1/2} \tag{8.8}$$

where $L_\epsilon \equiv k^{3/2}/\epsilon$ is the "dissipation length scale", actually the typical length scale of the stress-bearing motion used implicitly in all two-equation models. Now, L_ϵ is of the same order as ℓ so it follows from Equation (8.8) that also

$$Re_\lambda \sim Re_T^{-1/2} \tag{8.9}$$

Thus although λ is not a very meaningful length scale, Re_λ is an alternative to the Reynolds number of the energy-containing eddies. Finally, the **eddy turnover time**, $\tau_{turnover}$, is simply the ratio of the macroscales for length, ℓ or L_ϵ, and velocity, $k^{1/2}$, and is given by

$$\tau_{turnover} \sim \ell/k^{1/2} \sim L_\epsilon/k^{1/2} \tag{8.10}$$

The eddy turnover time is a measure of the time it takes an eddy to interact with its surroundings. As can be seen from the definition of L_ϵ it is also the reciprocal of the specific dissipation rate, $\omega \sim \epsilon/k$.

A second important consideration is the spectral representation of turbulence properties (see Subsection 1.3.4), which replaces the vague idea of "eddy size." If κ denotes wavenumber, defined as 2π/wavelength, and $E(\kappa)d\kappa$ is the turbulence kinetic energy contained between wavenumbers κ and $\kappa + d\kappa$, we can write

$$k \equiv \frac{1}{2}\overline{u_i'u_i'} = \int_0^\infty E(\kappa)\, d\kappa \tag{8.11}$$

Recall that k is half the trace of the autocorrelation tensor, $\mathcal{R}_{ij}$, defined in Equation (2.43), at zero time delay. Correspondingly, the **energy spectral density** or **energy spectrum function**, $E(\kappa)$, is related to the Fourier transform of half the trace of $\mathcal{R}_{ij}$. In general, we regard a spectral representation as a decomposition into wavenumbers (κ). In loose discussions of "eddy size," we regard the reciprocal of κ as the eddy size associated with κ. Small κ equals large wavelength equals large eddies, and conversely. Of course turbulence is not a superposition of simple waves; any definition of an "eddy" based on observed

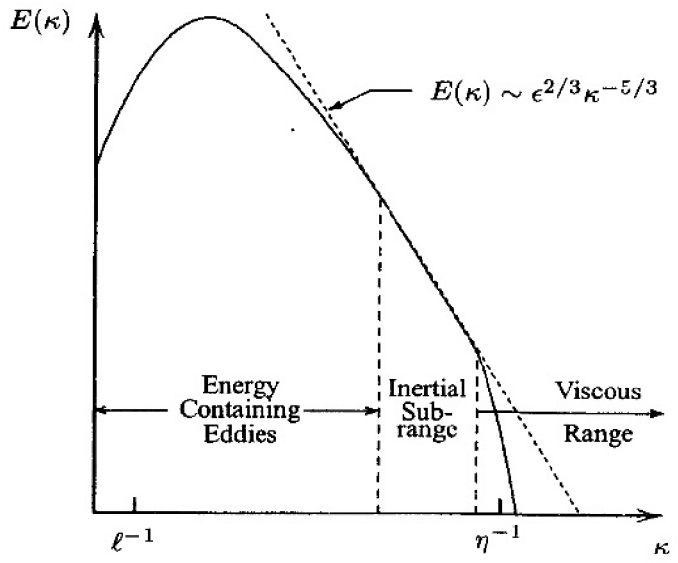

Figure 8.1: *Energy spectrum for a turbulent flow — log-log scales.*

flow patterns will actually cover a range of wavenumbers, and is still vague. However the definition of spectral density and the associated analysis are precise. The present discussion is simplified: see Tennekes and Lumley (1983) for a detailed discussion of energy spectra.

Again using dimensional analysis, Section 1.3.4 shows that, for wavenumbers small enough that viscosity does not affect the motion, but large enough that the overall dimensions of the flow such as boundary-layer thickness do not matter,

$$E(\kappa) = C_K \epsilon^{2/3} \kappa^{-5/3}, \qquad \frac{1}{\ell} \ll \kappa \ll \frac{1}{\eta} \tag{8.12}$$

where C_K is the Kolmogorov constant. This is the famous Kolmogorov $-5/3$ law that characterizes the **inertial subrange**. Figure 8.1 shows a typical energy spectrum for a turbulent flow. With these preliminary remarks in hand, we are now in a position to discuss DNS, LES and DES in the next three sections.

8.2 Direct Numerical Simulation

A direct numerical simulation, or DNS for short, means a complete three-dimensional and time-dependent solution of the Navier-Stokes and continuity equations. The value of such simulations is obvious: they are, in principle, numerically-accurate solutions of exact equations of motion and — in principle — the proper solution to the turbulence problem. From a practical standpoint, statistics computed from DNS results can be used to test proposed closure approximations in engineering models. At the most fundamental level, DNS can

be used to obtain understanding of turbulence structure and processes that can be of value in developing turbulence-control methods (e.g., drag reduction) or prediction methods. DNS can also be viewed as an additional source of experimental data, taken with unobtrusive measuring techniques. This is especially useful for obtaining information about essentially-unmeasurable properties like pressure fluctuations.

All of these comments assume the DNS is free of significant numerical, and other, forms of error. This is a nontrivial consideration, and the primary concerns in DNS are related to numerical accuracy, specification of boundary and initial conditions, and making optimum use of available computer resources. In this section, we discuss these issues only briefly. For more detail at an introductory level, with extensive references to recent research work, see the review article by Moin and Mahesh (1998). As a final reminder, remember that even the numerical solution of the exact equations of motion requires detailed understanding of the physics of turbulence if the solutions are to be economical and accurate.

Estimating the number of grid points and timesteps needed to perform an accurate DNS reveals the complexity of the problem from a computational point of view. As an example, consider incompressible turbulent flow in a channel of height H. The computational domain must be of sufficient extent to accommodate the largest turbulence scales. In channel flow, eddies are elongated in the direction parallel to the channel walls, and their length Λ is known to be about $2H$. Also, in principle, the grid must be fine enough to resolve the smallest eddies whose size is of the order of the Kolmogorov length scale, η. Assuming that at least 4 grid points in each direction are needed to resolve an eddy (since we need adequate resolution of derivatives), we estimate that the total number of grid points for uniform spacing, $N_{uniform}$, is

$$N_{uniform} \approx \left[4\frac{\Lambda}{\eta}\right]^3 = \left[8H\left(\frac{\epsilon}{\nu^3}\right)^{1/4}\right]^3 \tag{8.13}$$

Now, in channel flow, the average dissipation is $\epsilon \approx 2u_\tau^2 U_m/H$ where U_m is the average velocity across the channel, and $U_m/u_\tau \approx 20$. Substituting these estimates into Equation (8.13), we arrive at

$$N_{uniform} \approx (110 Re_\tau)^{9/4}, \quad Re_\tau = \frac{u_\tau H/2}{\nu} \tag{8.14}$$

In practice, it is wasteful to use uniformly-spaced grid points since there are regions where ϵ is small and the Kolmogorov length scale is much larger than it is near the surface where ϵ is largest. By using stretched grids to concentrate points where the smallest eddies reside, experience [Moser and Moin (1984), Kim, Moin and Moser (1987)] shows that the factor of 110 in Equation (8.14) can be replaced by about 3. Thus, the actual number of grid points typically

used in a DNS of channel flow, N_{DNS}, is

$$N_{DNS} \approx (3Re_\tau)^{9/4} \tag{8.15}$$

Similarly, the timestep in the computation, Δt, should be of the same order as the Kolmogorov time scale, $\tau = (\nu/\epsilon)^{1/2}$. Based on results of the computations done by Kim, Moin and Moser (1987), the timestep must be

$$\Delta t \approx \frac{0.003}{\sqrt{Re_\tau}} \frac{H}{u_\tau} \tag{8.16}$$

To appreciate how prohibitive these constraints are, consider the channel-flow experiments done by Laufer (1951) at Reynolds numbers of $1.23 \cdot 10^4$, $3.08 \cdot 10^4$ and $6.16 \cdot 10^4$ and the experiment of Comte-Bellot (1963) at a Reynolds number of $2.3 \cdot 10^5$. Table 8.1 lists the number of grid points and timesteps required to perform a DNS, assuming the time required to reach a statistically-steady state is $100H/U_m \approx 5H/u_\tau$. Clearly, computer memory limitations make all but the lowest Reynolds numbers considered by Laufer impractical with the computers of the early 21st century. The development of massively-parallel machines over the last decade has reduced execution times, but storage is still a problem, both during the computation and for later archiving of "fields" of raw data at selected timesteps.

Table 8.1: *Grid Point/Timestep Requirements for Channel-Flow DNS and LES.*

Re_H	Re_τ	N_{DNS}	DNS Timesteps	N_{LES}
$1.23 \cdot 10^4$	360	$6.7 \cdot 10^6$	32000	$6.1 \cdot 10^5$
$3.08 \cdot 10^4$	800	$4.0 \cdot 10^7$	47000	$3.0 \cdot 10^6$
$6.16 \cdot 10^4$	1450	$1.5 \cdot 10^8$	63000	$1.0 \cdot 10^7$
$2.30 \cdot 10^5$	4650	$2.1 \cdot 10^9$	114000	$1.0 \cdot 10^8$

The computations of Kim, Moin and Moser (1987) provide an example of the computer resources required for DNS of the geometrically simple case of channel flow. To demonstrate grid convergence of their methods, they compute channel flow with $Re_\tau = 180$, corresponding to $Re_H \approx 6000$ using grids with $2 \cdot 10^6$ and $4 \cdot 10^6$ points. For the finer grid, the CPU time on a Cray X/MP supercomputer was 40 seconds per timestep. The calculation was run for a total time $5H/u_\tau$, and required 250 CPU hours. The same computation would take about 100 CPU hours on a 3-GHz Pentium-D personal computer (see problems section).

Both second-order accurate and fourth-order accurate numerical algorithms have been used in DNS research to advance the solution in time. There are two primary concerns regarding numerical treatment of the spatial directions. The

first is achieving accurate representations of derivatives, especially at the smallest scales (or, equivalently, the highest wavenumbers). Spectral methods — Fourier series in the spatial directions — can be used to insure accurate computation of derivatives. Finite-difference methods usually underestimate derivatives of a given velocity field, leading to inaccuracies in the smallest (dissipating) scales. The dissipation as such is set by the rate of energy transfer from the larger eddies, so the underestimated derivatives are compensated by an excess in spectral density at the highest wavenumbers to achieve the right value for the dissipation as expressed by the right-hand side of Equation (4.6). This is usually just called "numerical dissipation," but is in no sense an addition to the dissipation rate set by the energy transfer.

Thus, the first concern in demonstrating grid convergence of a DNS is to verify that the energy spectrum, $E(\kappa)$, displays a rapid decay, often referred to as the **rolloff**, near the Kolmogorov length scale, η. The second concern is to avoid a phenomenon known as **aliasing**. This occurs when nonlinear interactions among the resolved wavenumbers produce waves with wavenumbers greater than κ_{max}, which can be misinterpreted numerically. If special precautions are not taken, this can result in a spurious transfer of energy to small wavenumbers [Ferziger (1976)].

While spectral methods are more accurate for computing derivatives at the smallest scales, they are difficult to use with arbitrarily nonuniform grids. Because of the wish to extend DNS and LES to more realistic geometries, bringing the need for more complicated grids, there has been a general swing towards finite-difference methods, but a higher order of accuracy is needed than for spectral methods. Unstructured grids, now well established in conventional CFD [e.g., Venkatakrishnan (1996)], are being introduced into DNS and LES for complicated geometries, but they carry a further penalty in storage and CPU time.

In their grid-convergence study, Kim, Moin and Moser (1987) show that their energy spectra display the characteristic rolloff approaching wavenumber $\kappa \approx 1/\eta$ where η is the Kolmogorov length scale. This corresponds to a wavelength of $2\pi\eta \approx 6\eta$, roughly the top of the dissipating range.

The primary difficulty with boundary conditions in any Navier-Stokes calculation, DNS, LES, DES or Reynolds-averaged, is at open boundaries. Because of the elliptic nature of the problem, the flow at such boundaries depends on the unknown flow outside the computational domain. In LES and DNS this problem is circumvented by imposing periodic boundary conditions for directions in which the flow is statistically homogeneous (e.g., the streamwise and spanwise directions in channel flow). Most simulations done to date have been homogeneous or periodic in at least one spatial direction, which has the additional advantage that statistics can be obtained by averaging over the homogeneous direction as well as over time, thus reducing the time sample needed to get converged statistics.

Flows that grow in the streamwise direction in a nearly self-similar manner (e.g., equilibrium boundary layers) can be reduced to approximate homogeneity by a coordinate transformation [Spalart (1986, 1988, 1989)]. Alternatives are to use the results of a previous simulation to give the incoming flow at the upstream boundary [Le, Moin and Kim (1997)] or use a suitably-rescaled version of the outgoing flow at the downstream boundary [the "fringe" method of Spalart; see Bertolotti et al. (1992)]. Finally one can add a synthetic random fluctuating velocity field to a prescribed mean-velocity field. After a few eddy-turnover times, the correct statistics evolve, but this may correspond to an unacceptably large downstream distance.

In nonperiodic flows the downstream boundary condition is usually taken as zero streamwise gradient of all variables. This is acceptable if the statistics of the real flow are changing slowly in the streamwise direction, because this implies negligible upstream influence — usually equivalent to validity of the boundary-layer approximation, which leads to parabolic equations.

Solid boundaries, where the no-slip velocity boundary condition applies, pose no special problems for DNS.

DNS results illustrate one of the curious features of turbulence and other chaotic systems. Suppose we generate a solution from a given set of initial conditions, and then repeat the computation with a very small perturbation in the initial conditions. We find that, after a few eddy-turnover times, the second solution, or **realization**, is very different from the first. However, in terms of all statistical measures, the two flows are identical! This is the classical problem of **predictability** discussed, for example, by Sandham and Kleiser (1992) (see also Section 8.5). It is a real phenomenon and has nothing to do with numerical error. Also, it occurs in everyday life, although usually with finite initial perturbations.

As a simple example, two strangers in a crowd, initially side by side, tend to drift apart — that is, a small difference in initial position tends to grow indefinitely, and the standard deviation of the difference, averaged over many trials, certainly grows. The public recognizes this in an empirical way: if one stranger steps on another's foot *twice*, the steppee is likely to suspect the stepper of doing it on purpose. Thus, while somewhat disconcerting to the mathematician, this phenomenon should come as no great surprise to the engineer.

DNS matured rapidly during the 1980's and continues to develop as more and more powerful computers appear. Although Reynolds numbers are usually well below those found in most branches of engineering, recent applications for simple geometries have been done for ever-increasing Reynolds numbers. Abe and Kawamura (2001), for example, have done channel-flow simulations for $Re_H = 2.4 \cdot 10^4$, which is nearly double the value achieved by Mansour, Kim and Moin in 1988. DNS data are currently available for many flows of interest to turbulence researchers (from the NASA Ames Research Center, for example), and the list of applications continues to grow.

8.3 Large Eddy Simulation

A Large Eddy Simulation, or LES for short, is a computation in which the large eddies are computed and the smallest, **subgrid-scale (SGS)**, eddies are modeled. The underlying premise is that the largest eddies are directly affected by the boundary conditions, carry most of the Reynolds stress, and must be computed. The small-scale turbulence is weaker, contributing less to the Reynolds stresses, and is therefore less critical. Also, it is more nearly isotropic and has nearly-universal characteristics; it is thus more amenable to modeling. Recent reviews are rapidly proliferating, including Ferziger (1996), Lesieur and Metais (1996), Rodi (1997, 1998), Ghosal (1999), Jiménez and Moser (2000) and Pitsch (2006) [focusing on combusting flows]. The comprehensive text by Sagaut and Germano (2004) is devoted entirely to LES.

Because LES involves modeling the smallest eddies, the smallest finite-difference cells can be much larger than the Kolmogorov length, and much larger timesteps can be taken than are possible in a DNS. Hence, for a given computing cost, it is possible to achieve much higher Reynolds numbers with LES than with DNS, or conversely to obtain a solution at a given Reynolds number more cheaply. See Table 8.1 for a comparison of estimated DNS and LES grid point requirements in a simple flow. An actual example, for a more complex flow, is comparison of calculations of the flow over a backward-facing step by DNS [Le, Moin and Kim (1997)] and by LES [Akselvoll and Moin (1993)], both at the low Reynolds number of 5000 based on step height. The LES required 3% of the number of grid points needed for the DNS and the computer time was 2% of that for the DNS: agreement with experiment was equally good.

Aside from the issue of the need to resolve the smallest eddies, the comments regarding DNS numerics, boundary and initial conditions in the previous section hold for LES as well. The primary issue in accuracy remains that of computing derivatives for the smallest scales (highest wavenumbers) resolved. The ultimate test of grid convergence is again the requirement that excessive energy must not accumulate in the smallest scales. The primary requirement is to get the dissipation rate right; details of the dissipating eddies are unimportant in LES. DNS nominally requires accurate simulation of the dissipating eddies, and the achievement of this in the classical channel simulation of Kim, Moin and Moser (1987) is verified by the accuracy of the dissipation-rate budget evaluated by Mansour, Kim and Moin (1988). However, marginally-resolved DNS often includes some numerical dissipation. If spectral or pseudo-spectral methods are used, the same boundary-condition difficulties hold in both DNS and LES.

A major difficulty in "Large" Eddy Simulation is that near a solid surface all eddies are small — to the extent that the stress-bearing and dissipation ranges of eddy size overlap. If one requires LES to resolve most of the stress-bearing range, the grid spacing, and timestep, required by LES gradually fall towards that

needed for full DNS as the surface is approached. This is, of course, a serious limitation on Reynolds number for LES, and later we will discuss the ways in which it can be avoided.

8.3.1 Filtering

To understand the primary difference between DNS and LES, we must introduce the concept of **filtering**. Note first that the values of flow properties at discrete points in a numerical simulation represent averaged values. To see this explicitly, consider the central-difference approximation for the first derivative of a continuous variable, $u(x)$, in a grid with points spaced a distance h apart. We can write this as follows.

$$\frac{u(x+h)-u(x-h)}{2h} = \frac{d}{dx}\left[\frac{1}{2h}\int_{x-h}^{x+h} u(\xi)\,d\xi\right] \tag{8.17}$$

This shows that the central-difference approximation can be thought of as an operator that **filters out scales smaller than the mesh size**. Furthermore, the approximation yields the derivative of an averaged value of $u(x)$.

There are many kinds of filters that can be used. The simplest type of filter is the **volume-average box filter** implemented by Deardorff (1970), one of the earliest LES researchers. The filter is

$$\overline{u}_i(\mathbf{x},t) = \frac{1}{\Delta^3}\int_{x-\frac{1}{2}\Delta x}^{x+\frac{1}{2}\Delta x}\int_{y-\frac{1}{2}\Delta y}^{y+\frac{1}{2}\Delta y}\int_{z-\frac{1}{2}\Delta z}^{z+\frac{1}{2}\Delta z} u_i(\boldsymbol{\xi},t)\,d\xi d\eta d\zeta \tag{8.18}$$

The quantity $\overline{u}_i$ denotes the **resolvable-scale filtered velocity**. The **subgrid-scale (SGS)** velocity, u_i', and the **filter width**, Δ, are given by

$$u_i' = u_i - \overline{u}_i \qquad \text{and} \qquad \Delta = (\Delta x \Delta y \Delta z)^{1/3} \tag{8.19}$$

Leonard (1974) defines a generalized filter as a convolution integral, viz.,

$$\overline{u}_i(\mathbf{x},t) = \iiint G(\mathbf{x}-\boldsymbol{\xi};\Delta)\,u_i(\boldsymbol{\xi},t)\,d^3\boldsymbol{\xi} \tag{8.20}$$

The **filter function**, G, is normalized by requiring that

$$\iiint G(\mathbf{x}-\boldsymbol{\xi};\Delta)\,d^3\boldsymbol{\xi} = 1 \tag{8.21}$$

In terms of the filter function, the volume-average box filter as defined in Equation (8.18) is

$$G(\mathbf{x}-\boldsymbol{\xi};\Delta) = \begin{cases} 1/\Delta^3, & |x_i-\xi_i| < \Delta x_i/2 \\ 0, & \text{otherwise} \end{cases} \tag{8.22}$$

The Fourier transform of Equation (8.20) is $\overline{U}_i(\kappa, t) = \mathcal{G}(\kappa)\mathcal{U}_i(\kappa, t)$ where $\mathcal{U}_i$ and $\mathcal{G}$ represent the Fourier transforms of u_i and G. Fourier spectral methods implicitly filter with

$$\mathcal{G}(\kappa; \Delta) = 0 \qquad \text{for} \qquad |\kappa| > \kappa_{max} = 2\pi/\Delta \tag{8.23}$$

As an example, Orszag et al. [see Ferziger (1976)] use the **Fourier cutoff filter**, i.e.,

$$G(\mathbf{x} - \boldsymbol{\xi}; \Delta) = \frac{1}{\Delta^3} \prod_{i=1}^{3} \frac{\sin(x_i - \xi_i)/\Delta}{(x_i - \xi_i)/\Delta} \tag{8.24}$$

The **Gaussian filter** [Ferziger (1976)] is popular in LES research, and is defined by

$$G(\mathbf{x}\text{-}\boldsymbol{\xi}; \Delta) = \left(\frac{6}{\pi\Delta^2}\right)^{3/2} \exp\left(-6\,\frac{|\mathbf{x} - \boldsymbol{\xi}|^2}{\Delta^2}\right) \tag{8.25}$$

Many other filters have been proposed and used, some of which are neither isotropic nor homogeneous. In all cases however, the filter introduces a scale Δ that represents the smallest turbulence scale allowed by the filter.

The filter provides a formal definition of the averaging process and separates the **resolvable scales** from the **subgrid scales**. We use filtering to derive the **resolvable-scale equations**. For incompressible flow, the continuity and Navier-Stokes equations assume the following form.

$$\frac{\partial \overline{u}_i}{\partial x_i} = 0 \tag{8.26}$$

$$\frac{\partial \overline{u}_i}{\partial t} + \frac{\partial}{\partial x_j}\left(\overline{\overline{u}_i \overline{u}_j}\right) = -\frac{1}{\rho}\frac{\partial \overline{p}}{\partial x_i} + \nu \frac{\partial^2 \overline{u}_i}{\partial x_k \partial x_k} \tag{8.27}$$

Now, the convective flux is given by

$$\overline{u_i u_j} = \overline{u}_i \overline{u}_j + L_{ij} + C_{ij} + R_{ij} \tag{8.28}$$

where

$$\left.\begin{aligned} L_{ij} &= \overline{\overline{u}_i \overline{u}_j} - \overline{u}_i \overline{u}_j \\ C_{ij} &= \overline{\overline{u}_i u_j'} + \overline{\overline{u}_j u_i'} \\ R_{ij} &= \overline{u_i' u_j'} \end{aligned}\right\} \tag{8.29}$$

Note that, with the exception of the Fourier cutoff filter [Equation (8.24)], filtering differs from standard averaging in one important respect:

$$\overline{\overline{u}}_i \neq \overline{u}_i \tag{8.30}$$

i.e., a second averaging yields a different result from the first averaging. The tensors L_{ij}, C_{ij} and R_{ij} are known as the **Leonard stress, cross-term stress** and the **SGS Reynolds stress**, respectively.

Leonard (1974) shows that the Leonard-stress term removes significant energy from the resolvable scales. It can be computed directly and need not be modeled. This is sometimes inconvenient, however, depending on the numerical method used. Leonard also demonstrates that since $\overline{u}_i$ is a smooth function, L_{ij} can be computed in terms of its Taylor-series expansion, the first term of which is

$$L_{ij} \approx \frac{\gamma_\ell}{2}\nabla^2\left(\overline{u}_i\overline{u}_j\right), \qquad \gamma_\ell = \iiint |\boldsymbol{\xi}|^2 G(\boldsymbol{\xi})\, d^3\boldsymbol{\xi} \tag{8.31}$$

Clark et al. (1979) verify that this representation is very accurate, at low Reynolds number, by comparing with DNS results. However, as shown by Shaanan, Ferziger and Reynolds (1975), the Leonard stresses are of the same order as the truncation error when a finite-difference scheme of second-order accuracy is used, and they are thus implicitly represented.

The cross-term stress tensor, C_{ij}, also drains significant energy from the resolvable scales. An expansion similar to Equation (8.31) can be made for C_{ij}. However, most current efforts model the sum of C_{ij} and R_{ij}. Clearly, the accuracy of a LES depends critically upon the model used for these terms.

We can now rearrange Equation (8.27) into a more conventional form,[1] i.e.,

$$\frac{\partial\overline{u}_i}{\partial t} + \frac{\partial}{\partial x_j}\left(\overline{u}_i\overline{u}_j\right) = -\frac{1}{\rho}\frac{\partial P}{\partial x_i} + \frac{\partial}{\partial x_j}\left[\nu\frac{\partial\overline{u}_i}{\partial x_j} + \tau_{ij}\right] \tag{8.32}$$

where

$$\left.\begin{aligned} \tau_{ij} &= -\left(Q_{ij} - \tfrac{1}{3}Q_{kk}\delta_{ij}\right) \\ P &= \overline{p} + \tfrac{1}{3}\rho Q_{kk}\delta_{ij} \\ Q_{ij} &= R_{ij} + C_{ij} \end{aligned}\right\} \tag{8.33}$$

At this point, **the fundamental problem of Large Eddy Simulation** is evident. Specifically, we must establish a satisfactory model for the SGS stresses as represented by the tensor Q_{ij}. To emphasize the importance of achieving an accurate SGS stress model, consider the following. In simulating the decay of homogeneous isotropic turbulence with $16^3 = 4096$ and $32^3 = 32768$ grid points, Ferziger (1976) reports that the SGS turbulence energy is 29% and 20%, respectively, of the total. Thus, the subgrid scales constitute a significant portion of the turbulence spectrum. The various attempts at developing a satisfactory SGS stress model during the past half century resemble the research efforts on

[1] Most LES practitioners reverse the sign of τ_{ij}. The notation chosen here is strictly for consistency with the rest of the text

engineering models discussed in Chapters 3 – 6. That is, models have been postulated that range from a simple gradient-diffusion model [Smagorinsky (1963)], to a one-equation model [Lilly (1966)], to the analog of a second-order closure model [Deardorff (1973)]. Nonlinear stress-strain rate relationships have even been postulated [Bardina, Ferziger and Reynolds (1983)]. Only the analog of the two-equation model appears to have been overlooked, most likely because the filter width serves as a readily-available length scale.

8.3.2 Subgrid-Scale (SGS) Modeling

Smagorinsky (1963) was the first to postulate a model for the SGS stresses. The model assumes the SGS stresses follow a gradient-diffusion process, similar to molecular motion. Consequently, τ_{ij} is given by

$$\tau_{ij} = 2\nu_T S_{ij}, \qquad S_{ij} = \frac{1}{2}\left(\frac{\partial \overline{u}_i}{\partial x_j} + \frac{\partial \overline{u}_j}{\partial x_i}\right) \tag{8.34}$$

where S_{ij} is called the "resolved strain rate," ν_T is the **Smagorinsky eddy viscosity**

$$\nu_T = (C_S\Delta)^2\sqrt{S_{ij}S_{ij}} \tag{8.35}$$

and C_S is the Smagorinsky coefficient. Note that Equation (8.35) is akin to a mixing-length formula with mixing length $C_S\Delta$. Obviously the grid scale Δ, or $(\Delta_1\Delta_2\Delta_3)^{1/3}$ if the steps in the three coordinate directions are different, is an overall scale of the SGS motion, but assuming it to be a unique one is clearly crude. If Δ were in the inertial subrange of eddy size in which Equation (8.12) holds, and sufficiently larger than the Kolmogorov viscous length scale η that the viscous-dependent part of the SGS motion was a small fraction of the whole, then no other length scale would be relevant and the Smagorinsky constant would be universal. This is rarely the case.

For all of the reasons discussed in Chapter 3, the physical assumption behind the mixing-length formula, that eddies behave like molecules, is simply not true. Nevertheless, just as the mixing-length model can be calibrated for a given class of flows, so can the Smagorinsky coefficient, C_S. Its value varies from flow to flow, and from place to place within a flow. In the early days of LES, the basic Smagorinsky subgrid-scale model was widely used, C_S being adjusted to get the best results for each flow [see e.g. Rogallo and Moin (1984) who quote a range $0.10 < C_S < 0.24$]. In the critical near-wall region, law-of-the-wall arguments — valid in well-behaved flows — suggest that C_S should be a function of Δ/y and an increasingly strong function of $u_\tau y/\nu$ as the latter decreases. However there seems to be no record of attempts to calibrate this function: virtually all users of the basic model keep C_S constant throughout the flow.

There are two key reasons why the basic Smagorinsky model enjoys some degree of success. First, the model yields sufficient diffusion and dissipation to stabilize the numerical computations. Second, low-order statistics of the larger eddies are usually insensitive to the SGS motions.

In an attempt to incorporate some representation of the dynamics of the subgrid scales, Lilly (1966) postulates that

$$\nu_T = C_L \Delta q \tag{8.36}$$

where q^2 is the SGS kinetic energy, and C_L is a closure coefficient. The subgrid-scale stress anisotropy now depends on the sign of the resolved strain rate, rather than on its magnitude as in the Smagorinsky formula. An equation for q^2 can be derived from a moment of the Navier-Stokes equation, which involves several terms that must be modeled. This model is very similar to Prandtl's one-equation model (Section 4.2), both in spirit and in results obtained. As pointed out by Schumann (1975) who used the model in his LES research, it is difficult to conclude that any significant improvement over the Smagorinsky model can be obtained with such a model.

Germano et al. (1991) [see also Ghosal et al. (1995), Yang and Ferziger (1993) and Carati and Eijnden (1997) for later developments], proposed what is known as a **Dynamic SGS Model**. Their formulation begins with the Smagorinsky eddy-viscosity approximation. However, rather than fixing the value of C_S a priori, they permit it to be computed as the LES proceeds. This is accomplished by using two filters, the usual LES filter at $\kappa = \kappa_{max}$ and the "test filter" which examines the resolved fluctuations between some lower wavenumber, usually $\kappa_{max}/2$, and κ_{max} itself. Then, the subgrid stresses are represented by rescaling the resolved stresses in the test-filter band. Usually, this is done by evaluating the Smagorinsky coefficient, C_S, from the resolved fluctuations in the test-filter band, and then using the same coefficient to evaluate the SGS stresses at the same point in space on the next timestep, for example. This "bootstrap" procedure could be rigorously justified on the same grounds as for the Smagorinsky formula, above. The test-filter band would have to lie in the inertial subrange and κ_{max} would have to be far below the viscous region.

Dynamic models undoubtedly work surprisingly well, even in cases where rigorous justification is not valid. Jiménez (1995) points out that the essential feature of an SGS model is to dissipate the kinetic energy cascaded down to it. Jiménez and Moser (2000) elaborate further on the efficacy of dynamic models. On the one hand, any eddy-viscosity model assumes the subgrid stresses are "perfectly related" to the strain rate, even though they are essentially uncorrelated. On the other hand, dynamic models are "very robust" to this fundamental error in physics, largely because "the formula for their eddy viscosity contains a sensor that responds to the accumulation of energy in the high wave numbers of the spectrum before it contaminates the energy containing range."

The dynamic-model concept has been implemented with intrinsically more realistic models than Smagorinsky's. Pomraning and Rutland (2002) and Krajnović and Davidson (2002), for example, have done computations with the dynamic one-equation model devised by Menon and Kim (1996). The equation they use is loosely based on the subgrid kinetic energy.

However, it is clear that, whatever SGS model is used, the *test-filter* concept implies that the structure of the SGS turbulence is similar to that in the test-filter band, which will not be the case when the local turbulence Reynolds number, Re_T, is small, as it is near a solid surface. Unfortunately, this is the most critical region for an SGS model. Unless the LES is to collapse into DNS, the SGS model must carry a significant portion of the Reynolds stresses.

It is a symptom of the inadequacy of the Smagorinsky mixing-length formula that dynamic-model values of C_S evaluated from the calculated motion in the test-filter band fluctuate wildly in space and time. "Dynamic" is all too apt a name for this model when used with the Smagorinsky formulation. A particular difficulty arising from this is that if the implied eddy viscosity is negative, kinetic energy can be transferred from the SGS motion to the resolved scales. This is, in principle, the real-life phenomenon of **backscatter**, i.e., reverse cascading of energy from smaller to larger eddies. The statistical-average energy transfer at high wavenumber is always towards the dissipating range, but this is not true instantaneously. However, negative eddy viscosity usually leads to instability of the calculation because there is nothing in the Smagorinsky formula to limit the depletion of SGS kinetic energy. A simple fix is to average C_S over a direction of homogeneity of the flow. As an alternative, Ghosal et al. (1995) and others have modeled an equation for SGS kinetic energy and used it to cut off the SGS eddy viscosity when the SGS energy falls to zero.

A subgrid-scale model with some general similarities to the dynamic model has been suggested by Domaradzki and Saiki (1997). The resolved motion is interpolated on a length scale of half the grid size, and the phases of the resulting subgrid modes are adjusted to correspond to the phases of the subgrid modes that would be generated (in a DNS) by nonlinear interactions of the resolved modes in the LES. This "bootstrap" procedure seems to be rigorously justifiable and initial results are promising.

8.3.3 "Off the Wall" Boundary Conditions

If LES is to be applied to wall flows at indefinitely high Reynolds numbers, the *viscous sublayer* or *viscous wall region* (typically $u_\tau y/\nu < 30$ — see Figure 1.7) must be excluded from the main computation. Moreover, the distance of the first LES grid point from the solid surface at $y = y_2$ must be independent of Reynolds number. It must be set at some suitable fraction of the shear-layer thickness, δ, so that the total number of grid points is also independent of Reynolds number.

We use y_2 to denote the first LES point from the wall for conformity with the rest of the book, irrespective of the arrangements $y < y_2$. If the first grid point is set at a given value of $u_\tau y/\nu$ and if, as usual, the y step increases proportional to y, the number of grid points required in the y direction increases proportional to $\ell n \delta^+$ where $\delta^+ = u_\tau \delta/\nu$ is the sublayer-scaled flow width (see problems section). This implies that the computer work required (number of grid points in the three-dimensional domain divided by timestep) will vary as $(\ell n \delta^+)^4$ approximately. Thus, a factor of 10 increase in Reynolds number means a factor of 30 increase in computer work.

Allowing the SGS model to bear more and more of the Reynolds stresses as the wall is approached [Speziale (1998)] does not remove the Reynolds-number dependence of the grid-point count. This is so even if the SGS model limits to a reliable *Reynolds-Averaged Navier Stokes* (RANS) model for a coarse mesh. The mesh must still be graded, so the number of points needed in the y direction is still proportional to $\ell n \delta^+$, with a different proportionality constant, even for full RANS calculations. For example, in Spalart's (1988) boundary-layer DNS, $u_\tau y_2/\nu$ is between 0.2 and 0.3, while most low-Reynolds-number RANS models require $u_\tau y_2/\nu < 1$. So, there is not usually an order-of-magnitude difference between the number of points in the y direction for simulations and for RANS calculations (RANS models can of course use much larger steps in x and z).

The current fashion in RANS modeling is integration to the wall rather than the use of off-the-wall boundary conditions (*wall functions* in RANS modeling terminology). For the geometrical-progression grid with **grading ratio**, $k_g = 1.14$ and $y_2^+ < 1$ recommended for typical computations with Program **EDDYBL** (see Appendix C), about 50 points are needed up to $y = \delta$ at momentum-thickness Reynolds number 1410 ($\delta^+ = 650$). The number increases by 17-18 points for every factor of 10 increase in δ^+. Spalart's DNS at this Reynolds number used 62 points up to $y = \delta$.

Note also that the above discussion is phrased, qualitatively at least, in "law-of-the-wall" language. However, if LES is to be a significant improvement on RANS models, it must deal with strongly-nonequilibrium flows, notably separated flows, in which the simple law of the wall is not valid. Indeed the status of the law of the wall is uncertain even in moderately three-dimensional boundary layers.

The earliest LES of a "laboratory" flow [Deardorff (1970)] used the logarithmic law of the wall for the mean velocity as an instantaneous boundary condition. This crude approach was followed by other early workers. However, experiments by Robinson (1986) showed that the instantaneous friction velocity is not a good scale for the instantaneous velocity in the logarithmic region.

If LES is to be applied to high-Reynolds-number engineering flows, not only must the "wall" boundary condition be applied at a distance y_2 from the surface which is a (not-too-small) fraction of δ, but any calculation for the region

$0 < y < y_2$ should be Reynolds-number independent. Quantitative use of law-of-the-wall concepts is not acceptable in the long term. For most purposes, details of the flow in $0 < y < y_2$ will not be important as long as the surface-flux rates (of momentum, heat and possibly mass) can be related to those at $y = y_2$.

Piomelli, Yu and Adrian (1996), Cabot (1997) and Baggett (1997) have studied "off the wall" boundary conditions. On the one hand, used with care, the instantaneous log law works satisfactorily for simple flows. On the other hand, Cabot found it to be unsatisfactory for separated flows such as the backward-facing step (where the law of the wall does not apply).

8.3.4 Applications

Estimates for the numbers of grid points, and computing times, needed for LES calculations of, say, the flow over a complete aircraft [e.g., Spalart et al. (1997), Moin and Kim (1997)] lie far beyond the capability of current computers, even if one assumes that a satisfactory "off the wall" boundary condition can be found. However, current Reynolds-averaged models perform acceptably well in two-dimensional or mildly three-dimensional boundary layers not too close to separation — that is, in most of the turbulent flow over an aircraft. Something better is needed in critical areas, such as wing-body junctions, tip vortices and separated flows. If LES is to be used in such areas, patched to a Reynolds-averaged calculation for the rest of the flow, some means is needed for providing time-dependent boundary conditions at the upstream end, and the sides, of the LES computational domain. This may involve enlarging the LES domain so that it considerably overlaps the region of reliable Reynolds-averaged prediction, imposing rough-and-ready boundary conditions at the edges of this domain, and then rescaling the LES in some way so that its statistics match those of the Reynolds-averaged model on the boundary of reliability of the latter. Spalart et al. (1997) suggest **Detached Eddy Simulation** or DES, combining Reynolds-averaged models in the boundary layers and coarse-mesh LES after a massive separation. We will discuss this approach in the next section.

Other engineering applications are less demanding than aircraft in terms of Reynolds number, but may be more demanding in terms of complex flow patterns. LES is likely to be applied first to internal flows.

Combustion is notoriously difficult to model at the Reynolds-averaged level, and fine-mesh DNS with the large number of species equations required for a realistic combustion model is currently out of the question for engineering use. Therefore, there is some interest in LES for combustion. Clearly the subgrid-scale model has to reproduce the statistics of fine-scale mixing of reactants, leading to the essentially molecular diffusion that finally brings the reactants together, and this seems a very severe requirement. Veynante and Poinsot (1997) and Pitsch (2006) review recent LES studies of combusting flows.

Two-phase flows [see Crowe et al. (1996) for a review] are central to many processes in technology and nature, from combustion of droplets or particles to cloud physics and bubble flows in fluidized-bed reactors. Several DNS studies have been reported. LES, with the need to add subgrid-scale motion of particles or bubbles to the larger-scale computed trajectories, is a longer-term prospect. Wang and Squires (1996) report good agreement between LES and DNS.

Compressible flow and heat transfer present no special difficulties to LES except for the presence of more equations to solve. Extension of subgrid-scale models to variable-density flows is straightforward and true compressibility effects in the weak small-scale motion are likely to be negligible. The review by Knight et al. (2003) includes results of LES applications to flows that include shock-induced boundary-layer separation. Figure 8.2 (a), for example, shows the convoluted shape of the shock wave for Mach 2.88 flow into a 25° compression corner. Figure 8.2 (b) shows results for an expansion followed by a compression, again at Mach 2.88. Despite having a Reynolds number in the LES that is significantly lower than in the experiments, computed and measured mean surface pressures are reasonably similar. The close agreement in this case is very likely due to the fact that this flow is remarkably insensitive to Reynolds number.

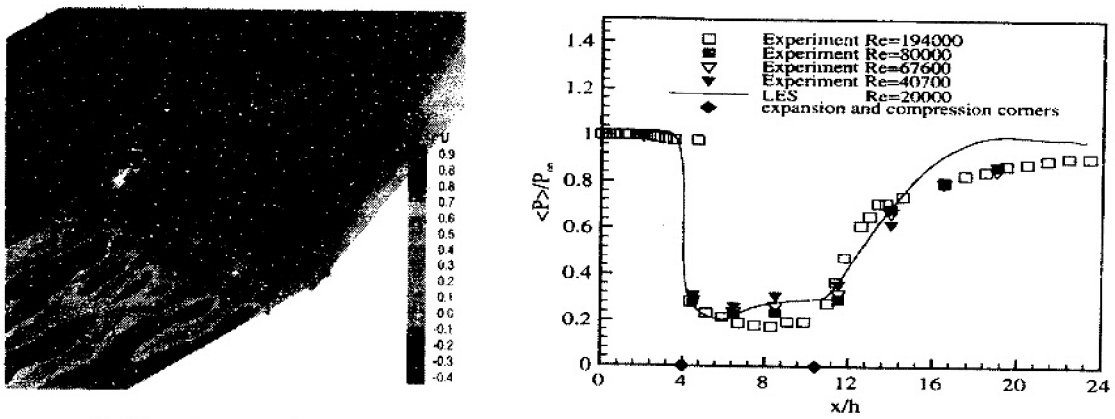

(a) Flow into a 25° corner: Instantaneous shock structure

(b) Flow through an expansion followed by a compression: Surface pressure

Figure 8.2: *Results of LES applications to Mach 2.88 compression-corner flows. [Figure provided by D. D. Knight.]*

In conclusion, LES holds promise as a future design tool, especially as computers continue to increase in speed and memory. Intense efforts are currently focused on devising a satisfactory SGS stress model, which is the primary deficiency of the method at this time. Even if LES is too expensive for modern design efforts, results of LES research can certainly be used to help improve engineering models of turbulence. The future of LES research appears very bright.

8.4 Detached Eddy Simulation

Spalart et al. (1997) introduced the Detached Eddy Simulation (DES) method as a cost-effective procedure that treats the largest eddies through a conventional LES, while handling boundary layers and thin shear layers with the conventional RANS approach. In practice, cell spacing, Δ, in a DES is of the same order of magnitude as the boundary-layer thickness.

One way of viewing DES is as an extension of a standard turbulence model based on Reynolds averaging into more complex flows. This is made possible by computing the geometry-dependent, three-dimensional eddies whose details are lost in Reynolds-averaging. Another way of viewing a DES is as a method for resolving the difficult task of establishing "off-the-wall" boundary conditions, with the hope that the DES converges toward an LES as the grid is refined. The discussion of "DES-blending functions" below strongly suggests that the latter view is unrealistic for DES as currently implemented.

As with DNS and LES, accurate numerical methods are imperative, especially for the LES part of the computation. Constantinescu and Squires (2000), for example, use "fifth-order accurate, one-point biased differences" in treating the convective terms for the momentum and turbulence-transport equations, while using conventional second-order accurate differencing for all other terms. Accurate methods have been devised to treat both inflow [Xiao, Edwards and Hassan (2003a)] and outflow [Schlüter, Pitsch and Moin (2005)] conditions for DES applications.

The RANS part of the computation requires selection of a suitable turbulence model. Most studies to date have been done with the Spalart-Allmaras (1992) one-equation model, a k-ω model or the Robinson et al. (1995) k-ζ (enstrophy) model.

8.4.1 DES-Blending Functions

A crucial ingredient in the DES methodology is the way the computation differentiates between the RANS and LES portions of the computation. Roughly speaking, we have two critical length scales. One is the effective turbulence length scale implied by the model, ℓ_{RANS}, i.e.,

$$\ell_{RANS} = \sqrt{k}/\omega \tag{8.37}$$

The other is the local finite-difference cell size, Δ, so that

$$\ell_{LES} = \Delta \tag{8.38}$$

Cells in which $\ell_{RANS} < \ell_{LES}$ are treated as part of the "subgrid" and deemed unresolvable. The hybrid RANS model is used as an effective subgrid scale (SGS) model.

The way in which we distinguish the appropriate length scale and computational mode (RANS or LES) is called blending. Although the terminology has been adopted by DES researchers, it holds potential for confusion. That is, the nomenclature "blending functions" was originally used to make k-ω model closure coefficients vary from one set of values near a solid boundary to another set near turbulent/nonturbulent interfaces [cf. Menter (1992c) or Hellsten (2005)]. To avoid confusion here, we will refer to "DES-blending functions."

The most popular way of blending in current usage is to modify the dissipation term in the RANS model. For the Spalart-Allmaras model, this means the equation for the working variable, $\tilde{\nu}$, which is proportional to the eddy viscosity, ν_T, is written as (see Section 4.2)

$$\begin{aligned} \frac{\partial \tilde{\nu}}{\partial t} + U_j \frac{\partial \tilde{\nu}}{\partial x_j} &= c_{b1} \tilde{S} \tilde{\nu} - c_{w1} f_w \left(\frac{\tilde{\nu}}{\tilde{d}} \right)^2 + \frac{c_{b2}}{\sigma} \frac{\partial \tilde{\nu}}{\partial x_k} \frac{\partial \tilde{\nu}}{\partial x_k} \\ &+ \frac{1}{\sigma} \frac{\partial}{\partial x_k} \left[(\nu + \tilde{\nu}) \frac{\partial \tilde{\nu}}{\partial x_k} \right] \end{aligned} \tag{8.39}$$

In the original Spalart-Allmaras model, the quantity $\tilde{d}$ is the distance to the nearest surface, d. For DES applications, $\tilde{d}$ is defined by

$$\tilde{d} \equiv \min(d, C_{DES} \Delta) \tag{8.40}$$

where Δ is the size of the smallest resolvable scale. Also, $C_{DES} = 0.65$ is a closure coefficient whose value has been determined by results of homogeneous turbulence computations.

In a similar spirit, most researchers rewrite the turbulence kinetic energy equation of the k-ω model as

$$\begin{aligned} \frac{\partial k}{\partial t} + U_j \frac{\partial k}{\partial x_j} &= \tau_{ij} \frac{\partial U_i}{\partial x_j} - (1 - \Gamma) \beta^* k \omega - \Gamma C_d \frac{k^{3/2}}{\Delta} \\ &+ \frac{\partial}{\partial x_j} \left[(\nu + \sigma^* \nu_T) \frac{\partial k}{\partial x_j} \right] \end{aligned} \tag{8.41}$$

The constant $C_d = 0.01$ and the function Γ have been introduced to effect the DES-blending. Xiao, Robinson and Hassan (2004) use a similar procedure with their k-ζ model in which ζ is the modeled enstrophy of the turbulence. They also include the function Γ in the equation for the eddy viscosity according to

$$\nu_T = (1 - \Gamma) \frac{k}{\omega} + \Gamma C_s \sqrt{k}\, \Delta \tag{8.42}$$

where $C_s = 0.01$ is a closure coefficient. As we will see below, the function Γ has a strong effect on turbulence-model predictions.

It is a straightforward exercise to demonstrate that, when production balances dissipation in either of these models, the eddy viscosity simplifies to an effective Smagorinsky-type model, viz.,

$$\nu_T = C_S \Delta^2 |S|, \qquad S = \sqrt{2 S_{ij} S_{ij}} \tag{8.43}$$

where C_S is an effective Smagorinsky coefficient that depends on the turbulence model's closure coefficients.

Ideally, the DES-blending procedure would have little impact on a RANS model's predictions in regions where the RANS model yields flow-property values that are in reasonably close agreement with measurements. The recent study by Xiao, Edwards and Hassan (2004) provides an example of how a DES is capable of corrupting a very good RANS solution. In their study, they assess three different DES-blending functions to determine the effect on a DES for two computations of supersonic flow into a compression corner. The functions tested are all of the form

$$\Gamma = \tanh(\eta^2) \tag{8.44}$$

The three different DES-blending functions differ in the choice of the parameter η, viz.,

$$\eta = \begin{cases} \dfrac{\ell_{vk}}{25\lambda}, & \text{Von Karman}: \ \ell_{vk} = \dfrac{S}{|\nabla S|}, \ \ \lambda = \sqrt{\dfrac{k}{\zeta}} \\ \dfrac{d}{25\lambda}, & d = \text{Distance to the nearest surface} \\ \dfrac{\ell_\epsilon}{5\Delta}, & \text{Integral scale}: \ \ell_\epsilon = \dfrac{\mathrm{k}^{3/2}}{\nu\zeta} \end{cases} \tag{8.45}$$

The various lengths appearing in Equation (8.45) are the Von Kármán length, ℓ_{vk}, the Taylor microscale, λ, and the dissipation length, ℓ_ϵ.

Figures 8.3 (a) and (b) show the effect of Γ_{vk} and Γ_Δ (based on ℓ_{vk} and ℓ_ϵ, respectively) on computed surface pressure for the two compression-corner flows. Although not shown, the DES-blending function based on distance to the nearest surface produces inferior solutions. Ironically, DES results actually show greater discrepancies from measurements than the pure k-ζ model, especially over the separation bubble.

Xiao, Edwards and Hassan provide a clue to why, rather than providing an improved solution, the DES yields the opposite. The clue lies in the behavior of the eddy viscosity, which is shown in Figure 8.3 (c) for the 20° compression corner. As shown, all three DES-blending functions make the RANS eddy viscosity very small compared to the value it would have in a pure RANS computation for $y^+ > 500$, which is well below the boundary-layer edge. This is, of course, necessary to avoid polluting the LES part of the computation. However, there

is a steep price that has been paid. Specifically, the RANS model's solution is dramatically altered not only in the outer part of the boundary layer, but in the near-wall region as well. That is, use of the DES-blending function changes the RANS model in a way that defeats some of its strengths.

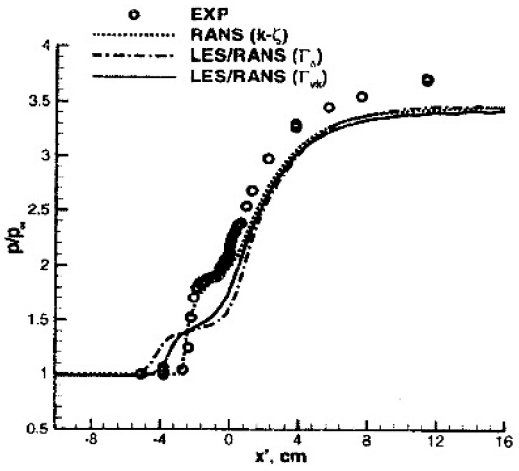

(a) Flow into a 20° corner: Mach 2.75

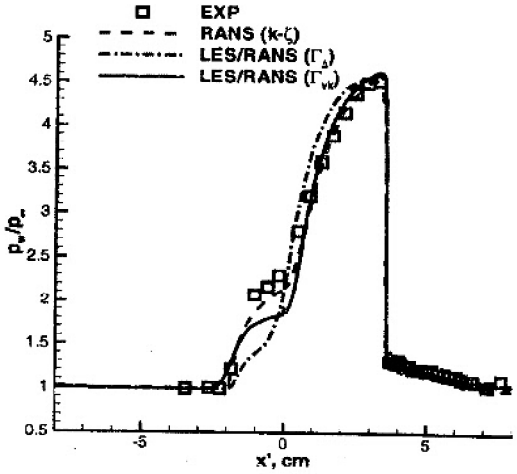

(b) Flow through a compression followed by an expansion: Mach 2.88

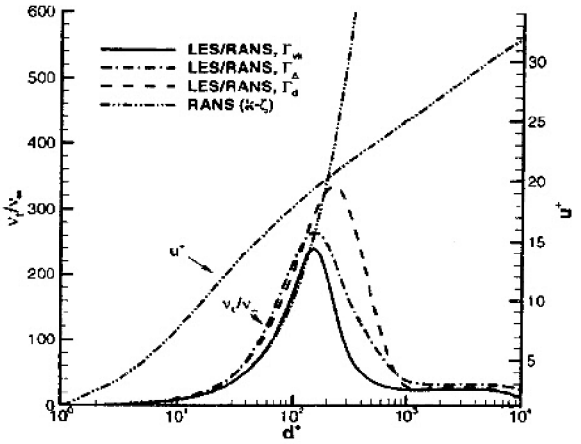

(c) 20° corner: Eddy Viscosity

Figure 8.3: *Results of DES applications to supersonic compression-corner flows. [From Xiao, Edwards and Hassan (2004) — Copyright © AIAA 2004 — Used with permission.]*

This problem was anticipated by Spalart et al. (1997), who warned that once the grid spacing becomes smaller than about half the boundary-layer thickness, the DES-limited eddy viscosity simultaneously corrupts the RANS model and precludes LES behavior. The net result is total Reynolds stresses that are representative of neither the RANS model nor the LES.

We can use Program **DEFECT** (see Appendix C) to illustrate the point. The following computations implement yet another DES-blending function, i.e., the one recommended by Menter [see Xiao, Edwards and Hassan (2000b)], viz.,

$$\Gamma = 1 - \tanh \eta^4 \tag{8.46}$$

where

$$\eta = \frac{\max(\tau_1, \tau_2)}{\omega}, \qquad \tau_1 = \frac{500\nu}{y^2}, \qquad \tau_2 = \frac{\sqrt{k}}{\beta^* y} \tag{8.47}$$

The quantity ν is kinematic molecular viscosity and y denotes distance normal to the surface. For the present analysis we are sufficiently far above the viscous sublayer that molecular viscosity is of negligible importance to the RANS model so that

$$\eta = \frac{\sqrt{k}/\omega}{\beta^* y} = \frac{1}{\beta^*} \frac{\ell_{RANS}}{y} \tag{8.48}$$

Figure 8.4 compares the computed wake-strength parameter, Π, with the baseline value of the Wilcox (1998) k-ω model for constant-pressure and adverse pressure gradient cases. The computations use the values of Γ and η defined in Equations (8.46) and (8.48). The alternative proposals for Γ in Equation (8.45) give results are similar to those presented in Figure 8.4.

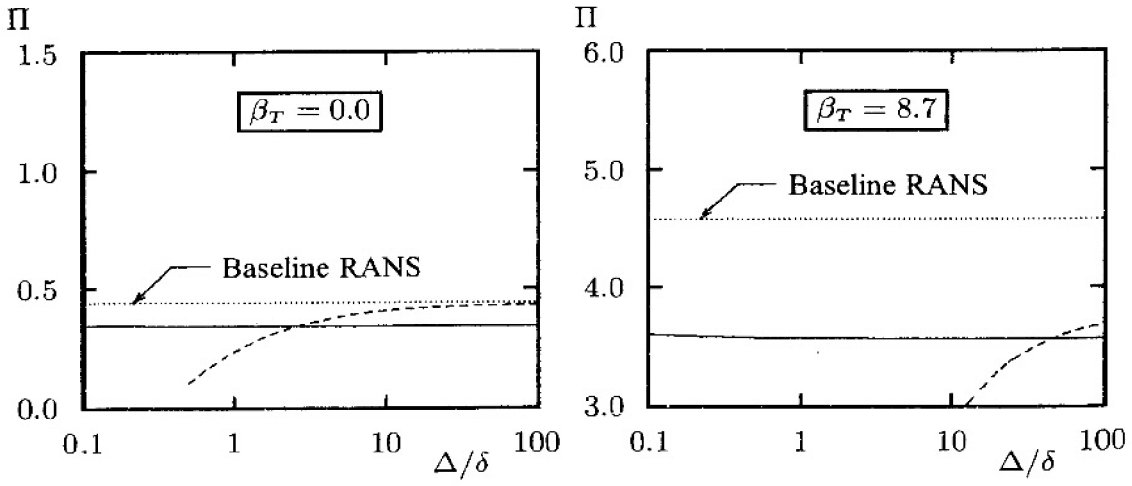

Figure 8.4: *Computed wake-strength parameter, Π, for the Wilcox (1998) k-ω two-equation RANS model; —— ν_T not modified, - - - ν_T modified.*

We obtain somewhat different results depending on whether or not Equation (8.42) is used to modify the kinematic eddy viscosity, ν_T. As shown, when we use Equation (8.42), the better the resolution of the flow, i.e., as Δ becomes smaller, the greater the distortion of the baseline model's predicted value for Π. When we use the value of ν_T as predicted by the RANS model, the k-ω model's

predictions are essentially insensitive to Δ. However, the computed value of Π lies far below the baseline k-ω model's solution even when Δ becomes very large compared to the entire boundary layer thickness! Although results are not included here, the Spalart-Allmaras model displays the same type of behavior.

This limitation on DES occurs because, until very recently, the RANS models used depend upon Δ. Spalart et al. (2006), by introducing an algebraic function to retain RANS within the boundary layer when $\Delta < \delta$, have suggested a remedy for this problem that they refer to as **Delayed Detached Eddy Simulation (DDES)**.

8.4.2 Applications

There is a growing list of successful DES applications to both research-oriented problems to very complicated industrial and military applications. Focusing first on a relatively simple research-oriented application, consider the flow on the base of a cylinder in a Mach 2.5 stream. Herrin and Dutton (1994) found experimentally that the pressure coefficient is nearly constant over the entire base region. By contrast, conventional RANS models predict a pressure coefficient, C_p, that varies with radial distance. Figure 8.5 compares computed and measured C_p for a DES based on the Spalart-Allmaras model [Forsythe et al. (2002)]. For reference, the figure includes results obtained with the Wilcox (1998) k-ω model, the Wilcox (1998) Stress-ω model and the RNG k-ϵ model [Papp and Ghia (2001)]. The DES clearly reproduces the experimentally-observed constant base pressure, which is the feature that has eluded RANS models.

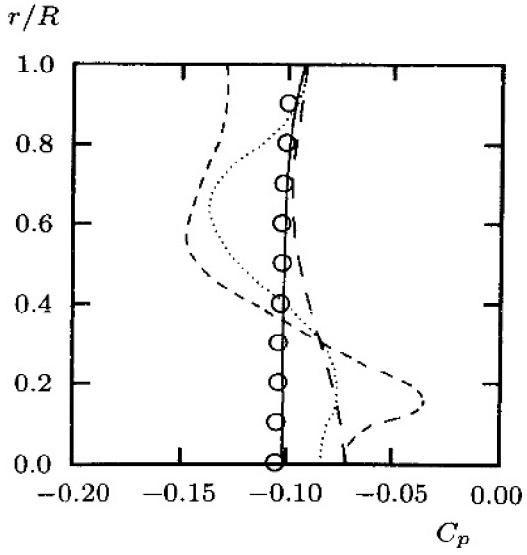

Figure 8.5: *Base pressure for Mach 2.5 flow past a cylindrical body with a square-cut base;* —— *DES;* · · · · · *Wilcox (1998) Stress-ω model;* - - - *Wilcox (1998) k-ω model;* – – – *RNG k-ϵ model;* o *Herrin-Dutton.*

Another major success is the accurate prediction of the drag force on Ahmed's body, the simplified automobile-like geometry experimentally documented by Ahmed et al. (1984). Recall from Section 4.10 that the Standard k-ϵ model predicts a drag coefficient that is 30% higher than measured. Kapadia, Roy and Wurtzler (2003) have performed a DES based on the Spalart-Allmaras model for Ahmed's body with an after-body slant angle of 25°. Figure 8.6 compares iso-surfaces of zero streamwise velocity for the DES and a pure RANS computation with the Spalart-Allmaras model. The presence of large, unsteady counter-rotating vortices dominate in the wake of the body — features that are not present in the RANS computation. The DES drag coefficient is within 5% of the measured value.

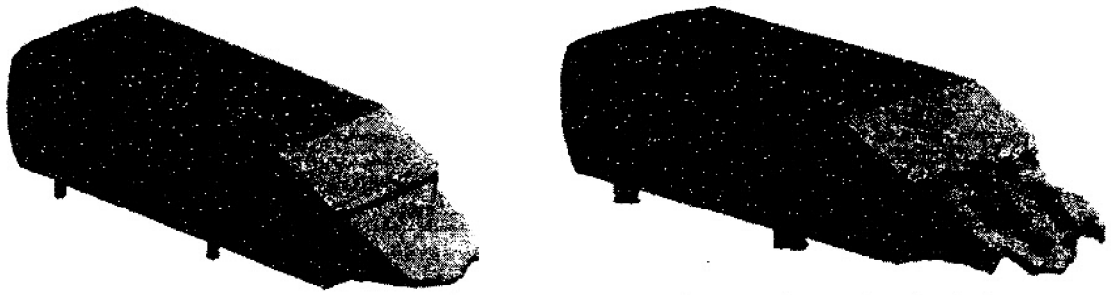

(a) Reynolds Averaged Navier Stokes (b) Detached Eddy Simulation

Figure 8.6: *Iso-surface of zero streamwise velocity for flow past Ahmed's body. [From Kapadia, Roy and Wurtzler (2003) — Copyright © AIAA 2003 — Used with permission.]*

The intense interest in DES is driven by its amenability to very complicated applications such as flow around an airplane. Such simulations have been and are continuing to be done by numerous researchers. Blessed by much shorter computing times than LES, the method holds great promise for enhancing our ability to use DES in a manner that can help in developing new designs.

8.5 Chaos

Our final topic is chaos, a mathematical theory that has attracted considerable attention in recent years. At the present time, no quantitative predictions for properties such as the reattachment length behind a backward-facing step or even the skin friction on a flat plate have been made. Hence, its relevance to turbulence modeling thus far has not been as a competing predictive tool. Rather, the theory's value is in developing qualitative understanding of turbulent-flow phenomena.

Chaos abounds with colorful terminology including **fractals, folded towel diffeomorphisms, smooth noodle maps, homeomorphisms, Hopf bifurcation** and the all-important **strange attractor**. Chaos theory stretches our imagination to think of noninteger dimensional space, and abounds with marvelous geometrical patterns with which the name Mandelbrot is intimately connected.

In the context of turbulence, the primary focus in chaos is upon **nonlinear dynamical systems**, i.e., a coupled system of nonlinear ordinary differential equations. Mathematicians have discovered that certain dynamical systems with a very small number of equations (degrees of freedom) possess extremely complicated (chaotic) solutions. Very simple models have been created that qualitatively reproduce observed physical behavior for nontrivial problems. For example, consider an initially motionless fluid between two horizontal heat-conducting plates in a gravitational field. Now suppose the lower plate is heated slightly. For small temperature difference, viscous forces are sufficient to suppress any mass motion. As the temperature is increased, a threshold is reached where fluid motion begins. A series of steady convective rolls forms, becoming more and more complicated as the temperature difference increases, and the flow ultimately becomes time-dependent and then nonperiodic/chaotic/turbulent. This is the **Rayleigh-Bénard instability**.

One of the famous successes of chaos theory is in qualitatively simulating the Rayleigh-Bénard flow with the following three coupled **ordinary** differential equations

$$\left.\begin{aligned} \frac{dX}{dt} &= (Y - X)/Pr_L \\ \frac{dY}{dt} &= -XZ + rX - Y \\ \frac{dZ}{dt} &= XY - bZ \end{aligned}\right\} \tag{8.49}$$

The quantity Pr_L is the Prandtl number, b and r are constants, and X, Y and Z are related to the streamfunction and temperature. The precise details of the model are given by Bergé, Pomeau and Vidal (1984), and are not important for the present discussion. What is important is that this innocent-looking set of equations yields a qualitative analog to the convection problem, including the geometry of the convection rolls and a solution that resembles turbulent flow.

The central feature of these equations is that they describe what is known as a strange attractor. This particular attractor was the first to be discovered and is more specifically referred to as the **Lorenz attractor**. For the general case, in some suitably defined **phase space** in which each point characterizes the velocity field within a three-dimensional volume (X, Y and Z for the Lorenz attractor), the dynamical system sweeps out a curve that we call the attractor. The concept of a phase space is an extension of classical phase-plane analysis of ordinary differential equations [c.f. Bender and Orszag (1978)]. In phase-plane

analysis, for example, linear equations have critical points such as the focus, the node and the saddle point. For a dynamical system, if the flow is steady, the "curve" is a single point, because the velocity is independent of time. If the flow is periodic in time the curve is closed and we have the familiar limit cycle. The interesting case in chaos is the unsteady, aperiodic case in which the curve asymptotically approaches the strange attractor. If the dynamical system is dissipative, as the Lorenz equations are, the solution trajectories always converge toward an attractor. Additionally, a slight change in the initial conditions for X, Y and Z causes large changes in the solution.

Chaos theory puts great emphasis on the strange attractor, and one of the primary goals of chaos research is to find a set of equations that correspond to the **turbulence attractor**. A dynamical regime is chaotic if two key conditions are satisfied.

1. Its power spectrum contains a continuous part, i.e., a broad band, regardless of the possible presence of peaks.

2. The autocorrelation function goes to zero in finite time.

Of course, both of these conditions are characteristic of turbulence. The latter condition means there is ultimately a loss of memory of the signal with respect to itself. This feature of chaos accounts for the strange attractor's **sensitive dependence on initial conditions**. That is, on a strange attractor, two neighboring trajectories always diverge, regardless of their initial proximity, so that the trajectory actually followed by the system is very sensitive to initial conditions. In chaos studies, this is known as the **butterfly effect** — the notion that a butterfly flapping its wings in Beijing today can change storm systems in New York next month.[2] It goes by the more formal name of **predictability** and was mentioned in Section 8.2 in discussion of the sensitivity of DNS and LES to initial conditions. The **predictability horizon** is the time beyond which predictions become inaccurate, however precise the calculations. Ruelle (1994), in a useful review of possible applications of chaos theory, points out that the motion of the planets in our Solar system is chaotic, with a **predictability time** of about 5 million years — only about 20000 times the orbital period of (the recently demoted "dwarf-planet") Pluto.

While all of these observations indicate there may be promise in using chaos theory to tackle the turbulence problem, there are some sobering realities that must be faced. The broad spectrum of wavelengths in the turbulence spectrum, ranging from the Kolmogorov length scale to the dimension of the flow, is far greater

[2] Although this is a colorful way to describe sensitivity to initial conditions, it is based on a gross exaggeration. To alter a storm system, the butterfly would have to trigger a substantial amount of backscatter, i.e., cause energy to cascade from the very smallest eddies to the energy-bearing eddies. Such an event is highly improbable.

than that of the dynamical systems that have been studied. Hence, as deduced by Keefe (1990) from analysis of DNS data, the dimension of the turbulence attractor (in essence, the number of equations needed to describe the attractor) must be several hundreds even at Reynolds numbers barely large enough for turbulence to exist. It seems essentially unlikely that a low-dimensional dynamical system can emulate turbulence to engineering standards of accuracy.

The layman-oriented book by Gleick (1988) provides an excellent introduction to this fascinating theory in general. See also the abovementioned short review by Ruelle (1994). As a more focused reference, Deissler (1989) presents a review of chaos studies in fluid mechanics.

8.6 Further Reading

Fluid dynamics is sometimes called a "mature science," but the capabilities of CFD are expanding rapidly as computer power increases, and the subject will have advanced considerably before this edition of *Turbulence Modeling for CFD* is replaced. Many bibliographies such as **Inspec** (general physical science) and **Ei Compendex** (engineering) are available on the Internet, generally via site licenses to institutions. A selected bibliography, with abstracts, of turbulence and related subjects is freely available on the World Wide Web at

http://navier.stanford.edu/bradshaw/resp_b.html

Maintained by Prof. Peter Bradshaw, this bibliography goes back to 1980, with some earlier references, and is updated periodically. The reader who wishes to remain up to date should use all of these resources.

Problems

8.1 To help gain an appreciation for how much computing power is needed for a DNS, consider the following. Table 8.1 lists the number of grid points and timesteps required to perform a DNS for channel flow as a function of Reynolds number. Evaluate the amount of 3-GHz Pentium-D microcomputer CPU time needed to do *a single multiplication* at each grid point and timestep for the four Reynolds numbers listed in the table. Assume the microcomputer is capable of 250 megaflops, where a flop is one floating-point operation (multiply, divide, add or subtract) per second. Express your CPU-time answers in hours.

8.2 A DNS of channel flow with $Re_\tau = 180$ using $4 \cdot 10^6$ grid points requires 250 hours of CPU time on a Cray X/MP. The computation runs for a total time, $T_{max} = 5H/u_\tau$. You can assume a Cray X/MP operates at 100 megaflops, where a flop is one floating-point operation (multiply, divide, add or subtract) per second.

(a) Estimate the number of timesteps taken in the computation.

(b) Ignoring time spent reading and writing to disk, estimate the number of floating-point operations per grid point, per iteration.

8.3 Assume a DNS of channel flow with $Re_\tau = 180$ using $4 \cdot 10^6$ grid points requires 225 hours of CPU time and 25 hours of disk I/O time on a Cray X/MP. When the "teraflop" computer becomes a reality, if its disk I/O time is 1000 times faster than that of the 100-megaflop X/MP, how much total computing time will be needed for this computation?

8.4 To help gain an appreciation for how much computer memory is needed for a DNS and an LES, consider the following. Table 8.1 lists the number of DNS and LES grid points for channel flow as a function of Reynolds number. There are three velocity components and, on a 64-bit computer, each requires 8 bytes of memory. Compute the amount of memory needed to hold all of the velocity components in memory for the four Reynolds numbers listed in the table. Express your answers in megabytes, noting that there are 1024^2 bytes in a megabyte.

8.5 This problem focuses on comparative grid requirements for LES and RANS.

(a) Assume the first grid point above a solid surface, $y = y_2$, is located at the outer edge of the viscous wall region, $u_\tau y_2/\nu = 30$. Also, assume that a simple expanding grid with $y_{n+1} = k_g y_n$ is used in $y_2 < y < \delta$. Verify that the number of grid points in the y direction is $1 + \ell n[u_\tau \delta/(30\nu)]/\ell n k_g$. Start by showing that $y_n = k_g^{n-2} y_2$.

(b) Deduce that if $k_g = 1.14$, as in a coarse-grid computation with Program **EDDYBL** (see Appendix C), a factor of 10 increase in $u_\tau \delta/\nu$ requires 18 more profile points.

(c) Near the stern of a ship 300 m long traveling at 10 m/sec (corresponding to a Reynolds number based on length of 10^9), $u_\tau \delta/\nu \approx 1.5 \cdot 10^5$. Show that if $k_g = 1.14$ and $y_2^+ = 30$ (wall function for RANS or *off-the-wall* boundary condition for LES), about 66 points are needed in the y direction. Also show that if $y_2^+ = 1$ (integration to the wall), about 92 points are needed.

8.6 Assuming production balances dissipation in the LES region, determine the effective Smagorinsky constant, C_S, implied by the k-ω model as defined in Equations (8.41) and (8.42). Assume the flow is incompressible and express your answer as a function of C_s and C_d.

Appendix A

Cartesian Tensor Analysis

The central point of view of tensor analysis is to provide a systematic way for transforming quantities such as vectors and matrices from one coordinate system to another. Tensor analysis is a very powerful tool for making such transformations, although the analysis generally is very involved. For our purposes, working with Cartesian coordinates is sufficient so that we only need to focus on issues of notation, nomenclature and some special tensors. This appendix presents elements of Cartesian tensor analysis.

We begin by addressing the question of notation. In Cartesian tensor analysis we make extensive use of subscripts. For consistency with general tensor-analysis nomenclature we use the terms subscript and index interchangeably. The components of an n-dimensional vector **x** are denoted as $x_1, x_2, \ldots, x_n$. For example, in three-dimensional space, we rewrite the coordinate vector **x** = (x, y, z) as **x** = (x_1, x_2, x_3). Now consider an equation describing a plane in three-dimensional space, viz.,

$$a_1 x_1 + a_2 x_2 + a_3 x_3 = c \tag{A.1}$$

where a_i and c are constants. This equation can be written as

$$\sum_{i=1}^{3} a_i x_i = c \tag{A.2}$$

In tensor analysis, we introduce the Einstein summation convention and rewrite Equation (A.2) in the shorthand form

$$a_i x_i = c \tag{A.3}$$

The Einstein summation convention is as follows:

> **Repetition of an index in a term denotes summation with respect to that index over its range.**

The **range** of an index i is the set of n integer values 1 to n. An index that is summed over is called a **dummy index**; one that is not summed is called a **free index**. Since a dummy index simply indicates summation, it is immaterial what symbol is used. Thus, $a_i x_i$ may be replaced by $a_j x_j$, which is obvious if we simply note that

$$\sum_{i=1}^{3} a_i x_i = \sum_{j=1}^{3} a_j x_j \tag{A.4}$$

As an example of an equation with a free index, consider a unit normal vector $\mathbf{n}$ in three-dimensional space. If the unit normals in the x_1, x_2 and x_3 directions are $\mathbf{i}_1$, $\mathbf{i}_2$ and $\mathbf{i}_3$, then the direction cosines α_1, α_2 and α_3 for the vector $\mathbf{n}$ are

$$\alpha_k = \mathbf{n} \cdot \mathbf{i}_k \tag{A.5}$$

There is no implied summation in Equation (A.5). Rather, it is a shorthand for the three equations defining the direction cosines. Because the length of a unit vector is one, we can take the dot product of $(\alpha_1, \alpha_2, \alpha_3)$ with itself and say that

$$\alpha_i \alpha_i = 1 \tag{A.6}$$

As another example, consider the total differential of a function of three variables, $p(x_1, x_2, x_3)$. We have

$$dp = \frac{\partial p}{\partial x_1} dx_1 + \frac{\partial p}{\partial x_2} dx_2 + \frac{\partial p}{\partial x_3} dx_3 \tag{A.7}$$

In tensor notation, this is replaced by

$$dp = \frac{\partial p}{\partial x_i} dx_i \tag{A.8}$$

Equation (A.8) can be thought of as the dot product of the gradient of p, namely ∇p, and the differential vector $d\mathbf{x} = (dx_1, dx_2, dx_3)$. Thus, we can also say that the i component of ∇p, which we denote as $(\nabla p)_i$, is given by

$$(\nabla p)_i = \frac{\partial p}{\partial x_i} = p_{,i} \tag{A.9}$$

where a comma followed by an index is tensor notation for differentiation with respect to x_i. Similarly, the divergence of a vector $\mathbf{u}$ is given by

$$\nabla \cdot \mathbf{u} = \frac{\partial u_i}{\partial x_i} = u_{i,i} \tag{A.10}$$

where we again denote differentiation with respect to x_i by "$,i$".

Thus far, we have dealt with scalars and vectors. The question naturally arises about how we might handle a matrix. The answer is we denote a matrix by using two subscripts, or indices. The first index corresponds to row number while the second corresponds to column number. For example, consider the 3×3 matrix $[A]$ defined by

$$[A] = \begin{bmatrix} A_{11} & A_{12} & A_{13} \\ A_{21} & A_{22} & A_{23} \\ A_{31} & A_{32} & A_{33} \end{bmatrix} \tag{A.11}$$

In tensor notation, we represent the matrix $[A]$ as A_{ij}. If we post-multiply an $m \times n$ matrix B_{ij} by an $n \times 1$ column vector x_j, their product is an $m \times 1$ column vector y_i. Using the summation convention, we write

$$y_i = B_{ij} x_j \tag{A.12}$$

Equation (A.12) contains both a free index (i) and a dummy index (j). The product of a square matrix A_{ij} and its inverse is the unit matrix, i.e.,

$$[A][A]^{-1} = \begin{bmatrix} 1 & 0 & 0 \\ 0 & 1 & 0 \\ 0 & 0 & 1 \end{bmatrix} \tag{A.13}$$

Equation (A.13) is rewritten in tensor notation as follows:

$$A_{ik}(A^{-1})_{kj} = \delta_{ij} \tag{A.14}$$

where δ_{ij} is the Kronecker delta defined by

$$\delta_{ij} = \begin{cases} 1, & i = j \\ 0, & i \neq j \end{cases} \tag{A.15}$$

We can use the Kronecker delta to rewrite Equation (A.6) as

$$\alpha_i \delta_{ij} \alpha_j = 1 \tag{A.16}$$

This corresponds to pre-multiplying the 3×3 matrix δ_{ij} by the row vector $(\alpha_1, \alpha_2, \alpha_3)$ and then post-multiplying their product by the column vector $(\alpha_1, \alpha_2, \alpha_3)^T$, where superscript T denotes transpose.

The determinant of a 3×3 matrix A_{ij} is

$$\begin{vmatrix} A_{11} & A_{12} & A_{13} \\ A_{21} & A_{22} & A_{23} \\ A_{31} & A_{32} & A_{33} \end{vmatrix} = \begin{array}{l} A_{11}A_{22}A_{33} + A_{21}A_{32}A_{13} + A_{31}A_{12}A_{23} \\ -A_{11}A_{32}A_{23} - A_{12}A_{21}A_{33} - A_{13}A_{22}A_{31} \end{array} \tag{A.17}$$

Tensor analysis provides a shorthand for this operation as well. Specifically, we replace Equation (A.17) by

$$det(A_{ij}) = |A_{ij}| = \epsilon_{rst} A_{r1} A_{s2} A_{t3} \tag{A.18}$$

where ϵ_{rst} is the **permutation tensor** defined by

$$\left.\begin{array}{l} \epsilon_{123} = \epsilon_{231} = \epsilon_{312} = 1 \\ \epsilon_{213} = \epsilon_{321} = \epsilon_{132} = -1 \\ \epsilon_{111} = \epsilon_{222} = \epsilon_{333} = \epsilon_{112} = \epsilon_{113} = \epsilon_{221} = \epsilon_{223} = \epsilon_{331} = \epsilon_{332} = 0 \end{array}\right\} \tag{A.19}$$

In other words, ϵ_{ijk} vanishes whenever the values of any two indices are the same; $\epsilon_{ijk} = 1$ when the indices are a permutation of 1, 2, 3; and $\epsilon_{ijk} = -1$ otherwise.

As can be easily verified, the cross product of two vectors **a** and **b** can be expressed as follows.

$$(\mathbf{a} \times \mathbf{b})_i = \epsilon_{ijk} a_j b_k \tag{A.20}$$

In particular, the curl of a vector **u** is

$$(\nabla \times \mathbf{u})_i = \epsilon_{ijk} \frac{\partial u_k}{\partial x_j} = \epsilon_{ijk} u_{k,j} \tag{A.21}$$

The Kronecker delta and permutation tensor are very important quantities that appear throughout this book. They are related by the ϵ-δ identity, which is the following.

$$\epsilon_{ijk} \epsilon_{ist} = \delta_{js} \delta_{kt} - \delta_{jt} \delta_{ks} \tag{A.22}$$

All that remains to complete our brief introduction to tensor analysis is to define a tensor. Tensors are classified in terms of their rank. To determine the rank of a tensor, we simply count the number of indices.

The lowest rank tensor is rank zero which corresponds to a scalar, i.e., a quantity that has magnitude only. Thermodynamic properties such as pressure and density are scalar quantities. Vectors such as velocity, vorticity and pressure gradient are tensors of rank one. They have both magnitude and direction. Matrices are rank two tensors. The stress tensor is a good example for illustrating physical interpretation of a second-rank tensor. It defines a force per unit area that has a magnitude and two associated directions, the direction of the force and the direction of the normal to the plane on which the force acts. For a normal stress, these two directions are the same; for a shear stress, they are (by convention) normal to each other.

As we move to tensors of rank three and beyond, the physical interpretation becomes more difficult to ascertain. This is rarely an issue of great concern since virtually all physically relevant tensors are of rank 2 or less. The permutation tensor is of rank 3, for example, and is simply defined by Equation (A.19).

A tensor a_{ij} is **symmetric** if $a_{ij} = a_{ji}$. Many important tensors in mathematical physics are symmetric, e.g., stress, strain and strain-rate tensors, moment of inertia tensor, virtual-mass tensor. A tensor is **skew symmetric** if $a_{ij} = -a_{ji}$. The rotation tensor, $\Omega_{ij} = \frac{1}{2}(u_{i,j} - u_{j,i})$ is skew symmetric.

As a final comment, in performing tensor-analysis operations with tensors that are not differential operators, we rarely have to worry about preserving the order of terms as we did in Equation (A.16). There is no confusion in writing $\delta_{ij}\alpha_i\alpha_j$ in place of $\alpha_i\delta_{ij}\alpha_j$. This is only an issue when the indicated summations actually have to be done. However, care should be exercised when differentiation occurs. As an example, $\nabla \cdot \mathbf{u} = \partial u_i/\partial x_i$ is a scalar number while $\mathbf{u} \cdot \nabla = u_i\partial/\partial x_i$ is a scalar differential operator.

Problems

A.1 Use the ϵ-δ identity to verify the well known vector identity

$$\mathbf{A} \times (\mathbf{B} \times \mathbf{C}) = (\mathbf{A} \cdot \mathbf{C})\mathbf{B} - (\mathbf{A} \cdot \mathbf{B})\mathbf{C}$$

A.2 Show that, when i, j, k range over 1, 2, 3

(a) $\delta_{ij}\delta_{ji} = 3$

(b) $\epsilon_{ijk}\epsilon_{jki} = 6$

(c) $\epsilon_{ijk}A_jA_k = 0$

(d) $\delta_{ij}\delta_{jk} = \delta_{ik}$

A.3 Verify that $2S_{ij,j} = \nabla^2 u_i$ for incompressible flow, where S_{ij} is the strain-rate tensor, i.e., $S_{ij} = \frac{1}{2}(u_{i,j} + u_{j,i})$.

A.4 Show that the scalar product $S_{ij}\Omega_{ji}$ vanishes identically if S_{ij} is a symmetric tensor and Ω_{ij} is skew symmetric.

A.5 If u_j is a vector, show that the tensor $\omega_{ik} = \epsilon_{ijk}u_j$ is skew symmetric.

A.6 Show that if A_{jk} is a skew-symmetric tensor, the unique solution of the equation $\omega_i = \frac{1}{2}\epsilon_{ijk}A_{jk}$ is $A_{mn} = \epsilon_{mni}\omega_i$.

A.7 The incompressible Navier-Stokes equation in a coordinate system rotating with constant angular velocity $\mathbf{\Omega}$ and with position vector $\mathbf{x} = x_k\mathbf{i}_k$ is

$$\frac{\partial \mathbf{u}}{\partial t} + \mathbf{u} \cdot \nabla \mathbf{u} + 2\mathbf{\Omega} \times \mathbf{u} = -\nabla\left(\frac{p}{\rho}\right) - \mathbf{\Omega} \times \mathbf{\Omega} \times \mathbf{x} + \nu\nabla^2\mathbf{u}$$

(a) Rewrite this equation in tensor notation.

(b) Using tensor analysis, show that for $\mathbf{\Omega} = \Omega\,\mathbf{k}$ ($\mathbf{k}$ is a unit vector aligned with $\mathbf{\Omega}$), the centrifugal force per unit mass is given by

$$-\mathbf{\Omega} \times \mathbf{\Omega} \times \mathbf{x} = \nabla(\frac{1}{2}\Omega^2 x_k x_k) - [\mathbf{k} \cdot \nabla(\frac{1}{2}\Omega^2 x_k x_k)]\mathbf{k}$$

A.8 Using tensor analysis, prove the vector identity

$$\mathbf{u} \cdot \nabla \mathbf{u} = \nabla(\frac{1}{2}\mathbf{u} \cdot \mathbf{u}) - \mathbf{u} \times (\nabla \times \mathbf{u})$$

Appendix B

Rudiments of Perturbation Methods

When we work with perturbation methods, we are constantly dealing with the concept of **order of magnitude**. There are three conventional **order symbols** that provide a mathematical measure of the order of magnitude of a given quantity, viz., **Big O**, **Little o**, and $\sim$. They are defined as follows.

Big O:

$f(\delta) = O[g(\delta)]$ as $\delta \to \delta_o$ if a neighborhood of δ_o exists and a constant M exists such that $|f| \leq M|g|$, i.e., $f(\delta)/g(\delta)$ is bounded as $\delta \to \delta_o$.

Little o:

$f(\delta) = o[g(\delta)]$ as $\delta \to \delta_o$ if, given any $\epsilon > 0$, there exists a neighborhood of δ_o such that $|f| \leq \epsilon|g|$, i.e., $f(\delta)/g(\delta) \to 0$ as $\delta \to \delta_o$.

$\sim$:

$f(\delta) \sim g(\delta)$ as $\delta \to \delta_o$ if $f(\delta)/g(\delta) \to 1$ as $\delta \to \delta_o$.

For example, the Taylor series for the exponential function is

$$e^{-x} = 1 - x + \frac{1}{2}x^2 - \frac{1}{6}x^3 + \cdots \tag{B.1}$$

where "$\cdots$" is conventional shorthand for the rest of the Taylor series, i.e.,

$$\cdots = \sum_{n=4}^{\infty} \frac{(-1)^n x^n}{n!} \tag{B.2}$$

In terms of the ordering symbols, we can replace "..." as follows.

$$e^{-x} = 1 - x + \frac{1}{2}x^2 - \frac{1}{6}x^3 + O(x^4) = 1 - x + \frac{1}{2}x^2 - \frac{1}{6}x^3 + o(x^3) \quad \text{(B.3)}$$

We define an **asymptotic sequence of functions** as a sequence $\phi_n(\delta)$ for $n = 1, 2, 3, \ldots$, satisfying the condition

$$\phi_{n+1}(\delta) = o[\phi_n(\delta)] \qquad \text{as} \qquad \delta \to \delta_o \quad \text{(B.4)}$$

Examples of asymptotic sequences are:

$$\left.\begin{array}{lcll} \phi_n(\delta) & = & 1, (\delta - \delta_o), (\delta - \delta_o)^2, (\delta - \delta_o)^3, \ldots & \delta \to \delta_o \\ \phi_n(\delta) & = & 1, \delta^{1/2}, \delta, \delta^{3/2}, \ldots & \delta \to 0 \\ \phi_n(\delta) & = & 1, \delta, \delta^2 \ell n \delta, \delta^2, \ldots & \delta \to 0 \\ \phi_n(x) & = & x^{-1}, x^{-2}, x^{-3}, x^{-4}, \ldots & x \to \infty \end{array}\right\} \quad \text{(B.5)}$$

We say that $g(\delta)$ is **transcendentally small** if $g(\delta)$ is $o[\phi_n(\delta)]$ for all n. For example,

$$e^{-1/\delta} = o(\delta^n) \qquad \text{for all } n \quad \text{(B.6)}$$

An asymptotic expansion is the sum of the first N terms in an asymptotic sequence. It is the asymptotic expansion of a function $F(\delta)$ as $\delta \to \delta_o$ provided

$$F(\delta) = \sum_{n=1}^{N} a_n \phi_n(\delta) + o[\phi_N(\delta)] \quad \text{(B.7)}$$

The following are a few useful asymptotic expansions generated from simple Taylor-series expansions, all of which are convergent as $\delta \to 0$.

$$\left.\begin{array}{lcl} (1+\delta)^n & \sim & 1 + n\delta + \frac{n(n-1)}{2}\delta^2 + O(\delta^3) \\ \ell n(1+\delta) & \sim & \delta - \frac{1}{2}\delta^2 + \frac{1}{3}\delta^3 + O(\delta^4) \\ (1-\delta)^{-1} & \sim & 1 + \delta + \delta^2 + O(\delta^3) \\ e^{\delta} & \sim & 1 + \delta + \frac{1}{2}\delta^2 + O(\delta^3) \\ \cos\delta & \sim & 1 - \frac{1}{2}\delta^2 + \frac{1}{24}\delta^4 + O(\delta^6) \\ \sin\delta & \sim & \delta - \frac{1}{6}\delta^3 + \frac{1}{120}\delta^5 + O(\delta^7) \\ \tan\delta & \sim & \delta + \frac{1}{3}\delta^3 + \frac{2}{15}\delta^5 + O(\delta^7) \end{array}\right\} \quad \text{(B.8)}$$

Not all asymptotic expansions are developed as a Taylor series, nor are they necessarily convergent. For example, consider the complementary error function, $\text{erfc}(x)$, i.e.,

$$\text{erfc}(x) = \frac{2}{\sqrt{\pi}} \int_x^{\infty} e^{-t^2}\, dt \quad \text{(B.9)}$$

We can generate an asymptotic expansion using a succession of integration-by-parts operations. (To start the process, for example, multiply and divide the integrand by t so that $t\exp(-t^2)$ becomes integrable in closed form.) The expansion is:

$$\begin{aligned} \operatorname{erfc}(x) &\sim \frac{2}{\sqrt{\pi}} e^{-x^2} \sum_{n=0}^{\infty} (-1)^n \frac{(1)(3)\ldots(2n-1)}{2^{n+1} x^{2n+1}} \qquad \text{as} \qquad x \to \infty \\ &\sim \frac{2}{\sqrt{\pi}} e^{-x^2} \left\{ \frac{x^{-1}}{2} - \frac{x^{-3}}{4} + O(x^{-5}) \right\} \end{aligned} \tag{B.10}$$

A simple ratio test shows that this series is divergent for all values of x. However, if we define the remainder after the first N terms of the series as $R_N(x)$, there are two limits we can consider, viz.,

$$\lim_{x \to \infty} |R_N(x)|_{Fixed\ N} = 0 \qquad \text{and} \qquad \lim_{N \to \infty} |R_N(x)|_{Fixed\ x} = \infty \tag{B.11}$$

Thus, this divergent series gives a good approximation to $\operatorname{erfc}(x)$ provided we don't keep too many terms! This is often the case for an asymptotic series.

Part of our task in developing a perturbation solution is to determine the appropriate asymptotic sequence. It is usually obvious, but not always. Also, more than one set of $\phi_n(\delta)$ may be suitable, i.e., we are not guaranteed uniqueness in perturbation solutions. These problems, although annoying from a theoretical viewpoint, by no means diminish the utility of perturbation methods. Usually, we have physical intuition to help guide us in developing our solution. This type of mathematical approach is, after all, standard operating procedure for the engineer. We are, in essence, using the methods Prandtl and von Kármán used before perturbation analysis was given a name.

A **singular-perturbation problem** is one in which no single asymptotic expansion is uniformly valid throughout the field of interest. For example, while $\delta/x^{1/2} = O(\delta)$ as $\delta \to 0$, the singularity as $x \to 0$ means this expression is not uniformly valid. Similarly, $\delta \ell n x = O(\delta)$ as $\delta \to 0$ and is not uniformly valid as $x \to 0$ and as $x \to \infty$. The two most common situations that lead to a singular-perturbation problem are:

(a) the coefficient of the highest derivative in a differential equation is very small;

(b) difficulties arise in behavior near boundaries.

Case (b) typically arises in analyzing the turbulent boundary layer where logarithmic behavior of the solution occurs close to a solid boundary. The following second-order ordinary differential equation illustrates Case (a).

$$\delta \frac{d^2F}{ds^2} + \frac{dF}{ds} + F = 0, \qquad 0 \le s \le 1 \tag{B.12}$$

We want to solve this equation subject to the following boundary conditions.

$$F(0) = 0 \quad \text{and} \quad F(1) = 1 \tag{B.13}$$

We also assume that δ is very small compared to 1, i.e.,

$$\delta \ll 1 \tag{B.14}$$

This equation is a simplified analog of the Navier-Stokes equation. The second-derivative term has a small coefficient just as the second-derivative term in the Navier-Stokes equation, in nondimensional form, has the reciprocal of the Reynolds number as its coefficient. An immediate consequence is that only one boundary condition can be satisfied if we set $\delta = 0$. This is similar to setting viscosity to zero in the Navier-Stokes equation, which yields Euler's equation, and the attendant consequence that only the normal-velocity surface boundary condition can be satisfied. That is, we cannot enforce the no-slip boundary condition for Euler-equation solutions.

The exact solution to this equation is

$$F(s;\delta) = \frac{e^{\alpha(1-s)} - e^{\alpha-\beta s/\delta}}{1 - e^{\alpha-\beta/\delta}} \tag{B.15}$$

where

$$\alpha = \frac{1-\sqrt{1-4\delta}}{2\delta} \quad \text{and} \quad \beta = \frac{1-\sqrt{1-4\delta}}{2} \tag{B.16}$$

which clearly satisfies both boundary conditions. If we set $\delta = 0$ in Equation (B.12), we have the following first-order equation:

$$\frac{dF}{ds} + F = 0 \tag{B.17}$$

and the solution, $F(s;0)$, is

$$F(s;0) = e^{1-s} \tag{B.18}$$

where we use the boundary condition at $s = 1$. However, the solution fails to satisfy the boundary condition at $s = 0$ because $F(0;0) = e = 2.71828\cdots$. Figure B.1 illustrates the solution to our simplified equation for several values of δ.

As shown, the smaller the value of δ, the more closely $F(s;0)$ represents the solution throughout the region $0 < s \leq 1$. Only in the immediate vicinity of $s = 0$ is the solution inaccurate. The thin layer where $F(s;0)$ departs from the exact solution is called a boundary layer, in direct analogy to its fluid-mechanical equivalent.

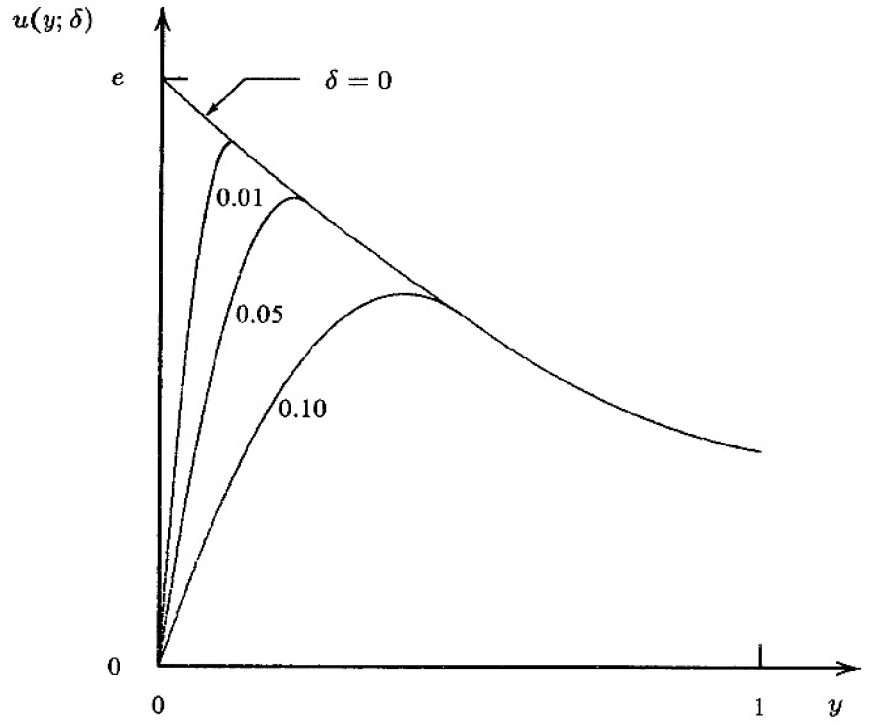

Figure B.1: *Solutions to the model equation for several values of* δ.

To solve this problem using perturbation methods, we seek a solution that consists of two separate asymptotic expansions, one known as the **outer expansion** and the other as the **inner expansion**. For the outer expansion, we assume a solution of the form

$$F_{outer}(s;\delta) \sim \sum_{n=0}^{N} F_n(s)\phi_n(\delta) \tag{B.19}$$

where the asymptotic sequence functions, $\phi_n(\delta)$, will be determined as part of the solution. Substituting Equation (B.19) into Equation (B.12) yields the following.

$$\sum_{n=0}^{N}\left[\frac{d^2F_n}{ds^2}\delta\phi_n(\delta) + \frac{dF_n}{ds}\phi_n(\delta) + F_n\phi_n(\delta)\right] = 0 \tag{B.20}$$

Clearly, if we select

$$\phi_n(\delta) = \delta^n \tag{B.21}$$

we, in effect, have a power-series expansion. Equating like powers of δ, the **leading-order** ($n = 0$) problem is Equation (B.17), while the second-derivative term makes its first appearance in the **first-order** ($n = 1$) problem. Thus, our

perturbation solution yields the following series of problems for the **outer expansion**.

$$\left.\begin{aligned} \frac{dF_0}{ds} + F_0 &= 0 \\ \frac{dF_1}{ds} + F_1 &= -\frac{d^2F_0}{ds^2} \\ \frac{dF_2}{ds} + F_2 &= -\frac{d^2F_1}{ds^2} \\ &\vdots \end{aligned}\right\} \tag{B.22}$$

Provided we solve the equations in sequence starting at the lowest order ($n = 0$) equation, the right-hand side of each equation is known from the preceding solution and serves simply to make each equation for $n \geq 1$ nonhomogeneous. Consequently, to all orders, the equation for $F_n(s)$ is of first order. Hence, no matter how many terms we include in our expansion, we can satisfy only one of the two boundary conditions. As in the introductory remarks, we elect to satisfy $F(1) = 1$. In terms of our expansion [Equations (B.19) and (B.21)], the boundary conditions for the F_n are

$$F_0(1) = 1 \quad \text{and} \quad F_n(1) = 0 \quad \text{for} \quad n \geq 1 \tag{B.23}$$

The solution to Equations (B.22) subject to the boundary conditions specified in Equation (B.23) is as follows.

$$\left.\begin{aligned} F_0(s) &= e^{1-s} \\ F_1(s) &= (1-s)e^{1-s} \\ &\vdots \end{aligned}\right\} \tag{B.24}$$

Hence, our **outer expansion** assumes the following form.

$$F_{outer}(s;\delta) \sim e^{1-s}\left[1 + (1-s)\delta + O(\delta^2)\right] \tag{B.25}$$

In general, for singular-perturbation problems, we have no guarantee that continuing to an infinite number of terms in the outer expansion yields a solution that satisfies both boundary conditions. That is, our expansion may or may not be convergent. Hence, we try a different approach to resolve the region near $s = 0$. We now generate an **inner expansion** in which we **stretch** the s coordinate. That is, we define a new independent variable σ as follows.

$$\sigma = \frac{s}{\mu(\delta)} \tag{B.26}$$

We assume an inner expansion in terms of a new set of asymptotic-sequence functions, $\psi_n(\delta)$, i.e.,

$$F_{inner}(\sigma;\delta) \sim \sum_{n=0}^{N} f_n(\sigma)\psi_n(\delta) \tag{B.27}$$

To best illustrate how we determine the appropriate stretching function, $\mu(\delta)$, consider the leading-order terms in the original differential equation, viz.,

$$\frac{d^2 f_0}{d\sigma^2}\left(\frac{\delta\psi_0}{\mu^2}\right) + \frac{df_0}{d\sigma}\left(\frac{\psi_0}{\mu}\right) + f_0\psi_0 = O\left(\frac{\delta\psi_1}{\mu^2}, \frac{\psi_1}{\mu}, \psi_1\right) \tag{B.28}$$

First of all, we must consider the three possibilities for the order of magnitude of $\mu(\delta)$, viz., $\mu \gg 1$, $\mu \sim 1$ and $\mu \ll 1$. If $\mu \gg 1$, inspection of Equation (B.28) shows that $f_0 = 0$ which is not a useful solution. If $\mu \sim 1$, we have the outer expansion. Thus, we conclude that $\mu \ll 1$.

We are now faced with three additional possibilities: $\delta\psi_0/\mu^2 \gg \psi_0/\mu$; $\delta\psi_0/\mu^2 \sim \psi_0/\mu$; and $\delta\psi_0/\mu^2 \ll \psi_0/\mu$. Using the boundary condition at $s = 0$, assuming $\delta\psi_0/\mu^2 \gg \psi_0/\mu$ yields $f_0 = A\sigma$ where A is a constant of integration. While this solution might be useful, we have learned nothing about the stretching function, $\mu(\delta)$. At the other extreme, $\delta\psi_0/\mu^2 \ll \psi_0/\mu$, we obtain the trivial solution, $f_0 = 0$, which doesn't help us in our quest for a solution. The final possibility, $\delta\psi_0/\mu^2 \sim \psi_0/\mu$, is known as the **distinguished limit**, and this is the case we choose. Thus,

$$\mu(\delta) = \delta \tag{B.29}$$

Again, the most appropriate choice for the $\psi_n(\delta)$ is

$$\psi_n(\delta) = \delta^n \tag{B.30}$$

The following sequence of equations and boundary conditions define the **inner expansion**.

$$\left.\begin{aligned} \frac{d^2 f_0}{d\sigma^2} + \frac{df_0}{d\sigma} &= 0 \\ \frac{d^2 f_1}{d\sigma^2} + \frac{df_1}{d\sigma} &= -f_0 \\ \frac{d^2 f_2}{d\sigma^2} + \frac{df_2}{d\sigma} &= -f_1 \\ &\vdots \end{aligned}\right\} \tag{B.31}$$

$$f_n(0) = 0 \qquad \text{for all } n \geq 0 \tag{B.32}$$

Solving the leading, or **zeroth**, order problem ($n = 0$) and the **first** order problem ($n = 1$), we find

$$\left.\begin{aligned} f_0(\sigma) &= A_0(1 - e^{-\sigma}) \\ f_1(\sigma) &= (A_1 - A_0\sigma) - (A_1 + A_0\sigma)e^{-\sigma} \\ &\vdots \end{aligned}\right\} \tag{B.33}$$

where A_0 and A_1 are constants of integration. These integration constants arise because each of Equations (B.31) is of second order and we have used only one boundary condition.

To complete the solution, we perform an operation known as **matching**. To motivate the matching procedure, note that on the one hand, the boundary $s = 1$ is located at $\sigma = 1/\delta \to \infty$ as $\delta \to 0$. Hence, we need a boundary condition for $F_{inner}(\sigma; \delta)$ valid as $\sigma \to \infty$. On the other hand, the independent variable in the outer expansion is related to σ by $s = \delta\sigma$. Thus, for any finite value of σ, the inner expansion lies very close to $s = 0$. We **match** these two asymptotic expansions by requiring that

$$\lim_{\sigma\to\infty} F_{inner}(\sigma; \delta) = \lim_{s\to 0} F_{outer}(s; \delta) \tag{B.34}$$

The general notion is that on the scale of the outer expansion, the inner expansion is valid in an infinitesimally thin layer. Similarly, on the scale of the inner expansion, the outer expansion is valid for a region infinitely distant from $s = 0$. For the problem at hand,

$$\lim_{\sigma\to\infty} f_0(\sigma) = A_0 \qquad \text{and} \qquad \lim_{s\to 0} F_0(s) = e \tag{B.35}$$

Thus, we conclude that

$$A_0 = e \tag{B.36}$$

Equivalently, we can visualize the existence of an **overlap region** between the inner and outer solutions. In the overlap region, we stretch the s coordinate according to

$$s^* = \frac{s}{\nu(\delta)}, \qquad \delta \ll \nu(\delta) \ll 1 \tag{B.37}$$

In terms of this intermediate variable, for any finite value of s^*,

$$s \to 0 \qquad \text{and} \qquad \sigma \to \infty \qquad \text{as} \qquad \nu(\delta) \to 0 \tag{B.38}$$

Using this method, we can match to as high an order as we wish. For example, matching to n^{th} order, we perform the following limit operation.

$$\lim_{\delta\to 0}\left[\frac{F_{inner} - F_{outer}}{\delta^n}\right] = 0 \tag{B.39}$$

For the problem at hand, the independent variables s and σ become

$$s = \nu(\delta)s^* \qquad \text{and} \qquad \sigma = \frac{\nu(\delta)s^*}{\delta} \tag{B.40}$$

Hence, replacing $e^{-\nu(\delta)s^*}$ by its Taylor-series expansion, we find

$$F_{outer} \sim e\{1 - \nu(\delta)s^* + \delta + O[\delta\nu(\delta)]\} \tag{B.41}$$

Similarly, noting that $e^{-\nu(\delta)s^*/\delta}$ is transcendentally small as $\delta \to 0$, we have

$$F_{inner} \sim A_0 - A_0\nu(\delta)s^* + A_1\delta + O(\delta^2) \tag{B.42}$$

Thus, holding s^* constant,

$$\lim_{\delta\to 0}\left[\frac{F_{inner} - F_{outer}}{\delta}\right] \sim \frac{(A_0 - e)(1 - \nu(\delta)s^*) + (A_1 - e)\delta + o(\delta)}{\delta} \tag{B.43}$$

Clearly, **matching to zeroth and first orders** can be achieved only if

$$A_0 = A_1 = e \tag{B.44}$$

In summary, the **inner and outer expansions** are given by

$$\left.\begin{aligned} &F_{outer}(s;\delta) \sim e^{1-s}\left[1 + (1-s)\delta + O(\delta^2)\right] \\ &F_{inner}(\sigma;\delta) \sim e\left\{(1 - e^{-\sigma}) + [(1-\sigma) - (1+\sigma)e^{-\sigma}]\delta + O(\delta^2)\right\} \\ &\sigma = s/\delta \end{aligned}\right\} \tag{B.45}$$

Finally, we can generate a single expansion, known as a **composite expansion**, that can be used throughout the region $0 \le s \le 1$. Recall that in the matching operations above, we envisioned an **overlap region**. In constructing a composite expansion, we note that the inner expansion is valid in the inner region, the outer expansion is valid in the outer region, and both are valid in the overlap region. Hence, we define

$$F_{composite} \equiv F_{inner} + F_{outer} - F_{cp} \tag{B.46}$$

where F_{cp} is the **common part**, i.e., the part of the expansions that cancel in the matching process. Again, for the case at hand, comparison of Equations (B.41) and (B.42) with A_0 and A_1 given by Equation (B.44) shows that

$$F_{cp} \sim e\left[1 + (1-\sigma)\delta + O(\delta^2)\right] \tag{B.47}$$

where we use the fact that $\nu(\delta)s^* = \delta\sigma$. Hence, the **composite expansion** is

$$F_{composite} \sim \left[e^{1-s} - e^{1-s/\delta}\right] + \left[(1-s)e^{1-s} - (1 + s/\delta)e^{1-s/\delta}\right]\delta + O(\delta^2) \tag{B.48}$$

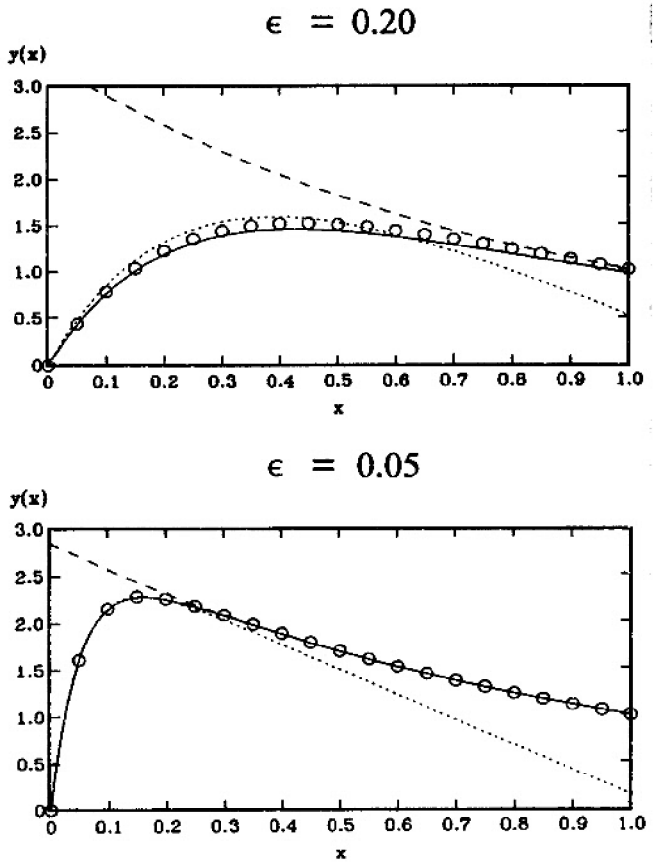

Figure B.2: *Comparison of asymptotic expansions and the exact solution for the sample boundary-value problem:* o *exact;* – – – *outer expansion;* · · · · · · *inner expansion;* —— *composite expansion.*

What we have done is combine two non-uniformly valid expansions to achieve a **uniformly-valid approximation** to the exact solution. Retaining just the zeroth-order term of the composite expansion yields an approximation to the exact solution that is accurate to within 7% for ϵ as large as 0.2! This is actually a bit fortuitous however, since the leading term in Equation (B.48) and the exact solution differ by a transcendentally small term. Figure B.2 compares the two-term inner, outer and composite expansions with the exact solution for $\epsilon = 0.05$ and $\epsilon = 0.20$.

For the obvious reason, perturbation analysis is often referred to as the theory of **matched asymptotic expansions**. The discussion here, although sufficient for our needs, is brief and covers only the bare essentials of the theory. For additional information, see the books by Van Dyke (1975), Bender and Orszag (1978), Kevorkian and Cole (1981), Nayfeh (1981) or Wilcox (1995a) on this powerful mathematical theory.

Problems

B.1 Consider the polynomial

$$x^3 - x^2 + \delta = 0$$

(a) For nonzero $\delta < 4/27$ this equation has three real and unequal roots. Why is this a singular-perturbation problem in the limit $\delta \to 0$?

(b) Use perturbation methods to solve for the first two terms in the expansions for the roots.

B.2 Determine the first two terms in the asymptotic expansion for the roots of the following polynomial valid as $\delta \to 0$.

$$\delta x^3 + x + 2 + \delta = 0$$

B.3 Consider the following nonlinear, first-order initial-value problem.

$$\frac{dy}{dt} + y + \delta y^2 = 0, \qquad y(0) = 1$$

Determine the exact solution and classify this problem as regular or singular in the limit $\delta \to 0$. Do the classification first for $t > 0$ and then for $t < 0$.

B.4 The following is an example of a perturbation problem that is singular because of nonuniformity near a boundary. Consider the following first-order equation in the limit $\epsilon \to 0$.

$$x^3 \frac{dy}{dx} = \epsilon y^2, \qquad y(1) = 1$$

The solution is known to be finite on the closed interval $0 \leq x \leq 1$.

(a) Solve for the first two terms in the outer expansion and show that the solution has a singularity as $x \to 0$.

(b) Show that there is a boundary layer near $x = 0$ whose thickness is of order $\epsilon^{1/2}$.

(c) Solve for the first two terms of the inner expansion. Note that the algebra simplifies if you do the zeroth-order matching before attempting to solve for the next term in the expansion.

B.5 Generate the first two terms in a perturbation solution for the following initial-value problem valid as $\delta \to 0$.

$$\frac{dy}{dx} = y^2 + 2y, \qquad y(0) = -2 + 5\delta$$

B.6 Generate the first two terms of the inner and outer expansions for the following boundary-value problem. Also, construct a composite expansion.

$$\delta \frac{d^2y}{dx^2} + \frac{dy}{dx} - xy = 0, \qquad \delta \ll 1$$

$$y(0) = 0 \qquad \text{and} \qquad y(1) = e^{1/2}$$

B.7 Generate the first two terms of the inner and outer expansions for the following boundary-value problem. Also, construct a composite expansion.

$$\delta \frac{d^2y}{dx^2} + \frac{dy}{dx} = \frac{1}{2}x^2, \qquad \delta \ll 1$$

$$y(0) = 1 \qquad \text{and} \qquad y(1) = 1/6$$

B.8 This problem demonstrates that the **overlap region** is not a layer in the same sense as the boundary layer. Rather, its thickness depends upon how many terms we retain in the matching process. Suppose we have solved a boundary-layer problem and the first three terms of the inner and outer expansions valid as $\epsilon \to 0$ are:

$$y_{outer}(x;\epsilon) \sim 1 + \epsilon e^{-x^2} + \epsilon^2 e^{-2x^2} + O(\epsilon^3)$$

$$y_{inner}(x;\epsilon) \sim A(1 - e^{-\xi}) + \epsilon B(1 - e^{-\xi}) + \epsilon^2 C(1 - \xi^2) + O(\epsilon^3)$$

where

$$\xi \equiv \frac{x}{\epsilon^{1/2}}$$

Determine the coefficients A, B and C. Explain why the thickness of the overlap region, $\nu(\epsilon)$, must lie in the range

$$\epsilon^{1/2} \ll \nu(\epsilon) \ll \epsilon^{1/4}$$

as opposed to the normally assumed range $\epsilon^{1/2} \ll \nu(\epsilon) \ll 1$.

Appendix C

Companion Software

The companion CD supplied with this book contains a collection of computer programs that can be used to develop and validate turbulence models. The CD includes the following.

- FORTRAN source code
- Executable programs built with the Lahey Fortran-90 compiler
- Menu-driven Visual C++ input-data preparation programs that should function on all versions of the Microsoft Windows operating system
- Visual C++ plotting programs to display program output in graphical form
- Detailed technical and user information

The programs supplied on the companion CD fall into five categories...

1. Free Shear Flows: Programs **JET**, **MIXER** and **WAKE** solve for free-shear-flow farfield behavior.

2. Channel and Pipe Flow: Program **PIPE** solves for two-dimensional channel flow and axisymmetric pipe flow under fully-developed conditions.

3. Boundary-Layer Perturbation Analysis: Programs **DEFECT** and **SUBLAY** generate solutions for the classical defect layer and the viscous sublayer.

4. Boundary Layers: Program **EDDYBL** is a two-dimensional/axisymmetric boundary-layer program applicable to compressible boundary layers under laminar, transitional and turbulent flow conditions.

5. Separated Flows: Program **EDDY2C** is a two-dimensional/axisymmetric Reynolds-Averaged Navier Stokes (RANS) program applicable to compressible separated flows under laminar and turbulent flow conditions.

The menu-driven input-data preparation programs include default input values that can be modified as needed. Additionally, for Programs **EDDYBL** and **EDDY2C**, the companion CD includes input-data files for many of the test cases discussed throughout this book. The documentation on the CD indicates the flow each file corresponds to.

NOTE: If you discover any bugs in the software or errors in its documentation, please report what you have found by sending email through DCW Industries' Internet site at **http://www.dcwindustries.com**. As they become available, revisions and/or corrections to the software will be downloadable from the site, so you might want to check for updates from time to time.

Bibliography

Abe, H. and Kawamura, H. (2001), "Direct Numerical Simulation of a Fully Developed Turbulent Channel Flow with Respect to the Reynolds Number Dependence," *Journal of Fluids Engineering*, Vol. 123, No. 2, pp. 382-393.

Abid, R. and Speziale, C. G. (1993), "Predicting Equilibrium States with Reynolds Stress Closures in Channel Flow and Homogeneous Shear Flow," *Physics of Fluids A*, Vol. 5, p. 1776.

Abid, R., Morrison, J. H., Gatski, T. B. and Speziale, C. G. (1996), "Prediction of Complex Aerodynamic Flows with Explicit Algebraic Stress Models," AIAA Paper 96-0565.

Abramowitz, M. and Stegun, I. A. (1965), *Handbook of Mathematical Functions*, Dover Publications, Inc., New York, NY.

Adams, N. (2000), "Direct Simulation of the Turbulent Boundary Layer along a Compression Ramp at $M = 3$ and $Re_\theta = 1685$," *Journal of Fluid Mechanics*, Vol. 420, pp. 47-83.

Afzal, N. and Narasimha, R. (1976), "Axisymmetric Turbulent Boundary Layer Along a Circular Cylinder," *Journal of Fluid Mechanics*, Vol. 74, pp. 113-128.

Ahmed, S. R., Ramm, G. and Faltin, G. (1984), "Some Salient Features of the Time-Averaged Ground Vehicle Wake," SAE Paper 840300, Society of Automotive Engineers, Warrendale, PA.

Akselvoll, K. and Moin, P. (1993), "Large-Eddy Simulation of a Backward-Facing Step Flow," *Engineering Turbulence Modelling and Experiments 2*, (W. Rodi and F. Martelli, eds.), Elsevier, pp. 303-313.

Andersen, P. S., Kays, W. M. and Moffat, R. J. (1972), "The Turbulent Boundary Layer on a Porous Plate: An Experimental Study of the Fluid Mechanics for Adverse Free-Stream Pressure Gradients," Report No. HMT-15, Dept. Mech. Eng., Stanford University, CA.

Anderson, D. A., Tannehill, J. C. and Pletcher, R. H. (1984), *Computational Fluid Dynamics and Heat Transfer*, Hemisphere Publishing, Washington, DC.

Bachalo, W. D. and Johnson, D. A. (1979), "An Investigation of Transonic Turbulent Boundary Layer Separation Generated on an Axisymmetric Flow Model," AIAA Paper 79-1479.

Baggett, J. S. (1997), "Some Modeling Requirements for Wall Models in Large Eddy Simulation," NASA Ames/Stanford Center for Turbulence Research, *Annual Research Briefs*, pp. 123-134.

Baldwin, B. S. and Lomax, H. (1978), "Thin-Layer Approximation and Algebraic Model for Separated Turbulent Flows," AIAA Paper 78-257.

Baldwin, B. S. and Barth, T. J. (1990), "A One-Equation Turbulence Transport Model for High Reynolds Number Wall-Bounded Flows," NASA TM-102847 [see also AIAA Paper 91-0610 (1991)].

Bardina, J., Ferziger, J. H. and Reynolds, W. C. (1983), "Improved Turbulence Models Based on Large Eddy Simulation of Homogeneous, Incompressible, Turbulent Flows," Report No. TF-19, Dept. Mech. Eng., Stanford University, CA.

Bardina, J., Huang, P. G. and Coakley, T. J. (1997), "Turbulence Modeling Validation," AIAA Paper 97-2121.

Barenblatt, G. I. (1979), *Similarity, Self-Similarity and Intermediate Asymptotics*, Consultants Bureau, NY.

Barenblatt, G. I. (1991), "Scaling Laws (Incomplete Self-Similarity with Respect to Reynolds Numbers) for the Developed Turbulent Flows in Pipes," *CR Acad. Sc. Paris*, Series II, Vol. 313, pp. 307-312.

Barenblatt, G. I. (1993), "Scaling Laws for Fully Developed Turbulent Shear Flows. Part 1: Basic Hypotheses and Analysis," *Journal of Fluid Mechanics*, Vol. 248, pp. 513-520.

Barenblatt, G. I., Chorin, A. J. and Prostokishin, V. M. (1997), "Scaling Laws for Fully Developed Flow in Pipes," *Applied Mechanics Reviews*, Vol. 50, No. 7, pp. 413-429.

Barnwell, R. W. (1992), "Nonadiabatic and Three-Dimensional Effects in Compressible Turbulent Boundary Layers," *AIAA Journal*, Vol. 30, No. 4, pp. 897-904.

Barone, M. F., Oberkampf, W. L. and Blottner, F. G. (2006), "Validation Case Study: Prediction of Compressible Turbulent Mixing Layer Growth Rate," *AIAA Journal*, Vol. 44, No. 7, pp. 1488-1497.

Beam, R. M. and Warming, R. F. (1976), "An Implicit Finite-Difference Algorithm for Hyperbolic Systems in Conservation Law Form," *Journal of Computational Physics*, Vol. 22, pp. 87-110.

Bearman, P. W. (1972), "Some Measurements of the Distortion of Turbulence Approaching a Two-Dimensional Bluff Body," *Journal of Fluid Mechanics*, Vol. 53, Part 3, pp. 451-467.

Benay, R. and Servel, P. (2001), "Two-Equation k-σ Turbulence Model: Application to a Supersonic Base Flow," *AIAA Journal*, Vol. 39, No. 3, pp. 407-416.

Bender, C. M. and Orszag, S. A. (1978), *Advanced Mathematical Methods for Scientists and Engineers*, McGraw-Hill, New York, NY.

Bergé, P., Pomeau, Y. and Vidal, C. (1984), *Order within Chaos: Towards a Deterministic Approach to Turbulence*, John Wiley & Sons, New York, NY.

Bertolotti, F. P., Herbert, T. and Spalart, P. R. (1992), "Linear and Nonlinear Stability of the Blasius Boundary Layer," *Journal of Fluid Mechanics*, Vol. 242, pp. 441-474.

Birch, S. F. and Eggers, J. M. (1972), "Free Turbulent Shear Flows," NASA SP-321, Vol. 1, pp. 11-40.

Blair, M. F. and Werle, M. J. (1981), "Combined Influence of Free-Stream Turbulence and Favorable Pressure Gradients on Boundary Layer Transition and Heat Transfer," United Technologies Report No. R81-914388-17.

Blair, M. F. (1983), "Influence of Free-Stream Turbulence on Boundary Layer Heat Transfer and Mean Profile Development, Part 1 — Experimental Data," *Transactions of the ASME, Journal of Heat Transfer*, Vol. 105, pp. 33-40.

Blottner, F. G. (1974), "Variable Grid Scheme Applied to Turbulent Boundary Layers," *Comput. Meth. Appl. Mech. & Eng.*, Vol. 4, No. 2, pp. 179-194.

Boussinesq, J. (1877), "Théorie de l'Écoulement Tourbillant," *Mem. Présentés par Divers Savants Acad. Sci. Inst. Fr.*, Vol. 23, pp. 46-50.

Bradbury, L. J. S. (1965), "The Structure of a Self-Preserving Turbulent Plane Jet," *Journal of Fluid Mechanics*, Vol. 23, pp. 31-64.

Bradshaw, P., Ferriss, D. H. and Atwell, N. P. (1967), "Calculation of Boundary Layer Development Using the Turbulent Energy Equation," *Journal of Fluid Mechanics*, Vol. 28, Pt. 3, pp. 593-616.

Bradshaw, P. (1969), "The Response of a Constant-Pressure Turbulent Boundary Layer to the Sudden Application of an Adverse Pressure Gradient," R. & M. Number 3575, British Aeronautical Research Council.

Bradshaw, P. (1972), "The Understanding and Prediction of Turbulent Flow," *The Aeronautical Journal*, Vol. 76, No. 739, pp. 403-418.

Bradshaw, P. (1973a), "Effects of Streamline Curvature on Turbulent Flow," AGARD-AG-169.

Bradshaw, P. (1973b), "The Strategy of Calculation Methods for Complex Turbulent Flows," Imperial College Aero. Report No. 73-05.

Bradshaw, P. and Perot, J. B. (1993), "A Note on Turbulent Energy Dissipation in the Viscous Wall Region," *Physics of Fluids A*, Vol. 5, p. 3305.

Bradshaw, P. (1994), "Turbulence: The Chief Outstanding Difficulty of Our Subject," *Experiments in Fluids*, Vol. 16, pp. 203-216.

Bradshaw, P. and Huang, G. P. (1995), "The Law of the Wall in Turbulent Flow," *Proc. R. Soc. A*, Vol. 451, pp. 165-188.

Briggs, D. A., Ferziger, J. H., Koseff, J. R. and Monismith, S. G. (1996), "Entrainment in a Shear-Free Turbulent Mixing Layer," *Journal of Fluid Mechanics*, Vol. 310, pp. 215-241.

Brown, G. L. and Roshko, A. (1974), "On Density Effects and Large Structure in Turbulent Mixing Layers," *Journal of Fluid Mechanics*, Vol. 64, p. 775.

Brusniak, L. and Dolling, D. S. (1996), "Engineering Estimation of Fluctuating Loads in Shock Wave/Turbulent Boundary-Layer Interactions," *AIAA Journal*, Vol. 34, No. 12, pp. 2554-2561.

Bush, W. B. and Fendell, F. E. (1972), "Asymptotic Analysis of Turbulent Channel and Boundary-Layer Flow," *Journal of Fluid Mechanics*, Vol. 56, Pt. 4, pp. 657-681.

Buschmann, M. H. and Gad-el-Hak, M. (2003), "Debate Concerning the Mean-Velocity Profile of a Turbulent Boundary Layer," *AIAA Journal*, Vol. 41, No. 4, pp. 565-572.

Cabot, W. (1997), "Wall Models in Large Eddy Simulation of Separated Flow," NASA Ames/Stanford Center for Turbulence Research, *Annual Research Briefs*, pp. 97-106.

Carati, D. and Eijnden, E. V. (1997), "On the Self-Similarity Assumption in Dynamic Models for Large Eddy Simulations," *Physics of Fluids*, Vol. 9, pp. 2165-2167.

Castro, I. P. and Bradshaw, P. (1976), "The Turbulence Structure of a Highly Curved Mixing Layer," *Journal of Fluid Mechanics*, Vol. 73, p. 265.

Cazalbou, J. B., Spalart, P. R. and Bradshaw, P. (1994), "On the Behavior of Two-Equation Models at the Edge of a Turbulent Region," *Physics of Fluids*, Vol. 6, No. 5, pp. 1797-1804.

Cebeci, T. and Smith, A. M. O. (1974), *Analysis of Turbulent Boundary Layers*, Ser. in Appl. Math. & Mech., Vol. XV, Academic Press, Orlando, FL.

Chambers, T. L. and Wilcox, D. C. (1977), "Critical Examination of Two-Equation Turbulence Closure Models for Boundary Layers," *AIAA Journal*, Vol. 15, No. 6, pp. 821-828.

Champagne, F. H., Harris, V. G. and Corrsin, S. (1970), "Experiments on Nearly Homogeneous Turbulent Shear Flow," *Journal of Fluid Mechanics*, Vol. 41, Pt. 1, pp. 81-139.

Champney, J. (1989), "Modeling of Turbulence for Compression Corner Flows and Internal Flows," AIAA Paper 89-2344.

Chapman, D., Kuehn, D. and Larson, H. (1957), "Investigation of Separated Flows in Supersonic and Subsonic Streams with Emphasis on the Effect of Transition," NACA Report 1356.

Chien, K.-Y. (1982), "Predictions of Channel and Boundary-Layer Flows with a Low-Reynolds-Number Turbulence Model," *AIAA Journal*, Vol. 20, No. 1, pp. 33-38.

Choi, K. S. and Lumley, J. L. (1984), "Return to Isotropy of Homogeneous Turbulence Revisited," *Turbulence and Chaotic Phenomena in Fluids*, T. Tatsumi, ed., New York: North-Holland, NY, pp. 267-272.

Chou, P. Y. (1945), "On the Velocity Correlations and the Solution of the Equations of Turbulent Fluctuation," *Quart. Appl. Math.*, Vol. 3, p. 38.

Clark, J. A. (1968), "A Study of Incompressible Turbulent Boundary Layers in Channel Flows," *Journal of Basic Engineering*, Vol. 90, pp. 455.

Clark, R. A., Ferziger, J. H. and Reynolds, W. C. (1979), "Evaluation of Subgrid-Scale Models Using an Accurately Simulated Turbulent Flow," *Journal of Fluid Mechanics*, Vol. 91, pp. 1-16.

Clauser, F. H. (1956), "The Turbulent Boundary Layer", *Advances in Applied Mechanics*, Vol. IV, Academic Press, New York, NY, pp. 1-51.

Clemens, N. T. and Mungal, M. G. (1995), "Large-Scale Structure and Entrainment in the Supersonic Mixing Layer," *Journal of Fluid Mechanics*, Vol. 284, p. 171.

Coakley, T. J. (1983), "Turbulence Modeling Methods for the Compressible Navier-Stokes Equations," AIAA Paper 83-1693.

Coakley, T. J. and Huang, P. G. (1992), "Turbulence Modeling for High Speed Flows," AIAA Paper 92-0436.

Coleman, G. N. and Mansour, N. N. (1991), "Simulation and Modeling of Homogeneous Compressible Turbulence under Isotropic Mean Compression," Eighth Symposium on Turbulent Shear Flows, Munich, Germany.

Coleman, G. N., Kim, J. and Moser, R. D. (1995), "A Numerical Study of Turbulent Supersonic Isothermal-Wall Channel Flow," *Journal of Fluid Mechanics*, Vol. 305, p. 159.

Coles, D. E. and Hirst, E. A. (1969), *Computation of Turbulent Boundary Layers-1968 AFOSR-IFP-Stanford Conference*, Vol. II, Thermosciences Division, Stanford University, CA.

Comte-Bellot, G. (1963), "Contribution a l'Étude de la Turbulence de Conduite," PhD Thesis, University of Grenoble, France.

Comte-Bellot, G. (1965), "Écoulement Turbulent entre Deux Parois Parallèles," Publ. Sci. Tech. Ministère de l'Air, No. 419.

Comte-Bellot, G. and Corrsin, S. (1971), "Simple Eulerian Time Correlation of Full- and Narrow-Band Velocity Signals in Grid Generated Isotropic Turbulence," *Journal of Fluid Mechanics*, Vol. 48, pp. 273-337.

Corrsin, S. and Kistler, A. L. (1954), "The Free-Stream Boundaries of Turbulent Flows," NACA TN 3133.

Courant, R. and Hilbert, D. (1966), *Methods of Mathematical Physics*, Vol. II, Interscience Publishers, John Wiley & Sons, New York, NY.

Courant, R., Friedrichs, K. and Lewy, H. (1967), "On the Partial Difference Equations of Mathematical Physics," *IBM Journal*, pp. 215-234.

Craft, T. J., Fu, S., Launder, B. E. and Tselepidakis, D. P. (1989), "Developments in Modeling the Turbulent Second-Moment Pressure Correlations," Report No. TFD/89/1, Mech. Eng. Dept., Manchester Institute of Science and Technology, England.

Craft, T. J. and Launder, B. E. (1992), "New Wall-Reflection Model Applied to the Turbulent Impinging Jet," *AIAA Journal*, Vol. 30, No. 12, pp. 2970-2972.

Craft, T. J., Launder, B. E. and Suga, K. (1996), "Development and Application of a Cubic Eddy-Viscosity Model of Turbulence," *International Journal of Heat and Fluid Flow*, Vol. 17, No. 2, pp. 108-115.

Crank, J. and Nicolson, P. (1947), "A Practical Method for Numerical Evaluation of Solutions of Partial Differential Equations of the Heat-Conduction Type," *Proceedings of the Cambridge Philosophical Society*, Vol. 43, No. 50, pp. 50-67.

Crow, S. C. (1968), "Viscoelastic Properties of Fine-Grained Incompressible Turbulence," *Journal of Fluid Mechanics*, Vol. 33, Pt. 1, pp. 1-20.

Crowe, C. T., Troutt, T. R. and Chung, J. N. (1996), "Numerical Models for Two-Phase Turbulent Flows," *Annual review of Fluid Mechanics*, Vol. 28, p. 11.

Daly, B. J. and Harlow, F. H. (1970), "Transport Equations in Turbulence," *Physics of Fluids*, Vol. 13, pp. 2634-2649.

Davidov, B. I. (1961), "On the Statistical Dynamics of an Incompressible Fluid," *Doklady Akademiya Nauk SSSR*, Vol. 136, p. 47.

Deardorff, J. W. (1970), "A Numerical Study of Three-Dimensional Turbulent Channel Flow at Large Reynolds Numbers," *Journal of Fluid Mechanics*, Vol. 41, Pt. 2, pp. 453-480.

Deardorff, J. W. (1973), "The Use of Subgrid Transport Equations in a Three-Dimensional Model of Atmospheric Turbulence," *ASME, Journal of Fluids Engineering*, Vol. 95, pp. 429-438.

Degani, D. and Schiff, L. B. (1986), "Computation of Turbulent Supersonic Flows Around Pointed Bodies Having Crossflow Separation," *Journal of Computational Physics*, Vol. 66, No. 1, pp. 173-196.

Deissler, R. G. (1989), "On the Nature of Navier-Stokes Turbulence," NASA TM-109183.

Demuren, A. O. (1991), "Calculation of Turbulence-Driven Secondary Motion in Ducts with Arbitrary Cross Section," *AIAA Journal*, Vol. 29, No. 4, pp. 531-537.

Dhawan, S. and Narasimha, R. (1958), "Some Properties of Boundary Layer Flow During the Transition from Laminar to Turbulent Motion," *Journal of Fluid Mechanics*, Vol. 3, pp. 418-436.

Dolling, D. S. and Murphy, M. T. (1983), "Unsteadiness of the Separation Shock-Wave Structure in a Supersonic Compression Ramp Flowfield," *AIAA Journal*, Vol. 21, No. 12, pp. 1628-1634.

Domaradzki, J. A. and Saiki, E. M. (1997), "A Subgrid-Scale Model Based on the Estimation of Unresolved Scales of Turbulence," *Physics of Fluids*, Vol. 9, pp. 2148-2164.

Donaldson, C. duP. and Rosenbaum, H. (1968), "Calculation of the Turbulent Shear Flows Through Closure of the Reynolds Equations by Invariant Modeling," ARAP Report 127, Aeronautical Research Associates of Princeton, Princeton, NJ.

Donaldson, C. duP. (1972), "Construction of a Dynamic Model of the Production of Atmospheric Turbulence and the Dispersal of Atmospheric Pollutants," ARAP Report 175, Aeronautical Research Associates of Princeton, Princeton, NJ.

Driver, D. M. and Seegmiller, H. L. (1985), "Features of a Reattaching Turbulent Shear Layer in Divergent Channel Flow," *AIAA Journal*, Vol. 23, No. 1, pp. 163-171.

Driver, D. M. (1991), "Reynolds Shear Stress Measurements in a Separated Boundary Layer," AIAA Paper 91-1787.

Dryden, H. L. (1959), *Aerodynamics and Jet Propulsion*, Vol. V, University Press, Princeton, NJ.

DuFort, E. C. and Frankel, S. P. (1953), "Stability Conditions in the Numerical Treatment of Parabolic Differential Equations," *Math. Tables and Other Aids to Computation*, Vol. 7, pp. 135-152.

Durbin, P. A. (1991), "Near Wall Turbulence Closure Modeling Without 'Damping Functions'," *Theoretical and Computational Fluid Dynamics*, Vol. 3, No. 1, pp. 1-13.

Durbin, P. A. (1995), "Separated Flow Computations with the k-ϵ-v^2 Model," *AIAA Journal*, Vol. 33, No. 4, pp. 659-664.

Durbin, P. A. (1996), "On the k-ϵ Stagnation Point Anomaly," *International Journal of Heat and Fluid Flow*, Vol. 17, No. 1, pp. 89-90.

Durbin, P. A. and Pettersson Reif, B. A. (2001), *Statistical Theory and Modeling for Turbulent Flows*, John Wiley & Sons, New York, NY.

Dutoya, D. and Michard, P. (1981), "A Program for Calculating Boundary Layers Along Compressor and Turbine Blades," *Numerical Methods in Heat Transfer*, edited by R. W. Lewis, Morgan and O. C. Zienkiewicz, John Wiley & Sons, New York, NY.

Eaton, J. K. and Johnston, J. P. (1980), "Turbulent Flow Reattachment: An Experimental Study of the Flow and Structure Behind a Backward-Facing Step," Report No. MD-39, Dept. Mech. Eng., Stanford University, CA.

Emmons, H. W. (1954), "Shear Flow Turbulence," Proceedings of the 2^{nd} U. S. Congress of Applied Mechanics, ASME.

Escudier, M. P. (1966), "The Distribution of Mixing-Length in Turbulent Flows Near Walls," Imperial College, Heat Transfer Section Report TWF/TN/12.

Fage, A. and Falkner, V. M. (1932), "Note on Experiments on the Temperature and Velocity in the Wake of a Heated Cylindrical Obstacle," *Proc. R. Soc., Lond.*, Vol. A135, pp. 702-705.

Fan, S., Lakshminarayana, B. and Barnett, M. (1993), "A Low-Reynolds Number k-ϵ Model for Unsteady Turbulent Boundary Layer Flows," *AIAA Journal*, Vol. 31, No. 10, pp. 1777-1784.

Favre, A. (1965), "Equations des Gaz Turbulents Compressibles," *Journal de Mecanique*, Vol. 4, No. 3, pp. 361-390.

Fendell, F. E. (1972), "Singular Perturbation and Turbulent Shear Flow Near Walls," *Journal of the Astronautical Sciences*, Vol. 20, No. 3, pp. 129-165.

Fernholz, H. H. and Finley, P. J. (1981), "A Further Compilation of Compressible Boundary Layer Data with a Survey of Turbulence Data," AGARDograph 263.

Ferziger, J. H. (1976), "Large Eddy Numerical Simulations of Turbulent Flows," AIAA Paper 76-347.

Ferziger, J. H. (1989), "Estimation and Reduction of Numerical Error," Forum on Methods of Estimating Uncertainty Limits in Fluid Flow Computations, ASME Winter Annual Meeting, San Francisco, CA.

Ferziger, J. H. (1996), "Recent Advances in Large-Eddy Simulation," *Engineering Turbulence Modelling and Experiments 3*, (W. Rodi and G. Begeles, eds.), Elsevier, p. 163.

Ferziger, J. H. and Perić, M. (1996), *Computational Methods for Fluid Dynamics*, Springer-Verlag, Berlin, Germany.

Fisher, D. F. and Dougherty, N. S. (1982), "Transition Measurements on a 10° Cone at Mach Numbers from 0.5 to 2.0," NASA TP-1971.

Forsythe, J. R., Strang, W. Z. and Hoffmann, K. A. (2000), "Validation of Several Reynolds-Averaged Turbulence Models in a 3-D Unstructured Grid Code," AIAA Paper 00-2552.

Forsythe, J. R., Hoffmann, K. A., Cummings, R. M. and Squires, K. D. (2002), "Detached-Eddy Simulation with Compressibility Corrections Applied to a Supersonic Axisymmetric Base Flow," *Journal of Fluids Engineering*, Vol. 124, No. 4, pp. 911-923.

Fu, S., Launder, B. E. and Tselepidakis, D. P. (1987), "Accommodating the Effects of High Strain Rates in Modelling the Pressure-Strain Correlation," Report No. TFD/87/5, Mech. Eng. Dept., Manchester Institute of Science and Technology, England.

Gatski, T. B. and Speziale, C. G. (1992), "On Explicit Algebraic Stress Models for Complex Turbulent Flows," *Journal of Fluid Mechanics*, Vol. 254, pp. 59-78.

Gee, K., Cummings, R. M. and Schiff, L. B. (1992), "Turbulence Model Effects on Separated Flow About a Prolate Spheroid," *AIAA Journal*, Vol. 30, No. 3, pp. 655-664.

George, W. K. Knecht, P. and Castillo, L. (1992), "The Zero-Pressure Gradient Turbulent Boundary Layer Revisited," *Proceedings of the 13th Biennial Symposium on Turbulence*, University of Missouri–Rolla.

Germano, M., Piomelli, U., Moin, P. and Cabot, W. (1991), "A Dynamic Subgrid-Scale Eddy Viscosity Model," *Physics of Fluids A*, Vol. 3, p. 1760.

Gerolymos, G. A. (1990), "Implicit Multiple-Grid Solution of the Compressible Navier-Stokes Equations Using k-ϵ Turbulence Closure," *AIAA Journal*, Vol. 28, pp. 1707-1717.

Gerolymos, G. A. and Vallet, I. (2001), "Wall-Normal-Free Near-Wall Reynolds-Stress Closure for Three-Dimensional Compressible Separated Flows," *AIAA Journal*, Vol. 39, pp. 1833-1842.

Gerolymos, G. A., Sauret, E. and Vallet, I. (2004a), "Oblique-Shock-Wave/Boundary-Layer Interaction Using Near-Wall Reynolds Stress Models," *AIAA Journal*, Vol. 42, No. 6, pp. 1089-1100.

Gerolymos, G. A., Sauret, E. and Vallet, I. (2004b), "Influence of Inflow Turbulence in Shock-Wave/Turbulent-Boundary-Layer Interaction Computations," *AIAA Journal*, Vol. 42, No. 6, pp. 1101-1106.

Ghalichi, F., Deng, X., DeChamplain, A., Douville, Y., King, M. and Guidoin, R. (1998), "Low Reynolds Number Turbulence Modeling of Blood Flow in Arterial Stenoses," *Biorheology*, Vol. 35, pp. 281-294.

Ghosal, S., Lund, T. S., Moin, P. and Akselvoll, K. (1995), "A Dynamic Localization Model for Large-Eddy Simulation of Turbulent Flows," *Journal of Fluid Mechanics*, Vol. 286, pp. 229-255.

Ghosal, S. (1999), "Mathematical and Physical Constraints on Large-Eddy Simulation of Turbulence," *AIAA Journal*, Vol. 37, No. 4, pp. 425-433.

Gibson, M. M. and Launder, B. E. (1978), "Ground Effects on Pressure Fluctuations in the Atmospheric Boundary Layer," *Journal of Fluid Mechanics*, Vol. 86, Pt. 3, pp. 491-511.

Gibson, M. M. and Younis, B. A. (1986), "Calculation of Swirling Jets with a Reynolds Stress Closure," *Physics of Fluids*, Vol. 29, pp. 38-48.

Gleick, J. (1988), *Chaos: Making a New Science*, Penguin Books, New York, NY.

Glushko, G. (1965), "Turbulent Boundary Layer on a Flat Plate in an Incompressible Fluid," *Izvestia Akademiya Nauk SSSR, Mekh.*, No. 4, p. 13.

Goddard, F. E. Jr. (1959), "Effect of Uniformly Distributed Roughness on Turbulent Skin-Friction Drag at Supersonic Speeds," *J. Aero/Space Sciences*, Vol. 26, No. 1, pp. 1-15, 24.

Godunov, S. K. (1959), "Finite Difference Method for Numerical Computation of Discontinuous Solutions of the Equations of Fluid Dynamics," *Matematicheskii Sbornik*, Vol. 47, No. 3, pp. 271-306.

Goldberg, U. C. (1991), "Derivation and Testing of a One-Equation Model Based on Two Time Scales," *AIAA Journal*, Vol. 29, No. 8, pp. 1337-1340.

Gulyaev, A. N., Kozlov, A. N., Ye, V. and Sekundov, A. N. (1993), "Universal Turbulence Model ν_t - 92," ECOLEN, Science Research Center, Preprint No. 3, Moscow.

Halleen, R. M. and Johnston, J. P. (1967), "The Influence of Rotation on Flow in a Long Rectangular Channel - An Experimental Study," Report No. MD-18, Dept. Mech. Eng., Stanford University, CA.

Han, T. (1989), "Computational Analysis of Three-Dimensional Turbulent Flow Around a Bluff Body in Ground Proximity," *AIAA Journal*, Vol. 27, No. 9, pp. 1213-1219.

Hanjalić, K. (1970), "Two-Dimensional Flow in an Axisymmetric Channel," PhD Thesis, University of London.

Hanjalić, K. and Launder, B. E. (1976), "Contribution Towards a Reynolds-Stress Closure for Low-Reynolds-Number Turbulence," *Journal of Fluid Mechanics*, Vol. 74, Pt. 4, pp. 593-610.

Hanjalić, K., Jakirlić, S. and Hadzić, I. (1997), "Expanding the Limits of 'Equilibrium' Second-Moment Turbulence Closures," *Fluid Dynamics Research*, Vol. 20, pp. 25-41.

Harlow, F. H. and Nakayama, P. I. (1968), "Transport of Turbulence Energy Decay Rate," Los Alamos Sci. Lab., University of California Report LA-3854.

Harris, V. G., Graham, J. A. H. and Corrsin, S. (1977), "Further Experiments in Nearly Homogeneous Turbulent Shear Flow," *Journal of Fluid Mechanics*, Vol. 81, p. 657.

Hassid, S. and Poreh, M. (1978), "A Turbulent Energy Dissipation Model for Flows with Drag Reduction," *ASME, Journal of Fluids Engineering*, Vol. 100, pp. 107-112.

Haworth, D. C. and Pope, S. B. (1986), "A Generalized Langevin Model for Turbulent Flows," *Physics of Fluids*, Vol. 29, pp. 387-405.

Hayes, W. D. and Probstein, R. F. (1959), *Hypersonic Flow Theory*, Academic Press, New York, NY, p. 290.

Hellsten, A. (2005), "New Advanced k-ω Turbulence Model for High-Lift Aerodynamics," *AIAA Journal*, Vol. 43, No. 9, pp. 1857-1869.

Henkes, R. A. W. M. (1998a), "Scaling of Equilibrium Boundary Layers Under Adverse Pressure Gradient Using Turbulence Models," *AIAA Journal*, Vol. 36, No. 3, pp. 320-326.

Henkes, R. A. W. M. (1998b), "Comparison of Turbulence Models for Attached Boundary Layers Relevant to Aeronautics," *Applied Scientific Research*, Vol. 57, No. 1, pp. 43-65.

Herrin, J. L. and Dutton, J. C. (1994), "Supersonic Base Flow Experiments in the Near Wake of a Cylindrical Afterbody," *AIAA Journal*, Vol. 32, No. 1, pp. 77-83.

Heskestad, G. (1965), "Hot-Wire Measurements in a Plane Turbulent Jet," *Journal of Applied Mechanics*, Vol. 32, No. 4, pp. 721-734.

Higuchi, H. and Rubesin, M. W. (1978), "Behavior of a Turbulent Boundary Layer Subjected to Sudden Transverse Strain," AIAA Paper 78-201.

Hinze, J. O. (1975), *Turbulence*, Second Ed., McGraw-Hill, New York, NY.

Hoffmann, G. H. (1975), "Improved Form of the Low-Reynolds-Number k-ϵ Turbulence Model," *Physics of Fluids*, Vol. 18, pp. 309-312.

Holden, M. S. (1978), "A Study of Flow Separation in Regions of Shock Wave-Boundary Layer Interaction in Hypersonic Flow," AIAA Paper 78-1168.

Horstman, C. C. (1992), "Hypersonic Shock-Wave/Turbulent-Boundary-Layer Interaction Flows," *AIAA Journal*, Vol. 30, No. 6, pp. 1480-1481.

Huang, P. G., Bradshaw, P. and Coakley, T. J. (1992), "Assessment of Closure Coefficients for Compressible-Flow Turbulence Models," NASA TM-103882.

Huang, P. G. and Coakley, T. J. (1992), "An Implicit Navier-Stokes Code for Turbulent Flow Modeling," AIAA Paper 92-547.

Huang, P. G. and Liou, W. W. (1994), "Numerical Calculations of Shock-Wave/Boundary-Layer Flow Interactions," NASA TM 106694.

Huang, P. G., Coleman, G. N. and Bradshaw, P. (1995), "Compressible Turbulent Channel Flows - DNS Results and Modelling," *Journal of Fluid Mechanics*, Vol. 305, p. 185.

Huang, P. G. (1999), "Physics and Computations of Flows with Adverse Pressure Gradients," *Modeling Complex Turbulent Flows* (M. Salas, et al. eds.), Kluwer, pp. 245-258.

Hung, C. M. (1976), "Development of Relaxation Turbulence Models," NASA CR-2783.

Hwang, C. B. and Lin, C. A. (1998), "Improved Low-Reynolds-Number k-$\tilde{\epsilon}$ Model Based on Direct Numerical Simulation Data," *AIAA Journal*, Vol. 36, No. 1, pp. 38-43.

Ibbetson, A. and Tritton, D. J. (1975), "Experiments on Turbulence in Rotating Fluid," *Journal of Fluid Mechanics*, Vol. 68, Pt. 4, pp. 639-672.

Inger, G. (1986), "Incipient Separation and Similitude Properties of Swept Shock/Turbulent Boundary Layer Interactions," AIAA Paper 86-345.

Jayaraman, R., Parikh, P. and Reynolds, W. C. (1982), "An Experimental Study of the Dynamics of an Unsteady Turbulent Boundary Layer," Report No. TF-18, Dept. Mech. Eng., Stanford University, CA.

Jeans, J. (1962), *An Introduction to the Kinetic Theory of Gases*, Cambridge University Press, London.

Jiménez, J. (1995), "On Why Dynamic Subgrid-Scale Models Work," NASA Ames/Stanford Center for Turbulence Research, *Annual Research Briefs*, pp. 25-34.

Jiménez, J. and Moser, R. D. (2000), "Large-Eddy Simulations: Where Are We and What Can We Expect?," *AIAA Journal*, Vol. 38, No. 4, pp. 605-612.

Johnson, D. A. and King, L. S. (1985), "A Mathematically Simple Turbulence Closure Model for Attached and Separated Turbulent Boundary Layers," *AIAA Journal*, Vol. 23, No. 11, pp. 1684-1692.

Johnson, D. A. (1987), "Transonic Separated Flow Predictions with an Eddy-Viscosity/Reynolds-Stress Closure Model," *AIAA Journal*, Vol. 25, No. 2, pp. 252-259.

Johnson, D. A. and Coakley, T. J. (1990), "Improvements to a Nonequilibrium Algebraic Turbulence Model," *AIAA Journal*, Vol. 28, No. 11, pp. 2000-2003.

Johnston, J. P., Halleen, R. M. and Lezius, D. K. (1972), "Effects of a Spanwise Rotation on the Structure of Two-Dimensional Fully-Developed Turbulent Channel Flow," *Journal of Fluid Mechanics*, Vol. 56, pp. 533-557.

Jones, W. P. and Launder, B. E. (1972), "The Prediction of Laminarization with a Two-Equation Model of Turbulence," *International Journal of Heat and Mass Transfer*, Vol. 15, pp. 301-314.

Jones, S. A. (1985), "A Study of Flow Downstream of a Constriction in a Cylindrical Tube at Low Reynolds Numbers with Emphasis on Frequency Correlations," PhD Thesis, University of California.

Jongen, T., Mompean, G. and Gatski, T. B. (1998), "Predicting S-Duct Flow Using a Composite Algebraic Stress Model," *AIAA Journal*, Vol. 36, No. 3, pp. 327-335.

Jovic, S. and Driver, D. (1994), "Backward-Facing Step Measurements at Low Reynolds Number," NASA TM-108870.

Jovic, S. and Driver, D. (1995), "Reynolds Number Effect on the Skin Friction in Separated Flows behind a Backward-Facing Step," *Experiments in Fluids*, pp. 464-467.

Kandula, M. and Wilcox, D. C. (1995), "An Examination of k-ω Turbulence Model for Boundary Layers, Free Shear Layers and Separated Flows," AIAA Paper 95-2317.

Kapadia, S., Roy, S. and Wurtzler, K. (2003), "Detached Eddy Simulation Over a Reference Ahmed Car Model," AIAA Paper 2003-0857.

Keefe, L. (1990), "Connecting Coherent Structures and Strange Attractors," in *Near-Wall Turbulence – 1988 Zaric Memorial Conference*, S. J. Kline and N. H. Afgan, eds., Hemisphere, Washington, DC.

Kevorkian, J. and Cole, J. D. (1981), *Perturbation Methods in Applied Mathematics*, Springer-Verlag, New York, NY.

Kim, J., Kline, S. J. and Johnston, J. P. (1980), "Investigation of a Reattaching Turbulent Shear Layer: Flow Over a Backward-Facing Step," *ASME, Journal of Fluids Engineering*, Vol. 102, pp. 302-308.

Kim, J., Moin, P. and Moser, R. (1987), "Turbulence Statistics in Fully Developed Channel Flow at Low Reynolds Number," *Journal of Fluid Mechanics*, Vol. 177, pp. 133-166.

Klebanoff, P. S. (1954), "Characteristics of Turbulence in a Boundary Layer with Zero Pressure Gradient," NACA TN 3178.

Klebanoff, P. S. (1955), "Characteristics of Turbulence in a Boundary Layer with Zero Pressure Gradient," NACA TN 1247.

Kline, S. J., Morkovin, M. V., Sovran, G. and Cockrell, D. J. (1969), *Computation of Turbulent Boundary Layers – 1968 AFOSR-IFP-Stanford Conference*, Vol. I, Thermosciences Division, Stanford University, CA.

Kline, S. J., Cantwell, B. J. and Lilley, G. M. (1981), *1980-81 AFOSR-HTTM-Stanford Conference on Complex Turbulent Flows*, Thermosciences Division, Stanford University, CA.

Knight, D. D., Horstman, C. C., Shapey, B and Bogdonoff, S. (1987), "Structure of Supersonic Flow Past a Sharp Fin," *AIAA Journal*, Vol. 25, No. 10, pp. 1331-1337.

Knight, D. D. (1993), "Numerical Simulation of 3-D Shock Wave Turbulent Boundary-Layer Interactions," AGARD/FDP Short Course on Shock Wave-Boundary Layer Interactions in Supersonic and Hypersonic Flows, von Kármán Institute for Fluid Dynamics, Brussels, Belgium, (May 24-28, 1993).

Knight, D. D. (1997), "Numerical Simulation of Compressible Turbulent Flows Using the Reynolds-Averaged Navier-Stokes Equations," AGARD Report R-819.

Knight, D. D., Yan, H., Panaras, A. G. and Zheltovodov, A. (2003), "Advances in CFD Prediction of Shock Wave Turbulent Boundary Layer Interactions," *Progress in Aerospace Sciences*, Vol. 39, pp. 121-184.

Kok, J. C. (2000), "Resolving the Dependence on Freestream Values for the k-ω Turbulence Model," *AIAA Journal*, Vol. 38, No. 7, pp. 1292-1295.

Kolmogorov, A. N. (1941), "Local Structure of Turbulence in Incompressible Viscous Fluid for Very Large Reynolds Number," *Doklady Akademiya Nauk SSSR*, Vol. 30, pp. 299-303.

Kolmogorov, A. N. (1942), "Equations of Turbulent Motion of an Incompressible Fluid," *Izvestia Academy of Sciences, USSR; Physics*, Vol. 6, Nos. 1 and 2, pp. 56-58.

Krajnović, S. and Davidson, L. (2002), "Large-Eddy Simulation of the Flow Around a Bluff Body," *AIAA Journal*, Vol. 40, No. 5, pp. 927-936.

Kuntz, D. W., Amatucci, V. A. and Addy, A. L. (1987), "Turbulent Boundary-Layer Properties Downstream of the Shock-Wave/Boundary-Layer Interaction," *AIAA Journal*, Vol. 25, No. 5, pp. 668-675.

Kussoy, M. I. and Horstman, C. C. (1989), "Documentation of Two- and Three-Dimensional Hypersonic Shock Wave/Turbulent Boundary Layer Interaction Flows," NASA TM 101075.

Lai, Y. G., So, R. M. C., Anwer, M. and Hwang, B. C. (1991), "Calculations of a Curved-Pipe Flow Using Reynolds Stress Closure," *Journal of Mechanical Engineering Science*, Vol. 205, Part C, pp. 231-244.

Lakshminarayana, B. (1986), "Turbulence Modeling for Complex Shear Flows," *AIAA Journal*, Vol. 24, No. 12, pp. 1900-1917.

Lam, C. K. G. and Bremhorst, K. A. (1981), "Modified Form of k-ϵ Model for Predicting Wall Turbulence," *ASME, Journal of Fluids Engineering*, Vol. 103, pp. 456-460.

Landahl, M. T. and Mollo-Christensen, E. (1992), *Turbulence and Random Processes in Fluid Mechanics*, 2^{nd} Ed., Cambridge Univ. Press, New York, NY.

Laufer, J. (1950), "Some Recent Measurements in a Two-Dimensional Turbulent Channel," *Journal of the Aeronautical Sciences*, Vol. 17, pp. 277-287.

Laufer, J. (1951), "Investigation of Turbulent Flow in a Two Dimensional Channel," NACA Rept. 1053.

Laufer, J. (1952), "The Structure of Turbulence in Fully Developed Pipe Flow," NACA Rept. 1174.

Launder, B. E. and Spalding, D. B. (1972), *Mathematical Models of Turbulence*, Academic Press, London.

Launder, B. E. and Sharma, B. I. (1974), "Application of the Energy Dissipation Model of Turbulence to the Calculation of Flow Near a Spinning Disc," *Letters in Heat and Mass Transfer*, Vol. 1, No. 2, pp. 131-138.

Launder, B. E., Reece, G. J. and Rodi, W. (1975), "Progress in the Development of a Reynolds-Stress Turbulence Closure," *Journal of Fluid Mechanics*, Vol. 68, Pt. 3, pp. 537-566.

Launder, B. E., Priddin, C. H. and Sharma, B. I. (1977), "The Calculation of Turbulent Boundary Layers on Spinning and Curved Surfaces," *ASME, Journal of Fluids Engineering*, Vol. 99, p. 231.

Launder, B. E. and Morse, A. (1979), "Numerical Prediction of Axisymmetric Free Shear Flows with a Second-Order Reynolds Stress Closure," *Turbulent Shear Flows I*, edited by F. Durst, B. E. Launder, F. W. Schmidt and J. Whitelaw, Springer-Verlag, Berlin.

Launder, B. E. and Shima, N. (1989), "Second-Moment Closure for the Near-Wall Sublayer: Development and Application," *AIAA Journal*, Vol. 27, No. 10, pp. 1319-1325.

Launder, B. E. (Ed.) (1992), *Fifth Biennial Colloquium on Computational Fluid Dynamics*, Manchester Institute of Science and Technology, England.

Launder, B. E. and Li, S.-P. (1994), "On the Elimination of Wall-Topography Parameters from Second-Moment Closure," *Physics of Fluids*, Vol. 6, p. 999.

Laurence, D. and Durbin, P. A. (1994), "Modeling Near Wall Effects in Second Moment Closures by Elliptic Relaxation," NASA Ames/Stanford Center for Turbulence Research, Summer Program 1994, p. 323.

Law, C. H. (1973), "Supersonic, Turbulent Boundary Layer Separation Measurements at Reynolds Numbers of 10^7 to 10^8," AIAA Paper 73-665.

Lax, P. D. and Wendroff, B. (1960), "Systems of Conservation Laws," *Communications on Pure and Applied Mathematics*, Vol. 13, pp. 217-237.

Le, H., Moin, P. and Kim, J. (1997), "Direct Numerical Simulation of Turbulent Flow over a Backward-Facing Step," *Journal of Fluid Mechanics*, Vol. 330, pp. 349-374.

Le Penven, L., Gence, J. N. and Comte-Bellot, G. (1984), "On the Approach to Isotropy of Homogeneous Turbulence — Effect of the Partition of Kinetic Energy Among the Velocity Components," *Frontiers in Fluid Mechanics*, S. H. Davis and J. L. Lumley, eds., Springer-Verlag, New York, NY, p. 1.

Lele, S. K. (1985), "A Consistency Condition for Reynolds Stress Closures," *Physics of Fluids*, Vol. 28, p. 64.

Leonard, A. (1974), "Energy Cascade in Large-Eddy Simulations of Turbulent Fluid Flows," *Advances in Geophysics*, Vol. 18A, pp. 237-248.

Lesieur, M. and Metais, O. (1996), "New Trends in Large-Eddy Simulations of Turbulence," *Annual Review of Fluid Mechanics*, Vol. 28, p. 45.

Libby, P. A. (1996), *Introduction to Turbulence*, Taylor and Francis, Bristol, PA.

Liepmann, H. W. and Laufer, J. (1947), "Investigations of Free Turbulent Mixing," NACA TN 1257.

Lilly, D. K. (1965), "On the Computational Stability of Numerical Solutions of Time-Dependent Non-Linear Geophysical Fluid Dynamics Problems," *Monthly Weather Review*, U. S. Weather Bureau, Vol. 93, No. 1, pp. 11-26.

Lilly, D. K. (1966), "On the Application of the Eddy Viscosity Concept in the Inertial Subrange of Turbulence," NCAR Manuscript 123.

Liou, W. W. and Huang, P. G. (1996), "Calculations of Oblique Shock Wave/Turbulent Boundary-Layer Interactions with New Two-Equation Turbulence Models," NASA CR-198445.

Lumley, J. L. (1970), "Toward a Turbulent Constitutive Equation," *Journal of Fluid Mechanics*, Vol. 41, pp. 413-434.

Lumley, J. L. (1972), "A Model for Computation of Stratified Turbulent Flows," Int. Symposium on Stratified Flow, Novisibirsk.

Lumley, J. L. (1978), "Computational Modeling of Turbulent Flows," *Adv. Appl. Mech.*, Vol. 18, pp. 123-176.

MacCormack, R. W. (1969), "The Effect of Viscosity in Hypervelocity Impact Cratering," AIAA Paper 69-354.

MacCormack, R. W. (1985), "Current Status of Numerical Solutions of the Navier-Stokes Equations," AIAA Paper 85-32.

Maise, G. and McDonald, H. (1967), "Mixing Length and Kinematic Eddy Viscosity in a Compressible Boundary Layer," AIAA Paper 67-199.

Mansour, N. N., Kim, J. and Moin, P. (1988), "Reynolds Stress and Dissipation Rate Budgets in Turbulent Channel Flow," *Journal of Fluid Mechanics*, Vol. 194, pp. 15-44.

Marshall, T. A. and Dolling, D. S. (1992), "Computation of Turbulent, Separated, Unswept Compression Ramp Interactions," *AIAA Journal*, Vol. 30, No. 8, pp. 2056-2065.

Marvin, J. G. and Huang, G. P. (1996), "Turbulence Modeling — Progress and Future Outlook," Keynote Lecture presented at the 15^{th} International Conference on Numerical Methods in Fluid Dynamics, June 24-28, Monterey, CA.

Mellor, G. L. (1972), "The Large Reynolds Number Asymptotic Theory of Turbulent Boundary Layers," *International Journal of Engineering Science*, Vol. 10, p. 851.

Mellor, G. L. and Herring, H. J. (1973), "A Survey of Mean Turbulent Field Closure Models," *AIAA Journal*, Vol. 11, No. 5, pp. 590-599.

Menon, S. and Kim, W.-W. (1996), "High Reynolds Number Flow Simulations Using the Localized Dynamic Subgrid-Scale Model," AIAA Paper 96-0425.

Menter, F. R. (1992a), "Influence of Freestream Values on k-ω Turbulence Model Predictions," *AIAA Journal*, Vol. 30, No. 6, pp. 1657-1659.

Menter, F. R. (1992b), "Performance of Popular Turbulence Models for Attached and Separated Adverse Pressure Gradient Flows," *AIAA Journal*, Vol. 30, No. 8, pp. 2066-2072.

Menter, F. R. (1992c), "Improved Two-Equation k-ω Turbulence Models for Aerodynamic Flows," NASA TM-103975.

Menter, F. R. (1994), "Eddy Viscosity Transport Equations and Their Relation to the k-ϵ Model," NASA TM-108854.

Menter, F. R. (1994), "A Critical Evaluation of Promising Eddy-Viscosity Models," International Symposium on Turbulence, Heat and Mass Transfer, August 9-12, 1994, Lisbon, Spain.

Merci, B., Steelant, J., Vierendeels, J., Riemslagh, K. and Dick, E. (2000), "Computational Treatment of Source Terms in Two-Equation Turbulence Models," *AIAA Journal*, Vol. 38, No. 11, pp. 2085-2093.

Meroney, R. N. and Bradshaw, P. (1975), "Turbulent Boundary-Layer Growth Over a Longitudinally Curved Surface," *AIAA Journal*, Vol. 13, pp. 1448-1453.

Millikan, C. B. (1938), "A Critical Discussion of Turbulent Flow in Channels and Circular Tubes," *Proceedings of the 5th International Conference of Theoretical and Applied Mechanics*, pp. 386-392, MIT Press, Cambridge, MA.

Minkowycz, W. J., Sparrow, E. M., Schneider, G. E. and Pletcher, R. H. (1988), *Handbook of Numerical Heat Transfer*, Wiley, New York.

Moin, P. and Kim, J. (1997), "Tackling Turbulence with Supercomputers," *Scientific American*.

Moin, P. and Mahesh, K. (1998), "Direct Numerical Simulation – A Tool in Turbulence Research," *Annual Review of Fluid Mechanics*, Vol. 30, pp. 539-578.

Moore, J. G. and Moore, J. (1999), "Realizability in Two-Equation Turbulence Models," AIAA Paper 99-3779.

Morkovin, M. V. (1962), "Effects of Compressibility on Turbulent Flow," *The Mechanics of Turbulence*, A. Favre, Ed., Gordon and Breach, p. 367.

Morris, P. J. (1984), "Modeling the Pressure Redistribution Terms," *Physics of Fluids*, Vol. 27, No. 7, pp. 1620-1623.

Moser, R. D. and Moin, P. (1984), "Direct Numerical Simulation of Curved Turbulent Channel Flow," NASA TM-85974.

Murthy, V. S. and Rose, W. C. (1978), "Wall Shear Stress Measurements in a Shock-Wave/Boundary-Layer Interaction," *AIAA Journal*, Vol. 16, No. 7, pp. 667-672.

Myong, H. K. and Kasagi, N. (1990), "A New Approach to the Improvement of k-ϵ Turbulence Model for Wall-Bounded Shear Flows," *JSME International Journal*, Vol. 33, pp. 63-72.

Narayanswami, N., Horstman, C. C. and Knight, D. D. (1993), "Computation of Crossing Shock/Turbulent Boundary Layer Interaction at Mach 8.3," *AIAA Journal*, Vol. 31, No. 8, pp. 1369-1376.

Nayfeh, A. H. (1981), *Introduction to Perturbation Techniques*, John Wiley and Sons, Inc., New York, NY.

Nee, V. W. and Kovasznay, L. S. G. (1968), "The Calculation of the Incompressible Turbulent Boundary Layer by a Simple Theory," *Physics of Fluids*, Vol. 12, p. 473.

Ng, K. H. and Spalding, D. B. (1972), "Some Applications of a Model of Turbulence to Boundary Layers Near Walls," *Physics of Fluids*, Vol. 15, No. 1, pp. 20-30.

Nichols, R. H. and Nelson, C. C. (2004), "Wall Function Boundary Conditions Including Heat Transfer and Compressibility," *AIAA Journal*, Vol. 42, No. 6, pp. 1107-1114.

Oh, Y. H. (1974), "Analysis of Two-Dimensional Free Turbulent Mixing," AIAA Paper 74-594.

Olsen, M. E. and Coakley, T. J. (2001), "The Lag Model, a Turbulence Model for Non Equilibrium Flows," AIAA Paper 2001-2564.

Olsen, M. E., Lillard, R. P. and Coakley, T. J. (2005), "The Lag Model Applied to High Speed Flows," AIAA Paper 2005-0101.

Papamoschou, D. and Roshko, A. (1988), "The Compressible Turbulent Shear Layer - An Experimental Study," *Journal of Fluid Mechanics*, Vol. 197, pp. 453-477.

Papp, J. L. and Ghia, K. N. (2001), "Application of the RNG Turbulence Model to the Simulation of Axisymmetric Supersonic Separated Base Flows," AIAA Paper 2001-0727.

Papp, J. L. and Dash, S. M. (2001), "Turbulence Model Unification and Assessment for High-Speed Aeropropulsive Flows," AIAA Paper 2001-0880.

Parneix, S., Laurence, D. and Durbin, P. A. (1998), "A Procedure for Using DNS Databases," *Journal of Fluids Engineering*, Vol. 120, pp. 40-46.

Patel, V. C. (1968), "The Effects of Curvature on the Turbulent Boundary Layer," Aeronautical Research Council Reports and Memoranda No. 3599.

Patel, V. C., Rodi, W. and Scheuerer, G. (1985), "Turbulence Models for Near-Wall and Low Reynolds Number Flows: A Review," *AIAA Journal*, Vol. 23, No. 9, pp. 1308-1319.

Patel, V. C. and Sotiropoulos, F. (1997), "Longitudinal Curvature Effects in Turbulent Boundary Layers," *Progress in Aerospace Sciences*, Vol. 33, p. 1.

Peaceman, D. W. and Rachford, H. H., Jr. (1955), "The Numerical Solution of Parabolic and Elliptic Differential Equations," *J. Soc. Indust. Applied Mathematics*, Vol. 3, No. 1, pp. 28-41.

Peng, S.-H., Davidson, L. and Holmberg, S. (1997), "A Modified Low-Reynolds Number k-ω Model for Recirculating Flows," *Journal of Fluids Engineering*, Vol. 119, pp. 867-875.

Petrov, G., Likhusin, V., Nekrasov, I. and Sorkin, L. (1952), "Influence of Viscosity on the Supersonic Flow with Shock Waves," *CIAM*, No. 224 [in Russian].

Peyret, R. and Taylor, T. D. (1983), *Computational Methods for Fluid Flow*, Springer-Verlag, New York, NY.

Piomelli, U., Yu, Y. and Adrian, R. J. (1996), "Subgrid-Scale Energy Transfer and Near-Wall Turbulence Structure," *Physics of Fluids*, Vol. 8, pp. 215-224.

Pitsch, H. (2006), "Large-Eddy Simulation of Turbulent Combustion," *Annual Review of Fluid Mechanics*, Vol. 38, pp. 453-482.

Pomraning, E. and Rutland, C. J. (2002), "Dynamic One-Equation Nonviscosity Large-Eddy Simulation Model," *AIAA Journal*, Vol. 40, No. 4, pp. 689-701.

Pope, S. B. (1975), "A More General Effective Viscosity Hypothesis," *Journal of Fluid Mechanics*, Vol. 72, pp. 331-340.

Pope, S. B. (1978), "An Explanation of the Turbulent Round-Jet/Plane-Jet Anomaly," *AIAA Journal*, Vol. 16, No. 3, pp. 279-281.

Prandtl, L. (1925), "Über die ausgebildete Turbulenz," *ZAMM*, Vol. 5, pp. 136-139.

Prandtl, L. (1945), "Über ein neues Formelsystem für die ausgebildete Turbulenz," *Nacr. Akad. Wiss. Göttingen, Math-Phys. Kl.*, pp. 6-19.

Rahman, M. M. and Siikonen, T. (2002), "Low-Reynolds-Number k-$\tilde{\epsilon}$ Model with Enhanced Near-Wall Dissipation," *AIAA Journal*, Vol. 40, No. 7, pp. 1462-1464.

Rastogi, A. K. and Rodi, W. (1978), "Calculation of General Three Dimensional Turbulent Boundary Layers," *AIAA Journal*, Vol. 16, No. 2, pp. 151-159.

Reda, D. C. and Murphy, J. D. (1972), "Shock-Wave/Turbulent-Boundary-Layer Interactions in Rectangular Channels," *AIAA Journal*, Vol. 11, No. 2, pp. 139-140; also AIAA Paper 72-715.

Reda, D. C., Ketter, F. C. Jr. and Fan, C. (1974), "Compressible Turbulent Skin Friction on Rough and Rough/Wavy Walls in Adiabatic Flow," AIAA Paper 74-574.

Reynolds, O. (1874), "On the Extent and Action of the Heating Surface for Steam Boilers," *Proc. Manchester Lit. Phil. Soc.*, Vol. 14, pp. 7-12.

Reynolds, O. (1895), "On the Dynamical Theory of Incompressible Viscous Fluids and the Determination of the Criterion," *Philosophical Transactions of the Royal Society of London, Series A*, Vol. 186, p. 123.

Reynolds, W. C. (1970), "Computation of Turbulent Flows-State of the Art," Report No. MD-27, Dept. Mech. Eng., Stanford University, CA.

Reynolds, W. C. (1976), "Computation of Turbulent Flows," *Annual Review of Fluid Mechanics*, Vol. 8, pp. 183-208.

Reynolds, W. C. (1987), "Fundamentals of Turbulence for Turbulence Modeling and Simulation," In Lecture Notes for von Kármán Institute, AGARD Lecture Series No. 86, pp. 1-66, New York: NATO.

Ristorcelli, J. R. (1993), "A Representation for the Turbulent Mass Flux Contribution to Reynolds Stress and Two-Equation Closures for Compressible Turbulence," ICASE Report No. 93-88, Universities Space Research Association, Hampton, VA.

Ristorcelli, J. R., Lumley, J. L. and Abid, R. (1995), "A Rapid-Pressure Correlation Representation Consistent with the Taylor-Proudman Theorem Materially Frame-Indifferent in the 2-D Limit," *Journal of Fluid Mechanics*, Vol. 292, pp. 111-152.

Rizzetta, D. P. (1998), "Evaluation of Explicit Algebraic Reynolds-Stress Models for Separated Supersonic Flows," *AIAA Journal*, Vol. 36, No. 1, pp. 24-30.

Roache, P. J. (1990), "Need for Control of Numerical Accuracy," *Journal of Spacecraft and Rockets*, Vol. 27, No. 2, pp. 98-102.

Roache, P. J. and Salari, K. (1990), "Weakly Compressible Navier-Stokes Solutions with an Implicit Approximate Factorization Code," AIAA Paper 90-235.

Roache, P. J. (1998a), *Fundamentals of Computational Fluid Dynamics*, Hermosa Publishers, Albuquerque, NM.

Roache, P. J. (1998b), *Verification and Validation in Computational Science and Engineering*, Hermosa Publishers, Albuquerque, NM.

Robinson, D. F., Harris, J. E. and Hassan, H. A. (1995), "Unified Turbulence Closure Model for Axisymmetric and Planar Free Shear Flows," *AIAA Journal*, Vol. 33, No. 12, pp. 2324-2331.

Robinson, S. K. (1986), "Instantaneous Velocity Profile Measurements in a Turbulent Boundary Layer," *Chem. Eng. Commun.*, Vol. 43, pp. 347 [see also AIAA Paper 82-0963 (1982)].

Rodi, W. and Spalding, D. B. (1970), "A Two-Parameter Model of Turbulence and its Application to Free Jets," *Wärme und Stoffübertragung*, Vol. 3, p. 85.

Rodi, W. (1975), "A New Method of Analyzing Hot-Wire Signals in Highly Turbulent Flows and Its Evaluation in Round Jets," Disa Information, No. 17.

Rodi, W. (1976), "A New Algebraic Relation for Calculating Reynolds Stresses," *ZAMM*, Vol. 56, p. 219.

Rodi, W. (1981), "Progress in Turbulence Modeling for Incompressible Flows," AIAA Paper 81-45.

Rodi, W. and Scheuerer, G. (1986), "Scrutinizing the k-ϵ Turbulence Model Under Adverse Pressure Gradient Conditions," *ASME, Journal of Fluids Engineering*, Vol. 108, pp. 174-179.

Rodi, W. (1991), "Experience with Two-Layer Models Combining the k-ϵ Model with a One-Equation Model Near the Wall," AIAA Paper 91-216.

Rodi, W. (1997), "Comparison of LES and RANS Calculations of the Flow Around Bluff Bodies," *Journal of Wind Engineering and Industrial Aerodynamics*, Vol. 69-71, pp. 55-75.

Rodi, W. (1998), "Large-Eddy Simulations of the Flow Past Bluff Bodies – State-of-the Art," *Japan Society of Mechanical Engineers International Journal*, Series B, Vol. 41, No. 2.

Roe, P. L. (1981), "Approximate Riemann Solvers, Parameter Vectors, and Difference Schemes," *Journal of Computational Physics*, Vol. 43, pp. 357-372.

Rogallo, R. S. and Moin, P. (1984), "Numerical Simulation of Turbulent Flows," *Annual Review of Fluid Mechanics*, Vol. 16, pp. 99-137.

Rotta, J. C. (1951), "Statistische Theorie nichthomogener Turbulenz," *Zeitschrift fur Physik*, Vol. 129, pp. 547-572.

Rotta, J. C. (1962), "Turbulent Boundary Layers in Incompressible Flow," *Progress in Aerospace Sciences*, Vol. 2, p. 1.

Rotta, J. C. (1968), "Über eine Methode zur Berechnung turbulenter Scherströmungen," Aerodynamische Versuchanstalt Göttingen, Rep. 69 A 14.

Rubel, A. and Melnik, R. E. (1984), "Jet, Wake and Wall Jet Solutions Using a k-ϵ Turbulence Model," AIAA Paper 84-1523.

Rubel, A. (1985), "On the Vortex Stretching Modification of the k-ϵ Turbulence Model: Radial Jets," *AIAA Journal*, Vol. 23, No. 7, pp. 1129-1130.

Rubesin, M. W. (1989), "Turbulence Modeling for Aerodynamic Flows," AIAA Paper 89-606.

Rubesin, M. W. (1990), "Extra Compressibility Terms for Favre Averaged Two-Equation Models of Inhomogeneous Turbulent Flows," NASA CR-177556.

Ruelle, D. (1994), "Where Can One Hope to Profitably Apply the Ideas of Chaos?" *Physics Today*, Vol. 47, No. 7, pp. 24-30.

Rumsey, C. L., Gatski, T. B., Ying, S. and Bertelrud, A. (1998), "Prediction of High-Lift Flows Using Turbulent Closure Models," *AIAA Journal*, Vol. 36, No. 5, pp. 765-774.

Rumsey, C. L., Pettersson Reif, B. A. and Gatski, T. B. (2006), "Arbitrary Steady-State Solutions with the k-ϵ Model," *AIAA Journal*, Vol. 44, No. 7, pp. 1586-1592.

Rung, T., Lübcke, H., Thiele, F., Fu, S., Wang, C. and Guo, Y. (2000), "Turbulence Closure Model Constraint Derived from Stress-Induced Secondary Flow," *AIAA Journal*, Vol. 38, No. 9, pp. 1756-1758.

Saad, A. A. and Giddens, D. P. (1983), "Velocity Measurements in Steady Flow through Axisymmetric Stenoses at Moderate Reynolds Numbers," *Journal Biomech.*, Vol. 16, pp. 505-516.

Saffman, P. G. (1970), "A Model for Inhomogeneous Turbulent Flow," *Proc. R. Soc., Lond.*, Vol. A317, pp. 417-433.

Saffman, P. G. and Wilcox, D. C. (1974), "Turbulence-Model Predictions for Turbulent Boundary Layers," *AIAA Journal*, Vol. 12, No. 4, pp. 541-546.

Saffman, P. G. (1976), "Development of a Complete Model for the Calculation of Turbulent Shear Flows," April 1976 Symposium on Turbulence and Dynamical Systems, Duke Univ., Durham, NC.

Sagaut, P. and Germano, M. (2004), *Large Eddy Simulation for Incompressible Flows*, Second Edition, Springer-Verlag, New York, NY.

Sai, V. A. and Lutfy, F. M. (1995), "Analysis of the Baldwin-Barth and Spalart-Allmaras One-Equation Turbulence Models," *AIAA Journal*, Vol. 33, No. 10, pp. 1971-1974.

Samimy, M., Petrie, H. L. and Addy, A. L. (1985), "Reattachment and Redevelopment of Compressible Turbulent Free Shear Layers," *International Symposium on Laser Anemometry*, FED-Vol. 33, pp. 159-166.

Sandham, N. D. and Kleiser, L. (1992), "The Late Stages of Transition to Turbulence in Channel Flow," *Journal of Fluid Mechanics*, Vol. 245, p. 319.

Sarkar, S., Erlebacher, G., Hussaini, M. Y. and Kreiss, H. O. (1989), "The Analysis and Modeling of Dilatational Terms in Compressible Turbulence," NASA CR-181959.

Sarkar, S. and Speziale, C. G. (1990), "A Simple Nonlinear Model for the Return to Isotropy in Turbulence," *Physics of Fluids A*, Vol. 2, pp. 84-93.

Sarkar, S., Erlebacher, G. and Hussaini, M. Y. (1991), "Compressible and Homogeneous Shear — Simulation and Modeling," 8^{th} Symposium on Turbulent Shear Flows, Munich, Paper No. 21-2.

Sarkar, S. (1992), "The Pressure-Dilatation Correlation in Compressible Flows," *Physics of Fluids A*, Vol. 4, pp. 2674-2682.

Schlüter, J. U., Pitsch, H. and Moin, P. (2005), "Outflow Conditions for Integrated Large Eddy Simulation/Reynolds-Averaged Navier-Stokes Simulations," *AIAA Journal*, Vol. 43, No. 1, pp. 156-164.

Schubauer, G. B. and Klebanoff, P. S. (1955), "Contributions on the Mechanics of Boundary-Layer Transition," NASA TN 3489.

Schubauer, G. B. and Skramstad, H. K. (1948), "Laminar-Boundary-Layer Oscillations and Transition on a Flat Plate," NACA 909.

Schumann, U. (1975), "Subgrid Scale Model for Finite Difference Simulations of Turbulent Flows in Plane Channels and Annuli," *Journal of Computational Physics*, Vol. 18, pp. 376-404.

Schwarz, W. R. and Bradshaw, P. (1994), "Term-by-Term Tests of Stress-Transport Turbulence Models in a Three-Dimensional Boundary Layer," *Physics of Fluids*, Vol. 6, p. 986.

Sekundov, A. N. (1971), "Application of the Differential Equation for Turbulent Viscosity to the Analysis of Plane Nonself-Similar Flows," *Akademiya Nauk SSSR*, Izvestiia, Mekhanika Zhidkosti i Gaza, pp. 114-127 (in Russian).

Settles, G. S., Vas, I. E. and Bogdonoff, S. M. (1976), "Details of a Shock Separated Turbulent Boundary Layer at a Compression Corner," *AIAA Journal*, Vol. 14, No. 12, pp. 1709-1715.

Settles, G. S. and Dodson, L. J. (1994), "Supersonic and Hypersonic Shock Boundary-Layer Interaction Database," *AIAA Journal*, Vol. 32, No. 7, p. 1377.

Shaanan, S., Ferziger, J. H. and Reynolds, W. C. (1975), "Numerical Simulation of Turbulence in the Presence of Shear," Report No. TF-6, Dept. Mech. Eng., Stanford University, CA.

Shang, J. S. and Hankey, W. L. (1975), "Numerical Solution of the Navier Stokes Equations for Compression Ramp," AIAA Paper 75-4.

Shang, J. S., Hankey, W. L. and Law, C. (1976), "Numerical Simulation of Shock Wave Turbulent Boundary Layer Interaction," *AIAA Journal*, Vol. 14, No. 10, pp. 1451-1457.

Shih, T. H. and Lumley, J. L. (1985), "Modeling of Pressure Correlation Terms in Reynolds Stress and Scalar Flux Equations," Report No. FDA-85-3, Cornell University, Ithaca, NY.

Shih, T. H., Mansour, N. and Chen, J. Y. (1987), " Reynolds Stress Models of Homogeneous Turbulence," *Studying Turbulence Using Numerical Simulation Databases*, NASA Ames/Stanford CTR-S87, p. 191.

Shih, T. H. and Hsu, A. T. (1991), "An Improved k-ϵ Model for Near-Wall Turbulence," AIAA Paper 91-611.

Shih, T. H., Zhu, J. and Lumley, J. L. (1995), "A New Reynolds Stress Algebraic Equation Model," *Comput. Meth. Appl. Mech. & Eng.*, Vol. 125, Nos. 1-4, pp. 287-302.

Shih, T. S., Povinelli, L. A., Liu, N.-S., Potapczuk, M. G. and Limley, J. L. (1999), "Turbulence Surface Flow and Wall Function," AIAA Paper 99-2392.

Shih, T. I.-P., Steinthorsson, E. and Chyu, W. J. (1993), "Implicit Treatment of Diffusion Terms in Lower-Upper Algorithms," *AIAA Journal*, Vol. 31, No. 4, pp. 788-791.

Shur, M. L., Strelets, M. K., Travin, A. K. and Spalart, P. R. (2000), "Turbulence Modeling in Rotating and Curved Channels: Assessing the Spalart-Shur Correction," *AIAA Journal*, Vol. 38, No. 5, pp. 784-792.

Simpson, R. L. and Wallace, D. B. (1975), "Laminarescent Turbulent Boundary Layers: Experiments on Sink Flows," Project SQUID, Report SMU-1-PU.

Skare, P. and Krogstad, P. (1994), "A Turbulent Equilibrium Boundary Layer near Separation," *Journal of Fluid Mechanics*, Vol. 272, pp. 319-348.

Smagorinsky, J. (1963), "General Circulation Experiments with the Primitive Equations. I. The Basic Experiment," *Mon. Weather Rev.*, Vol. 91, pp. 99-164.

Smith, A. M. O. and Cebeci, T. (1967), "Numerical Solution of the Turbulent Boundary-Layer Equations," Douglas Aircraft Division Report DAC 33735.

Smith, B. R. (1990), "The k-$k\ell$ Turbulence and Wall Layer Model for Compressible Flows," AIAA Paper 90-1483.

Smith, B. R. (1994), "A near Wall Model for the k-ℓ Two Equation Turbulence Model," AIAA Paper 94-2386.

So, R. M. C. and Mellor, G. L. (1972), "An Experimental Investigation of Turbulent Boundary Layers Along Curved Surfaces," NASA CR-1940.

So, R. M. C. and Mellor, G. L. (1978), "Turbulent Boundary Layers with Large Streamline Curvature Effects," *ZAMP*, Vol. 29, pp. 54-74.

So, R. M. C., Lai, Y. G., Hwang, B. C. and Yoo, G. J. (1988), "Low Reynolds Number Modeling of Flows Over a Backward Facing Step," *ZAMP*, Vol. 39, pp. 13-27.

So, R. M. C., Lai, Y. G., Zhang, H. S. and Hwang, B. C. (1991), "Second-Order Near-Wall Turbulence Closures: A Review," *AIAA Journal*, Vol. 29, No. 11, pp. 1819-1835.

So, R. M. C. and Yuan, S. P. (1998), "Near-Wall Two-Equation and Reynolds-Stress Modeling of Backstep Flow," *International Journal of Engineering Science*, Vol. 36, No, 3, pp. 283-298.

So, R. M. C., Gatski, T. B. and Sommer, T. P. (1998), "Morkovin Hypothesis and the Modeling of Wall-Bounded Compressible Turbulent Flows," *AIAA Journal*, Vol. 36, No, 9, pp. 1583-1592.

Spalart, P. R. (1986), "Numerical Study of Sink-Flow Boundary Layers," *Journal of Fluid Mechanics*, Vol. 172, pp. 307-328.

Spalart, P. R. (1988), "Direct Simulation of a Turbulent Boundary Layer up to $Re_\theta = 1400$," *Journal of Fluid Mechanics*, Vol. 187, pp. 61-98.

Spalart, P. R. (1989), "Direct Numerical Study of Leading-Edge Contamination," AGARD CP 438.

Spalart, P. R. and Allmaras, S. R. (1992), "A One-Equation Turbulence Model for Aerodynamic Flows," AIAA Paper 92-439 [see also *La Recherche Aerospatiale* No. 1, p. 5 (1994)].

Spalart, P. R., Jou, W.-H., Strelets, M. and Allmaras, S. R. (1997), "Comments on the Feasibility of LES for Wings, and on a Hybrid RANS/LES Approach," *Advances in DNS/LES* (C. Liu and Z. Liu, eds. - Proceedings of 1st AFOSR Internat. Conf. on DNS and LES, Louisiana Tech.), Greyden Press, Columbus, OH.

Spalart, P. R., Deck, S., Shur, M. L., Squires, K. D., Strelets, M. and Travin, A. (2006), "A New Version of Detached-Eddy Simulation, Resistant to Ambiguous Grid Densities," *Theoretical and Computational Fluid Dynamics*, Vol. 20, pp. 181-195.

Spalding, D. B. (1961), "A Single Formula for the Law of the Wall," *Journal of Applied Mechanics*, Vol. 28, No. 3, pp. 444-458.

Speziale, C. G. (1985), "Modeling the Pressure-Gradient-Velocity Correlation of Turbulence," *Physics of Fluids*, Vol. 28, pp. 69-71.

Speziale, C. G. (1987a), "Second-Order Closure Models for Rotating Turbulent Flows," *Q. Appl. Math.*, Vol. 45, pp. 721-733.

Speziale, C. G. (1987b), "On Nonlinear k-ℓ and k-ϵ Models of Turbulence," *Journal of Fluid Mechanics*, Vol. 178, pp. 459-475.

Speziale, C. G., Abid, R. and Anderson, E. C. (1990), "A Critical Evaluation of Two-Equation Models for Near Wall Turbulence," AIAA Paper 90-1481.

Speziale, C. G. (1991), "Analytical Methods for the Development of Reynolds Stress Closures in Turbulence," *Annual Review of Fluid Mechanics*, Vol. 23, pp. 107-157.

Speziale, C. G. Sarkar, S. and Gatski, T. B. (1991), "Modeling the Pressure-Strain Correlation of Turbulence," *Journal of Fluid Mechanics*, Vol. 227, pp. 245-272.

Speziale, C. G., Abid, R. and Durbin, P. A. (1994), "On the Realizability of Reynolds Stress Turbulence Closures," *Journal of Scientific Computing*, Vol. 9, pp. 369-403.

Speziale, C. G. and Abid, R. (1995), "Near-Wall Integration of Reynolds Stress Turbulence Closures with No Wall Damping," *AIAA Journal*, Vol. 33, No. 10, pp. 1974-1977.

Speziale, C. G. and So, R. M. C. (1996), "Turbulence Modeling and Simulation," Technical Report No. AM-96-015, Boston University, Boston, MA.

Speziale, C. G. and Xu, X. H. (1996), "Towards the Development of Second-Order Closure Models for Non-Equilibrium Turbulent Flows," *Int. Journal of Heat and Fluid Flow*, Vol. 17, pp. 238-244.

Speziale, C. G. (1997), "Comparison of Explicit and Traditional Algebraic Stress Models of Turbulence," *AIAA Journal*, Vol. 35, No. 9, pp. 1506-1509.

Speziale, C. G. (1998), "Turbulence Modeling for Time-Dependent RANS and VLES: A Review," *AIAA Journal*, Vol. 36, No. 2, pp. 173-184.

Steger, J. and Warming, R. F. (1979), "Flux Vector Splitting of the Inviscid Gasdynamics Equations with Application to Finite Difference Methods," NASA TM-78605.

Stewartson, K. (1981), "Some Recent Studies in Triple-Deck Theory," in *Numerical and Physical Aspects of Aerodynamic Flows*, T. Cebeci, ed., Springer-Verlag, New York, NY, p. 142.

Stratford, B. S. (1959), "An Experimental Flow with Zero Skin Friction Throughout its Region of Pressure Rise," *Journal of Fluid Mechanics*, Vol. 5, pp. 17-35.

Tanaka, T. and Tanaka, E. (1976), "Experimental Study of a Radial Turbulent Jet," *Bulletin of the JSME*, Vol. 19, pp. 792-799.

Tavoularis, S. and Corrsin, S. (1981), "Experiments in Nearly Homogeneous Turbulent Shear Flow with Uniform Mean Temperature Gradient. Part I," *Journal of Fluid Mechanics*, Vol. 104, pp. 311-347.

Tavoularis, S. and Karnik, U. (1989), "Further Experiments on the Evolution of Turbulent Stresses and Scales in Uniformly Sheared Turbulence," *Journal of Fluid Mechanics*, Vol. 204, p. 457.

Taylor, G. I. (1935), "Statistical Theory of Turbulence," *Proc. R. Soc., Lond.*, Vol. A151, p. 421.

Tennekes, H. and Lumley, J. L. (1983), *A First Course in Turbulence*, MIT Press, Cambridge, MA.

Thangam, S. and Speziale, C. G. (1992), "Turbulent Flow Past a Backward Facing Step: A Critical Evaluation of Two-Equation Models," *AIAA Journal*, Vol. 30, No. 5, pp. 1314-1320.

Thomann, H. (1968), "Effect of Streamwise Wall Curvature on Heat Transfer in a Turbulent Boundary Layer," *Journal of Fluid Mechanics*, Vol. 33, pp. 283-292.

Townsend, A. A. (1956), "The Uniform Distortion of Homogeneous Turbulence," *Q. J. Mech. Appl. Math.*, Vol. 7, p. 104.

Townsend, A. A. (1976), *The Structure of Turbulent Shear Flow*, Second Ed., Cambridge University Press, Cambridge, England.

Tucker, H. J. and Reynolds, A. J. (1968), "The Distortion of Turbulence by Irrotational Plane Strain," *Journal of Fluid Mechanics*, Vol. 32, Pt. 4, pp. 657-673.

Uberoi, M. S. (1956), "Effect of Wind Tunnel Contraction on Free Stream Turbulence," *Journal of the Aeronautical Sciences*, Vol. 23, pp. 754-764.

Van Driest, E. R. (1951), "Turbulent Boundary Layer in Compressible Fluids," *Journal of the Aeronautical Sciences*, Vol. 18, pp. 145-160, 216.

Van Driest, E. R. (1956), "On Turbulent Flow Near a Wall," *Journal of the Aeronautical Sciences*, Vol. 23, p. 1007.

Van Dyke, M. D. (1975), *Perturbation Methods in Fluid Mechanics*, Parabolic Press, Stanford, CA.

Van Leer, B. (1982), "Flux-Vector Splitting for the Euler Equations," ICASE Report 82-30, Univ. Space Research Assoc., Hampton, VA.

Vasiliev, V. I., Volkov, D. V., Zaitsev, S. A. and Lyubimov, D. A. (1997), "Numerical Simulation of Channel Flows by a One-Equation Turbulence Model," *Journal of Fluids Engineering*, Vol. 119, pp. 885-892.

Venkatakrishnan, V. (1996), "Perspective in Unstructured Grid Flow Solvers," *AIAA Journal*, Vol. 34, pp. 533-547.

Veynante, D. and Poinsot, T. (1997), "Large Eddy Simulation of Combustion Instabilities in Turbulent Premixed Burners," NASA Ames/Stanford Center for Turbulence Research, *Annual Research Briefs*, pp. 253-274.

Viegas, J. R. and Horstman, C. C. (1979), "Comparison of Multiequation Turbulence Models for Several Shock Boundary-Layer Interaction Flows," *AIAA Journal*, Vol. 17, No. 8, pp. 811-820.

Viegas, J. R., Rubesin, M. W. and Horstman, C. C. (1985), "On the Use of Wall Functions as Boundary Conditions for Two-Dimensional Separated Compressible Flows," AIAA Paper 85-180.

Vollmers, H. and Rotta, J. C. (1977), "Similar Solutions of the Mean Velocity, Turbulent Energy and Length Scale Equation," *AIAA Journal*, Vol. 15, No. 5, pp. 714-720.

von Kármán, T. (1930), "Mechanische Ähnlichkeit und Turbulenz," *Proc. Int. Congr. Appl. Mech., 3^{rd}, Stockholm*, Part 1, pp. 85-105.

von Kármán, T. (1934), "Some Aspects of the Turbulence Problem," *Proc. Int. Congr. Appl. Mech., 4^{th}, Cambridge*, p. 54.

von Kármán, T. (1937), "Turbulence," Twenty-Fifth Wilbur Wright Memorial Lecture, *Journal of the Aeronautical Sciences*, Vol. 41, p. 1109.

Vreman, A. W., Sandham, N. D. and Luo, K. H. (1996), "Compressible Mixing Layer Growth Rate and Turbulence Characteristics," *Journal of Fluid Mechanics*, Vol. 320, p. 235.

Wang, Q. and Squires, K. D. (1996), "Large Eddy Simulation of Particle-Laden Turbulent Channel Flow," *Physics of Fluids*, Vol. 8, pp. 1207-1223.

Weinstock, J. (1981), "Theory of the Pressure-Strain Rate Correlation for Reynolds Stress Turbulence Closures," *Journal of Fluid Mechanics*, Vol. 105, pp. 369-396.

Weygandt, J. H. and Mehta, R. D. (1995), "Three-Dimensional Structure of Straight and Curved Plane Wakes," *Journal of Fluid Mechanics*, Vol. 282, p. 279.

Wieghardt, K. and Tillman, W. (1951), "On the Turbulent Friction Layer for Rising Pressure," NACA TM 1314.

Wigeland, R. A. and Nagib, H. M. (1978), "Grid-Generated Turbulence With and Without Rotation About the Streamwise Direction," Fluids and Heat Transfer Report R78-1, Illinois Institute of Technology, Chicago, IL.

Wilcox, D. C. and Alber, I. E. (1972), "A Turbulence Model for High Speed Flows," *Proc. of the 1972 Heat Trans. & Fluid Mech. Inst.*, Stanford Univ. Press, Stanford, CA, pp. 231-252.

Wilcox, D. C. and Traci, R. M. (1974), "Analytical Study of Freestream Turbulence Effects on Stagnation Point Flow and Heat Transfer," AIAA Paper 74-515.

Wilcox, D. C. (1974), "Numerical Study of Separated Turbulent Flows," AIAA Paper 74-584.

Wilcox, D. C. and Chambers, T. L. (1975), "Further Refinement of the Turbulence Model Transition Prediction Technique," DCW Industries Report DCW-R-03-02, La Cañada, CA.

Wilcox, D. C. and Traci, R. M. (1976), "A Complete Model of Turbulence," AIAA Paper 76-351.

Wilcox, D. C. and Chambers, T. L. (1977), "Streamline Curvature Effects on Turbulent Boundary Layers," *AIAA Journal*, Vol. 15, No. 4, pp. 574-580.

Wilcox, D. C. (1977), "A Model for Transitional Flows," AIAA Paper 77-126.

Wilcox, D. C. and Rubesin, M. W. (1980), "Progress in Turbulence Modeling for Complex Flow Fields Including Effects of Compressibility," NASA TP-1517.

Wilcox, D. C. (1981a), "Alternative to the e^9 Procedure for Predicting Boundary Layer Transition," *AIAA Journal*, Vol. 19, No. 1, pp. 56-64.

Wilcox, D. C. (1981b), "Algorithm for Rapid Integration of Turbulence Model Equations on Parabolic Regions," *AIAA Journal*, Vol. 19, No. 2, pp. 248-251.

Wilcox, D. C. (1988a), "Reassessment of the Scale Determining Equation for Advanced Turbulence Models," *AIAA Journal*, Vol. 26, No. 11, pp. 1299-1310.

Wilcox, D. C. (1988b), "Multiscale Model for Turbulent Flows," *AIAA Journal*, Vol. 26, No. 11, pp. 1311-1320.

Wilcox, D. C. (1989), "Wall Matching, A Rational Alternative to Wall Functions," AIAA Paper 89-611.

Wilcox, D. C. (1990), "Supersonic Compression-Corner Applications of a Multiscale Model for Turbulent Flows," *AIAA Journal*, Vol. 28, No. 7, p. 1194.

Wilcox, D. C. (1991), "Progress in Hypersonic Turbulence Modeling," AIAA Paper 91-1785.

Wilcox, D. C. (1992a), "The Remarkable Ability of Turbulence Model Equations to Describe Transition," Fifth Symposium on Numerical and Physical Aspects of Aerodynamic Flows, 13-15 January 1992, California State University, Long Beach, CA.

Wilcox, D. C. (1992b), "Dilatation-Dissipation Corrections for Advanced Turbulence Models," *AIAA Journal*, Vol. 30, No. 11, pp. 2639-2646.

Wilcox, D. C. (1993a), "A Two-Equation Turbulence Model for Wall-Bounded and Free-Shear Flows," AIAA Paper 93-2905.

Wilcox, D. C. (1993b), "Comparison of Two-Equation Turbulence Models for Boundary Layers with Pressure Gradient," *AIAA Journal*, Vol. 31, No. 8, pp. 1414-1421.

Wilcox, D. C. (1994), "Simulation of Transition with a Two-Equation Turbulence Model," *AIAA Journal*, Vol. 32, No. 2, pp. 247-255.

Wilcox, D. C. (1995a), *Perturbation Methods in the Computer Age*, DCW Industries, Inc., La Cañada, CA.

Wilcox, D. C. (1995b), "Back of the Envelope Analysis of Turbulence Models," *IUTAM Symposium on Asymptotic Methods for Turbulent Shear Flows at High Reynolds Numbers*, pp. 309-322, Kluwer Academic Publishers, Dordrecht, The Netherlands.

Wilcox, D. C. (1998), *Turbulence Modeling for CFD*, Second Edition, DCW Industries, Inc., La Canada, CA.

Winter, K. and Gaudet, L. (1973), "Turbulent Boundary-Layer Studies at High Reynolds Number at Mach Numbers Between 0.2 and 2.8," R. & M. Number 3712, British Aeronautical Research Council.

Witze, P. O. and Dwyer, H. A. (1976), "The Turbulent Radial Jet," *Journal of Fluid Mechanics*, Vol. 75, pp. 401-417.

Wolfshtein, M. (1967), "Convection Processes in Turbulent Impinging Jets," Imperial College, Heat Transfer Section Report SF/R/2.

Wygnanski, I. and Fiedler, H. E. (1969), "Some Measurements in the Self-Preserving Jet," *Journal of Fluid Mechanics*, Vol. 38, pp. 577-612.

Xiao, X., Edwards, J. R. and Hassan, H. A. (2003a), "Inflow Boundary Conditions for Hybrid Large Eddy/Reynolds Averaged Navier-Stokes Simulations," *AIAA Journal*, Vol. 41, No. 8, pp. 1481-1489.

Xiao, X., Edwards, J. R. and Hassan, H. A. (2003b), "Investigation of Flow Dependent Blending Functions in Hybrid LES/RANS Simulations," AIAA Paper 2003-3462.

Xiao, X., Edwards, J. R. and Hassan, H. A. (2004), "Blending Functions in Hybrid Large Eddy/Reynolds Averaged Navier-Stokes Simulations," *AIAA Journal*, Vol. 42, No. 12, pp. 2508-2515.

Yakhot, V. and Orszag, S. A. (1986), "Renormalization Group Analysis of Turbulence: 1. Basic Theory," *Journal of Scientific Computing*, Vol. 1, pp. 3-51.

Yakhot, V., Orszag, S. A., Thangam, S., Gatski, T. B. and Speziale, C. G. (1992), "Development of Turbulence Models for Shear Flows by a Double Expansion Technique," *Physics of Fluids A*, Vol. 4, p. 1510-1520.

Yang, K.-S. and Ferziger, J. H. (1993), "Large-Eddy Simulation of Turbulent Obstacle Flow Using a Dynamic Subgrid-Scale Model," *AIAA Journal*, Vol. 31, pp. 1406-1413.

Yang, Z. and Shih, T.-H. (1993), "A New Time Scale Based k-ϵ Model for Near Wall Turbulence," *AIAA Journal*, Vol. 31, No. 7, pp. 1191-1198.

Yap, C. (1987), "Turbulent Heat and Momentum Transfer in Recirculating and Impinging Flows," PhD Thesis, Faculty of Technology, Univ. of Manchester.

Zagarola, M. V. (1996), "Mean Flow Scaling in Turbulent Pipe Flow," PhD Thesis, Princeton University, Princeton, NJ.

Zagarola, M. V., Perry, A. E. and Smits, A. J. (1997), "Log Laws or Power Laws: The Scaling in the Overlap Region," *Physics of Fluids*, Vol. 9, No. 7, pp. 2094-2100.

Zeierman, S. and Wolfshtein, M. (1986), "Turbulent Time Scale for Turbulent Flow Calculations," *AIAA Journal*, Vol. 24, No. 10, pp. 1606-1610.

Zeman, O. (1990), "Dilatational Dissipation: The Concept and Application in Modeling Compressible Mixing Layers," *Physics of Fluids A*, Vol. 2, No. 2, pp. 178-188.

Zeman, O. (1991), "The Role of Pressure-Dilatation Correlation in Rapidly Compressed Turbulence and in Boundary Layers," NASA Ames, Stanford Center for Turbulence Research Annual Research Briefs, p. 105.

Zeman, O. (1993), "A New Model for Super/hypersonic Turbulent Boundary Layers," AIAA Paper 93-0897.

Zhang, H. S., So, R. M. C., Speziale, C. G. and Lai, Y. G. (1993), "Near-Wall Two-Equation Model for Compressible Turbulent Flows," *AIAA Journal*, Vol. 31, pp. 196-199

Zijlema, M., Segal, A. and Wesselinh, P. (1995), "Finite Volume Computation of 2D Incompressible Turbulent Flows in General Coordinates on Staggered Grids," *Int. J. Numer. Methods in Fluids*, Vol. 20, pp. 621-640.

Index

A

B

C

D

E

F

G

H

I

J

K

L

M

N

O

P

R

S

T

W

Y

Z

Has the time arrived to select a new introductory fluid mechanics text?

If it is, you should know that DCW Industries has published a book that deserves your consideration.

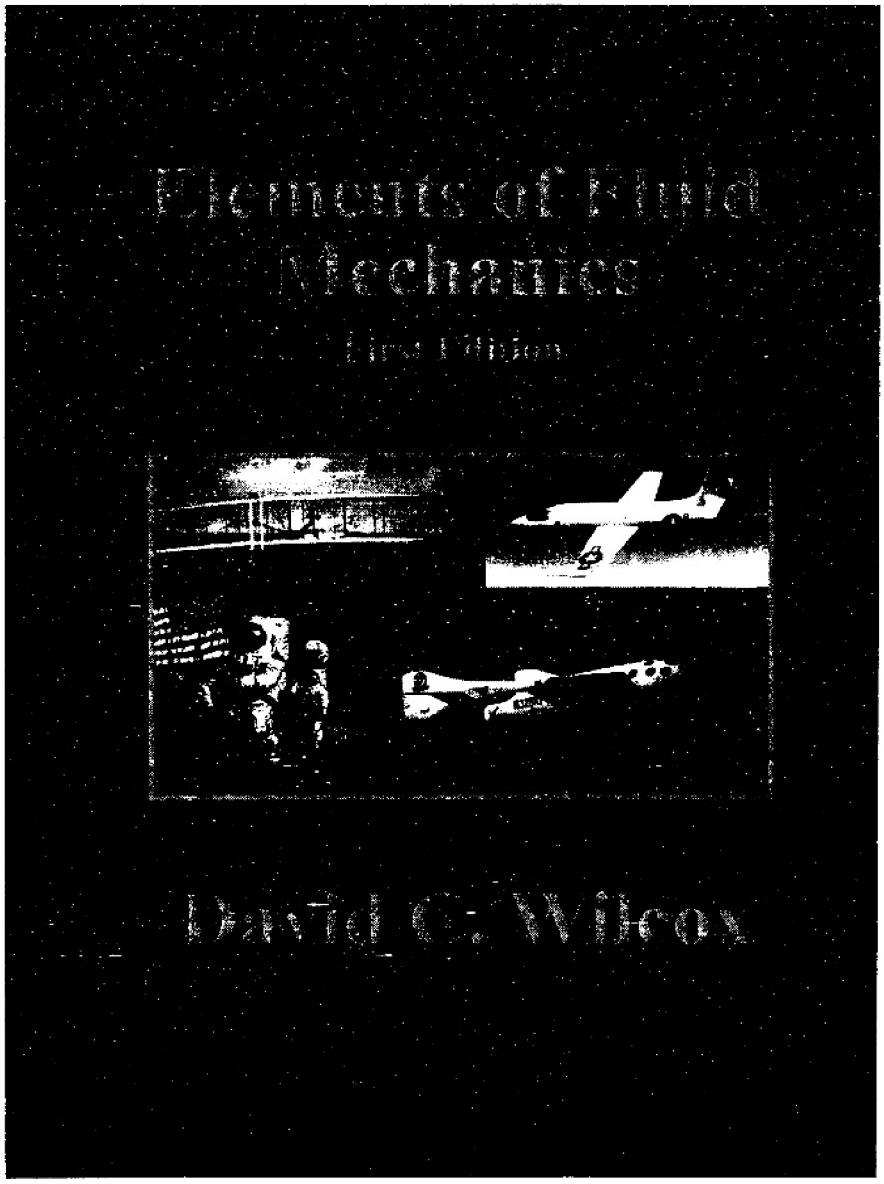

ISBN 1-928729-17-7, 570 pages

Elements of Fluid Mechanics (2005) is designed to counter the modern trend away from an emphasis on fundamentals. With the revived interest in aeronautics spurred by both private enterprise and government to expand mankind's travel in and exploration of space, a return to rigor is overdue in universities. This text has been written in that spirit and will challenge the reader's intellect and encourage aiming for excellence. *If you're a teacher*, this text will help you lay the foundation for your students to be tomorrow's innovators. *If you're a practicing engineer* and you want to firm up your knowledge of the basic principles of fluid mechanics, this book is exactly what you've been looking for.

Scope: Based on Dr. Wilcox's 25+ years of experience teaching introductory fluid mechanics, this book is suitable for a one-semester introduction to fluid mechanics. The primary focus is on the control-volume approach with minimal focus on the differential equations of fluid motion. The text maintains rigor while using only the most basic elements of vector calculus. Topics covered are as follows.

- Thorough development of the control-volume approach
- Dimensional analysis
- Fluid statics
- Open-channel flow
- Pipe flow, including pipe systems
- Elements of flow through turbomachines
- One-dimensional compressible flow including Fanno and Rayleigh flow
- Elements of potential-flow theory
- Introduction to boundary-layer theory

Companion CD: The book includes a CD with fluid-mechanics pictures and movies illustrating basic fluid physics.

Solutions Manual: The 1285-page manual is typeset in LaTeX, and is supplied on CD without charge to schools that have adopted the book.

Lecture Notes: The Solutions Manual CD includes a complete set of lecture notes in Microsoft Power Point format.

Has the time arrived to select a new intermediate fluid mechanics text?

If it is, you should know that DCW Industries has published a book that deserves your consideration.

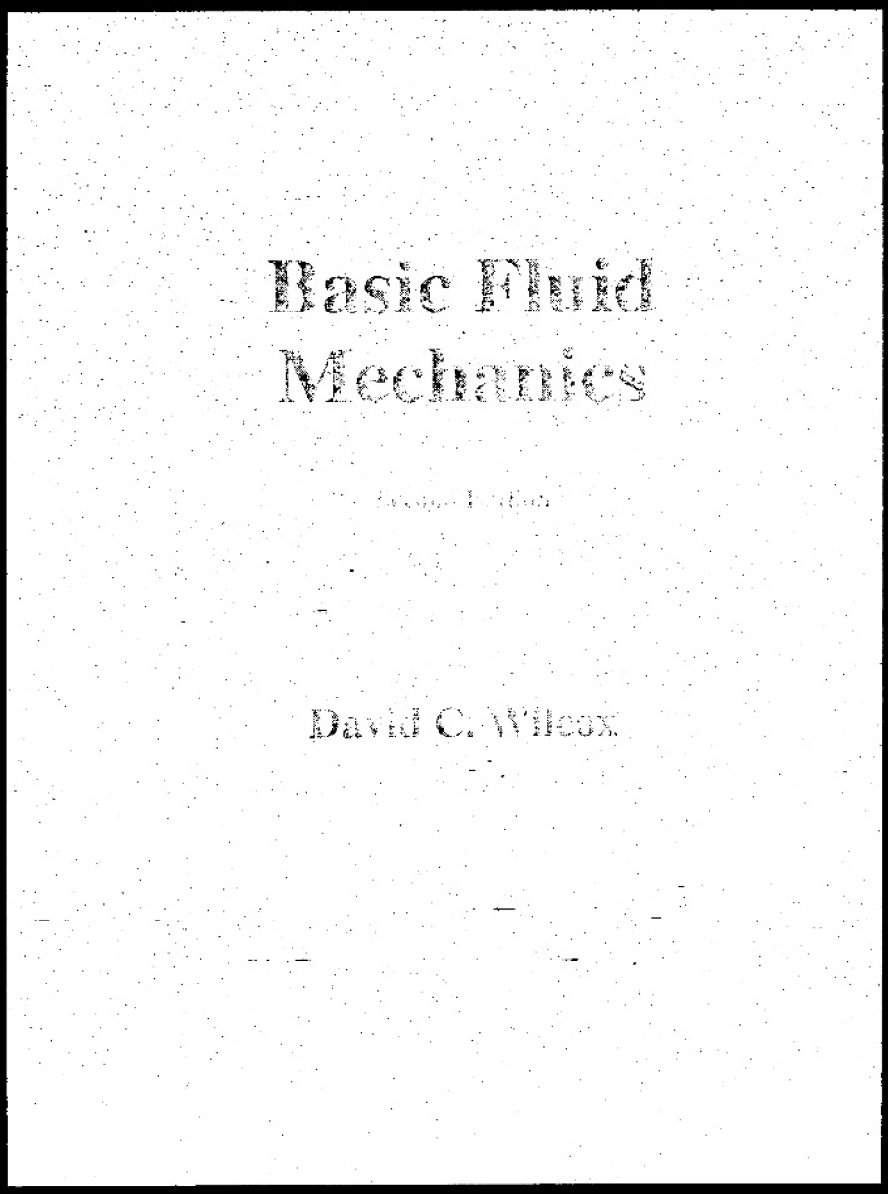

ISBN 1-928729-03-7, 786 pages

Basic Fluid Mechanics (2003) is designed to counter the modern trend away from an emphasis on fundamentals. With the revived interest in aeronautics spurred by both private enterprise and government to expand mankind's travel in and exploration of space, a return to rigor is overdue in universities. This text has been written in that spirit and will challenge the reader's intellect and encourage aiming for excellence. *If you're a teacher*, this text will help you lay the foundation for your students to be tomorrow's innovators. *If you're a practicing engineer* and you want to firm up your knowledge of the basic principles of fluid mechanics, this book is exactly what you've been looking for.

Scope: Based on Dr. Wilcox's 25+ years of experience teaching introductory and intermediate fluid mechanics, this book is suitable for a two-semester sequence of fluid-mechanics courses. The first 10 chapters of the text include:

- Thorough development of the control-volume approach
- Dimensional analysis
- Fluid statics and open-channel flow
- Pipe flow, including pipe systems
- Elements of flow through turbomachines
- One-dimensional compressible flow

Chapters 11-15 cover the differential equations of fluid motion, including:

- Potential-flow theory
- Detailed development of the Navier-Stokes equation
- Exact Navier-Stokes solutions
- Boundary-layer theory including an introduction to turbulent flow
- Prandtl-Meyer expansion and oblique shocks, Fanno and Rayleigh flow
- CFD concepts integrated throughout

Companion CD: The book includes a CD with useful engineering software, and fluid-mechanics pictures and movies illustrating basic fluid physics.

Solutions Manual: The 1512-page manual is typeset in LaTeX, and is supplied on CD without charge to schools that have adopted the book.

Lecture Notes: The Solutions Manual CD includes a complete set of lecture notes in Microsoft Power Point format.

Has the time arrived to select a new perturbation methods text?

If it is, you should know that DCW Industries has published a book that deserves your consideration.

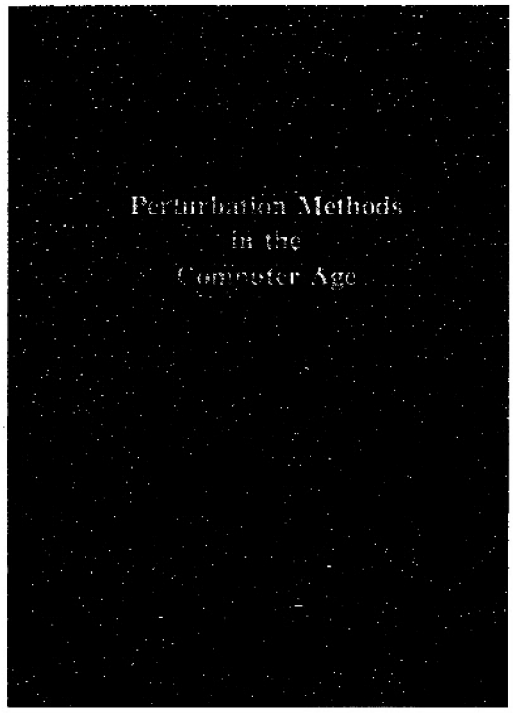

ISBN 0-9636051-2-7, 224 pages

Perturbation Methods in the Computer Age (1995) is an advanced undergraduate or first-year graduate text on asymptotic and perturbation methods. It discusses asymptotic expansion of integrals, including Laplace's method, stationary phase and steepest descent. The book introduces the general principles of singular-perturbation theory, with examples for ODE's and PDE's. It covers multiple-scale analysis, including the method of averaging and the WKB method. Through a collection of practical examples, the text shows how useful asymptotics can be when used in conjunction with computational methods.

Solutions Manual: The 164-page manual is typeset in LaTeX, and is available on CD from DCW Industries, Inc.

Would you like to understand some of the mystery surrounding entropy and the science of thermodynamics?

If it is, you should know that DCW Industries has published a book that deserves your consideration.

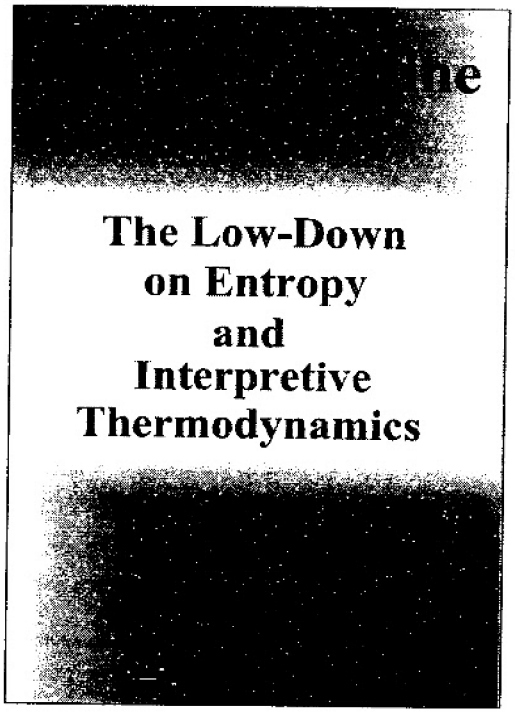

ISBN 1-928729-01-0, 120 pages

The Low-Down on Entropy and Interpretive Thermodynamics (1999) is the final book written by Professor Stephen Kline of Stanford University. It is a delightful treatise on the subtleties of entropy and the second law of thermodynamics.

For other educational books, please visit DCW Industries' Home Page . . .

DCW Industries
5354 Palm Drive, La Cañada, CA 91011
http://www.dcwindustries.com

NOTE: We have taken great pains to assure the accuracy of this manuscript. However, if you find errors, please report them to DCW Industries' Home Page on the Worldwide Web at **http://dcwindustries.com**. As long as we maintain a WWW page, we will provide an updated list of known typographical errors.